ESCUELA TÉCNICA SUPERIOR DE INGENIERÍA
Universidad de Sevilla

Filiberto Fele

Coalitional model predictive control for systems of systems

DOCTORAL THESIS

Sevilla, 2016

ESCUELA TÉCNICA SUPERIOR DE INGENIERÍA
Universidad de Sevilla

Filiberto Fele

Coalitional model predictive control for systems of systems

DOCTORAL THESIS

Supervisors: Professor Eduardo F. Camacho
Dr. José María Maestre

Sevilla, 2016

This Doctoral thesis has been made at Escuela Técnica Superior de Ingeniería de Sevilla, University of Seville, Department of Systems and Automation Engineering

Supervisors: Professor Eduardo F. Camacho
Dr. José María Maestre

This Doctoral thesis contains 159 pages

Abstract

Coalitional model predictive control for systems of systems

An aspect so far rarely contemplated in distributed control problems is the explicit consideration of individual (local) interests of the components of a complex system. Indeed, the focus of the majority of the literature about distributed control has been the overall system performance. While on one hand this permitted to address fundamental properties of centralized control, such as system-wide optimality and stability, one the other hand it implied assuming unrestricted cooperation across local controllers. However, when dealing with multi-agent systems with a strong heterogeneous character, cooperation between the agents cannot be taken for granted (due to, for example, logistics, market competition), and selfish interests may not be neglected. Another critical point that must be kept into consideration is the *diversity* characterizing systems of systems (SoS), yielding very complex interactions between the agents involved (one example of such system is the smart grid).

In order to tackle such inherent aspects of SoS, the research presented in this thesis has been concerned with the development of a novel framework, the *coalitional control*, that extends the scope of advanced control methods (in particular MPC) by drawing concepts from cooperative game theory that are suited for the inherent heterogeneity of SoS, providing as well an economical interpretation useful to explicitly take into account local selfish interests. Thus, coalitional control aims at governing the association/dissociation dynamics of the agents controlling the system, according to the expected benefits of their possible cooperation. From a control theoretical perspective, this framework is founded on the theory of switched systems and variable structure/topology networked systems, topics that are recently experiencing a renewed interest within the community. The main concepts and challenges in coalitional control, and the links with cooperative network game theory are presented in this document, tracing a path from model partitioning to the control schemes whose principles delin-

eate the idea of coalitional control. This thesis focuses on two basic architectures: *(i)* a hierarchically supervised evolution of the coalitional structure, and *(ii)* a protocol for autonomous negotiation between the agents, with specific mechanisms for benefit redistribution, leading to the emergence of cooperating clusters.

Keywords: model predictive control, cooperative MPC control, cooperative game theory, multi-agent systems, systems of systems, microgrid, smart grid, irrigation canals

Contents

Chapter 1

Introduction

The evolution of information and communication technologies (ICT) has yielded means of sharing measures and other information in an efficient and flexible way [1], increasing the size and complexity of control applications [2]. At the same time, the improvements in the computational and communicational capabilities of control devices have fostered the development of noncentralized control architectures, already motivated by the inherent structural constraints of large-scale systems. Computer-based control approaches such as model predictive control (MPC) are visible beneficiaries of these advances and have registered a significant growth regarding both theoretical and applied fields [3, 4].

Whether or not the system arises from the interaction of different entities, it is generally possible to identify a set of coupled *local* control problems, often defining a clear structure, that jointly configure the global one. Hence, the variables of a system can be grouped to highlight weakly coupled blocks: within each block (usually designated as *neighborhood*) dynamic interactions propagate quickly, affecting the rest of the system on a longer time scale [5]. In most cases centralized strategies do not exploit such structure, sometimes leading to unviable computational or communicational requirements.

As a natural way of avoiding the dependence on unavailable information—as well as to keep computational requirements at a minimum—it is desirable to formulate control laws based exclusively on local information [6, 7]. Noncentralized control strategies seek a tradeoff between performance loss and a scalable and flexible implementation [1]. In general, though, the stronger the interaction among different parts of a system, the denser the communication required between the control agents—the extreme case corresponding to a distributed solution of the centralized control problem [8].

An extra degree of flexibility in the optimization of the computational and communicational requirements can be derived by the online identification of subsystems' interactions and the consequent real-time adjustment of the control law structure. This is the idea behind *coalitional control*, a novel theory inspired by cooperative games, where the control strategy adapts to the varying coupling conditions between the controllers, promoting the formation of coalitions—clusters of controllers that cooperate in order to benefit from a jointly optimized control action. The adaptation of the controller topology may be the result of a top-down architecture, that is, imposed by a supervisor [9, 10, 11], or of a bottom-up approach [12], an autonomous coalition formation process occurring between the control agents. In all cases, the outcome will be a dynamically evolving coalitional structure of the overall controller.

Coalitional control focuses on the local interests that motivate the controllers to assemble, an aspect so far rarely contemplated in the distributed control literature. Indeed, although a well-defined global organizational objective may be present in large-scale infrastructures, it is not uncommon for the individual components to show interests that do not align with the global one [13]. The smart grid and the intelligent transportation system are clear examples: a consistent research effort is being devoted to the issues associated with their management, typically involving different game-theoretic models in order to grasp the complex interaction phenomena produced by their heterogeneous user population [14, 15].

This thesis presents the main concepts and challenges in coalitional control, and the links with cooperative network game theory. In Section 1.1, a path is traced from the issues related with model partitioning—a fundamental step in the design of distributed controllers—to the solutions proposed in the literature whose principles delineate the idea of coalitional control.

1.1 Controlling large-scale systems: the path to coalitional control

Consider a large-scale system described by the following discrete-time model:

$$\begin{aligned} x^+ &= f(x,u), \\ y &= g(x), \end{aligned} \tag{1.1}$$

where $x \in \mathbb{R}^n$ and $u \in \mathbb{R}^q$ are the global state and control input vectors, respectively, constrained in the sets $\mathcal{X}$ and $\mathcal{U}$, and $y \in \mathbb{R}^p$ is the vector gathering the outputs of the system.

A standard practice is to implement controllers on top of an already defined plant's structure—usually following structural constraints and fault tolerance requirements. This typically involves a prior partition of (1.1) into a set $\mathcal{N} = \{1, \dots, N\}$ of submodels, such that the essential dynamics characterizing the system are retained. Dynamic interactions typically occur between adjacent subsystems: coupling effects sensed beyond neighboring subsystems are seen through intermediate subsystems. Hence, the system's topology appears as a fundamental guideline for the reduction of the overall information exchange, which represents a critical aspect of distributed cooperative MPC schemes [8]. The problems of system partitioning and distributed control are closely related. Coalitional control encompasses both of them, allowing the *dynamic* partitioning of the system into cooperative components.

1.1.1 Model partitioning

Model partitioning consists in the assignment of subsets of the global state and input variables to each of the agents involved in the control of a system, such that $x = (x_i)_{i \in \mathcal{N}} \in \mathbb{R}^n$, $u = (u_i)_{i \in \mathcal{N}} \in \mathbb{R}^q$. According to the classification provided by [16], the system decomposition can be either *horizontal* or *hierarchical*. The first type relates to the physical structure of the system, while the second is based on the nature of the process, its characteristic time scales, and the control objectives. Hierarchical decompositions provide larger flexibility in shaping the controller to the heterogeneity of many large-scale systems—different sampling times, asynchronous operation of the different parts [17, 5]. A general systematic methodology is hard to define due to the manifold nature (subsystems' interactions, time-scale, communication constraints, privacy concerns) of controlled systems, so that ad hoc approaches are frequently implemented.

Once the global model has been partitioned, each resulting subsystem $i \in \mathcal{N}$ is assigned to a local control agent that has partial knowledge of the overall system, such that its behavior can be described by

$$\begin{aligned} x_i^+ &= f_i(x_i, u_i) + w_i, \\ y_i &= g_i(x_i) + \varpi_i, \end{aligned} \tag{1.2}$$

where $x_i \in \mathbb{R}^{n_i}$ and $u_i \in \mathbb{R}^{q_i}$ are respectively the local state and input vectors, constrained in the sets $\mathcal{X}_i$ and $\mathcal{U}_i$ respectively, and $y_i \in \mathbb{R}^{p_i}$ is the local output vector. The vector $w_i \in \mathbb{R}^{n_i}$ represents the measurable state disturbances resulting from the coupling with other subsystems,

$$w_i = \sum_{j \in \mathcal{M}_i} f_{ij}(x_j, u_j), \tag{1.3}$$

where $\mathcal{M}_i \triangleq \{j \in \mathcal{N} \setminus \{i\} : \exists (x_j, u_j) \in \mathcal{X}_j \times \mathcal{U}_j \mid f_{ij}(x_j, u_j) \neq \mathbf{0}\}$ is referred to as the *neighborhood* of subsystem i. Similarly, $\varpi_i \in \mathbb{R}^{p_i}$ expresses the measurable disturbances on the local output. Notice that neither the external state and inputs x_j and u_j nor their relation f_{ij} with the local ones are known a priori by the local agent, eventually inducing some modeling error due to possibly neglected state–state, input–state, or input–output interactions.

In the search for the optimal structure of the control system, an important limiting factor comes from the available computation and communication resources. For instance, the excessive partitioning of the system may reduce the model size and hence the computational requirements at each node, yet at the expense of an increased communication load—which in turn limits the possibilities of a parallel implementation of the control algorithm. Similarly, while a small sampling time allows to obtain a model that reflects the actual structure of the system, it will result in high communication rates between nodes, as well as in a shorter time available for computation [1].

Besides, more often than not, large-scale systems are characterized by multi-scale dynamics—typically slower overall dynamics arising out of a group of subsystems with fast dynamics. With specific attention towards the strong relationship between model decomposition and sampling time, a structural analysis for decomposition is presented in [1], oriented to the implementation of a hierarchical multi-rate estimation and control architecture. In [18], the coupling structure of the plant is analyzed prior to the design of feedback laws in order to decompose the model into hierarchically coupled clusters. A two-layer multi-rate control for such hierarchical decomposition is proposed in [19], where information is exchanged at each time step within clusters of strongly coupled subsystems, while a slower communication rate is required between different clusters.

The interaction among subsystems can be as well viewed as multiplicative output uncertainty. In [20], the selection of best model partition within a given set of candidates is based on their associated (open loop) uncertainty bounds. The implications of system decomposition on robustness are investigated in [21]. The robustness of distributed MPC schemes characterized by different levels of knowledge of the non-local dynamics of the system is evaluated by means of an H_∞ index. The formulation of a multi-objective mixed-integer nonlinear programming problem (MINLP) based on this index allows to seek a tradeoff between global robust performance and the degree of connectivity among agents (translated in terms of local interaction model coverage). Given N subsystems, the MINLP considers $N(N-1)$ binary variables to choose the structure of the controller over all possible connections among the subsystems. Simulation results show how controllers characterized by dense connectivity are more sensitive to errors in the interaction models. When these are affected by significant uncertainty, a fully decentralized structure can provide higher robustness.

Several other methods have been proposed in the literature. In [22], the most relevant variables of the system are controlled by a central coordinator MPC, and a set of decentralized controllers complete the control action by responding to the inputs of the coordinator. The work of [23] addresses the assignment of actuators to a given set of controllers on the basis of two criteria, in order to achieve submodels of manageable size for MPC control. The first is an open-loop criterion based on maximizing the connectivity of the weighted graph representing the system, as an expression of the Hankel norm resulting by the controllability and observability Grammians. The second is a closed-loop criterion that aims at minimizing the performance degradation due to model partitioning, measured through the MPC's cost function. A method for the derivation of a distributed model is suggested in [24], based on the Kalman canonical form of the linear state-space model for each input-output pair [25].

An exhaustive study of the issues related to model partitioning for the decentralized control of large-scale systems can be found in [6]. One contribution of [6] is that of showing how graph theory methods are well suited to gain an insight about the structural controllability and observability of large-scale systems, and employ these as a basis for model decomposition. Graph theory methods have been as well employed for the analysis of the impact of system topology on controllability and observability in [26, 27]. Based on graph partitioning is the work of [28], where a decomposition method providing a set of non-overlapping subgraphs, with balanced number of vertices and minimal number of interconnecting edges, was developed. More recently, a threshold on the Shapley value [29] of the potential communication links between the controllers was proposed in [30] as a criterion for partitioning.

1.1.2 Cooperative control

We assume in the following that the objective of each local controller is to drive the subsystem's state towards the origin of the state space. The cost of subsystem i at any given time step k is expressed by the stage cost $\ell_i(x_i, u_i)$. At time k, a control sequence is derived by the solution of the MPC problem

$$\min_{\mathbf{u}_i} J_i = \sum_{t=0}^{N_p-1} \ell_i(x_i(t|k), u_i(t|k)) + V_i(x_i(N_p|k)) \tag{1.4a}$$

$$\text{s.t.}$$

$$x_i(t+1|k) = f_i(x_i(t|k), u_i(t|k)) + \hat{w}_i(t|k), \tag{1.4b}$$

$$h_i^{\text{in}}(x_i(t|k), u_i(t|k)) \leq 0,\ t = 0, \ldots, N_p, \tag{1.4c}$$

$$h_i^{\text{eq}}(x_i(t|k), u_i(t|k)) = 0,\ t = 0, \ldots, N_p - 1, \tag{1.4d}$$

$$x_i(0|k) = x_i(k). \tag{1.4e}$$

The first element of the minimizer $\mathbf{u}_i^* \triangleq [u_i(0|k)^*, u_i(1|k)^*, \ldots, u_i(N_p-1|k)^*]$ is applied as input to the subsystem, and the problem is solved again at subsequent time steps in a receding horizon fashion.

Notice that, in absence of measures from the rest of the system, an estimate of the disturbance term (1.3) is employed in the solution of (1.4). For this reason, decentralized schemes generally require either assuming a priori bounds on the coupling between subsystems, or considering worst-case interactions, resulting in a loss of performance [1]. Communication between local controllers allows to achieve a visible enhancement in the overall control performance; however, it is difficult to synthesize a general result, due to the dependence on the particular scheme used [31, 32]. It is essential that the communication serves as a means to reach a shared consensus—an improvement over the decision that each agent would be able to make by relying merely on locally available information. Once the model partitioning is given, the control by means of a cooperative scheme requires to answer fundamental questions. We analyze some of them in the following.

How communication improves performance? According to the degree of *selfishness* of the objective function employed, two categories of controllers emerge in the distributed MPC literature: *noncooperative*, where the agents pursue a local objective, and *cooperative*, where the influence on the rest of the system, including how nonlocal objectives are affected, is taken into account in the choice of the inputs locally applied by each agent. More specifically, a global objective—consisting of a given (weighted) combination of individual objectives—is optimized over local inputs $\mathbf{u}_i$, $i \in \mathcal{N}$,

$$\min_{\mathbf{u}_i} J = \sum_{t=0}^{N_p-1} \ell(x_i(t|k), u_i(t|k), x_{-i}(t|k), u_{-i}(t|k)) + V(x_i(N_p|k), x_{-i}(N_p|k)), \quad (1.5)$$

subject to (1.4b)–(1.4e) (subscript '$-i$' designates all subsystems $j \in \mathcal{N} \setminus \{i\}$). Several techniques can be applied to obtain feedback about the values of nonlocal variables in (1.5): typically, controllers update these values over intermediate iterations, by direct exchange or through Lagrangian multipliers.

The importance of *cooperation* among MPC control agents is underlined in [8]: the exchange of information among subsystems provided with mutual interaction models does not constitute a sufficient guarantee for closed-loop stability, due to the *competition* arising from the pursuit of conflicting objectives. Similar conclusions are given by [33], showing that increased cooperation not always translates to a gain in performance; indeed, in some cases it may even lead to a performance loss. This emphasizes the importance of the criteria upon which the cooperation is based. In case that the interests of local controllers diverge from the global benefit, a reward scheme may be implemented at the supervisory layer in order to bring these interests as much in line as possible [13].

Who should communicate with whom? The control agents communicate through a data network whose topology can be described by means of the undirected graph $\mathcal{G} = (\mathcal{N}, \mathcal{E})$, where to each subsystem in $\mathcal{N}$ is assigned a node. Dependence of the optimal topology $\mathcal{E} \subseteq \mathcal{N} \times \mathcal{N}$ of the communication graph on the coupling between the local control problems is expected. The answer can be derived from a case-oriented evaluation of the performance deterioration due to the absence of communication between a given pair of local controllers. Control architectures for large-scale systems typically include a supervisory level, which may act as a coordinator to set the necessary information flows [13].

The sharing of information in a networked system can be represented through a *knowledge graph*, where each node stands for the model of a given subsystem, and the edges

indicate that the information about the models is available to the agents controlling the pointed nodes. The *connectivity* and the *degree distribution* of such graph can be interpreted in quantitative terms [34].
In [33], a graph representing the coupling between subsystems is updated at each time step by identifying the constraints that were active at the previous time step. Then, the cooperating sets are formed by those subsystems that are connected by a path in the graph. Further control-related studies, such as [35, 36], focus on the PageRank index, a variant of the eigenvector centrality measure, used to quantify the relevance of nodes from a coalition formation viewpoint.

What information should be available to each local agent? The answer to this problem depends on the coupling source and the type of distributed control strategy that is implemented. In general, the need for information exchange is inversely proportional to the coverage of the locally available information. In [37], the control is performed by means of a (global) linear feedback law. A continuous exchange of information is avoided by providing models of the coupled subsystems to each agent. In the interval between broadcasts, these models are used to predict a local estimate of the evolution of the neighbors' state. In [10] the effect of input coupling is viewed—on the grounds of the slow dynamics of the plant under study—as a constant disturbance along the prediction horizon, which is then estimated with a Kalman filter. Usual choices are the expected state and/or input sequences [38, 39], or auxiliary coordination variables such as prices [40] or sensitivities [41]. See also [42] for further details regarding the information exchange in different schemes.
Regardless of the knowledge of the global dynamics that may be available to each agent, the closed-loop behavior can range from stable and almost optimal, to unstable Nash equilibria if conflicting objectives are pursued. This sensible difference in performance is likely to be detected when dealing with strongly coupled subsystems [8].

How to deal with constrained communications? The system dynamics impose limits on the time available to make agreements over cooperative decisions. Limitations in bandwidth or in energy consumption, as well as communication delays or packet losses concerning the data link infrastructure, need to be taken into account. Some algorithms are more flexible than others in this regard, providing superior robustness to delays or failures in communication. For example, the strategy presented in [24] admits the injection of suboptimal control actions in order to relax the heavy communicational requirement typical of iterative distributed schemes. Through a hierarchical design, this same strategy has been later extended to allow the asynchronous update among different neighborhoods [5]. Another example of algorithms showing such properties can be found in [39], where the robust tube feedback formulation admits steps with no updates (by employing shifted input sequences).

1.1.3 Dynamic neighborhoods and coalitional control

The coupling among subsystems can be categorized over three classes. In presence of *dynamical coupling*, a subsystem's behavior may be influenced by the value of the state and/or input of some other subsystems. Output coupling is a particular case of state coupling. This class of coupling can be described as in (1.2)–(1.3). When the system is characterized by constraints involving multiple subsystems, the coupling is seen *through the constraints*. This wide class includes constraints on input and/or state variables (such as physical limits of the plant or common-pool resources), and constraints not involving physical limits but related with the objective functions of the subsystems (for example, limited benefit within a free market with limited demand). Such problems may be analyzed under a zero-sum games perspective. Notice that constraint-coupled subsystems are not necessarily dynamically coupled. In this case, constraints (1.4c)–(1.4e) take the form:

$$h^{\text{in}}(x,u) \leq 0, \quad h^{\text{eq}}(x,u) = 0, \tag{1.6}$$

where h^{in} and h^{eq} cannot be fully decomposed into independent equations $h_i^{\text{in}}(x_i,u_i)$, $h_i^{\text{eq}}(x_i,u_i)$, $i \in \mathcal{N}$.
Lastly, coupling can appear *through the objective function*: subsystems are part of a larger interacting environment and, therefore, it is likely that external variables exert some influence on their performance. These variables are usually related with the state of other subsystems, and often express economic indices. Notice that this category may overlap with the previous ones.

Broadly speaking, a *neighborhood* designates a group of agents whose control problems show appreciable coupling that can be sensed within a limited time delay. Although the coupling structure may be fixed for a given system, in most cases the effect of coupling fluctuates. At this point, a natural question is *what to do when coupling varies with time*? Is it reasonable to consider *time-varying neighborhoods*?

Some distributed control schemes in the literature have already moved in this direction. The notion of *cooperating sets* is employed in [33, 39]. Within any given cooperating set, one subsystem at each time step locally computes optimal control actions for all the subsystems involved in the set, even if only the results relative to that subsystem are broadcast. The rationale behind computing such "hypothetical" non-local control inputs is to optimize the individual strategy considering what others may be able to achieve, so that cooperation is indirectly promoted among the agents. The composition of such sets is updated according to a graph representing the active coupling constraints. Interestingly, the results of [33] show that the optimal cooperating set is not necessarily restricted to *directly* coupled subsystems.

In the distributed MPC scheme of [43], the cost incurred by each local controller is dynamically adjusted to fulfill minimum local requirements, on the basis of situational altruism criteria. On a similar line is the work of [44], where a flexible hierarchical MPC scheme is proposed for a hydro-power valley, where the priority of the agents in optimizing their control actions can be rearranged according to the different operational conditions.

The work of [10] investigates the design of a hierarchical control scheme characterized by some flexibility over the employ of the data network through which the local control agents exchange information. The application on an irrigation canal is considered as a case study. The design of an optimal communication topology and its associated set of decentralized feedback control laws can be posed as a mixed-integer problem. However, such formulation generally suffers from high computational complexity as the number of control nodes and the possible communication links between them grow. This issue is addressed through a two-layer greedy approach in [10], with the aim of optimizing the data links usage and decomposing the global MPC problem in small sized subproblems whenever possible. The goal of the supervisory layer is to find the best compromise between control performance and communication costs by actively modifying the network topology. The actions taken at the supervisory layer alter the control agents' knowledge of the complete system, and the set of agents with which they can communicate. Each group of linked subsystems constitutes a coalition, independently controlled on the basis of a decentralized MPC scheme managed at the bottom layer. This feature is particularly interesting for communication infrastructures based on battery-powered wireless communication devices. The properties of a multi-agent control scheme based on this same idea are discussed in [9], where the time-variant relevance of the communication within a set of dynamically coupled linear systems is analyzed using tools from cooperative game theory.

A different approach is found in [45], where the distributed MPC problem for dynamically-coupled subsystems is analyzed under a *dynamic bargaining game* perspective. The formulation follows a few recent proposals in which the classic (static) bargaining theory has been extended to dynamic decision environments (see references in [45]). These works focus on the *coalition as the objective of the bargaining*, as a means of implementing a coalition-wide solution (the same for all members). However, the application of the same control input by all the agents in a coalition is likely to provide poor performances—if not an infeasible strategy—in a controlled system. Filling this gap, the work of [45] provides a distributed MPC formulation where cooperation is subject to bargaining: an agent accepts to be part of a coalition only if a benefit is foreseen over the performance expected by acting independently. Guarantees for the satisfaction of a minimum individual performance are imposed by means of a *disagreement point*, defined as the threshold of maximum allowed loss of performance in case of cooperation. An agent's disagreement point is decreased whenever it decides to cooperate, and increased otherwise such as to foster a later participation; in this way, the disagreement point tends to the optimal expected value of the objective function.

The recent advances on ICT, particularly the spread of wireless networks and *cloud-based* applications, simplify the deployment of a communication infrastructure between local controllers. The use of a distributed database of systemwide measures to achieve a globally optimal, yet scalable, control is a promising line of research yet to be explored [1]. Nonetheless, when non-local information is critical for adequate global feedback, issues derived by privacy-concerned subsystems not inclined to share local models and/or state information need to be specifically addressed.

1.2 Coalitional MPC control

The distinct feature of such adaptive schemes, namely the rerouting of information flows among changing sets of controllers, can be schematized by the dynamical graph $\mathcal{G}(k) = (\mathcal{N}, \mathcal{E}(k))$, where the time dependence of $\mathcal{E}(k) \subseteq \mathcal{N} \times \mathcal{N}$ reflects the possibility to activate or shut down data links at any given time step k. A coalition is constituted by establishing flows of information—a broadened control feedback—within a given set of agents. The cooperation of the agents within a coalition can be carried out in different ways: the agents can exchange whichever information is required to enhance their performance by jointly solving the control problem—commonly state or output trajectories, or planned input sequences. The flow of such information from agent i to agent j is enabled by the activation of the associated link $l_{ij} = \{i, j\} \in \mathcal{E}$.

The description provided by $\mathcal{G}(k)$ delineates a partition $\mathcal{P}(\mathcal{N}, \mathcal{G}(k)) = \{\mathcal{C}_1, \dots, \mathcal{C}_{N_c}\}$ of the set of controllers into N_c connected components, referred to as coalitions [46].

Coalitions are disjoint sets such that [47]

$$\mathcal{C}_i \subseteq \mathcal{N}, \text{ for all } i \in \{1,\ldots,N_c\}, \text{ and } \bigcup_{i=1}^{N_c} \mathcal{C}_i = \mathcal{N}.$$

The number of coalitions N_c pertains to the interval $[1, |\mathcal{N}|]$, whose extremes correspond to the centralized control case (all the $|\mathcal{N}|$ subsystems connected) and the case where each subsystem "forms a coalition" on its own (all links disabled). The dynamics (1.2) of all subsystems relative to a given connected component $i \in \{1,\ldots,N_c\}$ can be aggregated as

$$\xi_i^+ = F_i(\xi_i, \nu_i) + \omega_i, \tag{1.7}$$

with $\xi_i \triangleq (x_j)_{j\in\mathcal{C}_i}$, $\nu_i \triangleq (u_j)_{j\in\mathcal{C}_i}$ the aggregate state and input vectors, and $F_i(\xi_i, \nu_i)$ the relative state transition function, describing the state and input coupling between members of the same coalition. Finally, the vector

$$\omega_i = (w_j')_{j\in\mathcal{C}_i} \tag{1.8a}$$

gathers the disturbances due to the coupling with subsystems external to $\mathcal{C}_i$. Following (1.3) it holds that

$$w_j' = \sum_r f_{jr}(x_r, u_r), \text{with } r \in \mathcal{M}_j \setminus \mathcal{C}_i, \tag{1.8b}$$

pointing out how, for each $j \in \mathcal{C}_i$, the set of unknown coupling from neighboring subsystems is reduced to the neighbors left out of the coalition. That is, from the coalition standpoint, the uncertainty comes from any subsystems $r \in (\bigcup_{j\in\mathcal{C}_i} \mathcal{M}_j) \setminus \mathcal{C}_i$. Notice that in case of singleton coalition, i.e., $\mathcal{C}_i \equiv \{i\}$, the description given by (1.7) coincides with (1.2).

1.2.1 Objective of coalitional control

In the remainder, we refer to the stage cost extended to $\mathcal{C}_i \subseteq \mathcal{N}$ as $\boldsymbol{\ell}_i(\xi_i, \nu_i)$. Although the most straightforward example would be $\boldsymbol{\ell}_i \equiv \sum_{j\in\mathcal{C}_i} \ell_j$, the coalitional stage cost can be formulated differently to exploit the added knowledge provided by cooperation. One such example is provided in 3.6. Local controllers aggregate into a coalition with the aim of coordinating the effort and achieving a better overall performance. At time k, a control sequence for all subsystems $j \in \mathcal{C}_i$ is derived by the joint solution of the

MPC problem

$$\min_{\boldsymbol{\nu}_i} \mathbf{J}_i = \sum_{t=0}^{N_p-1} \boldsymbol{\ell}_i(\xi_i(t|k), \nu_i(t|k)) + \mathbf{V}_i(\xi_i(N_p|k)) \tag{1.9a}$$

s.t.

$$\xi_i(t+1|k) = F_i(\xi_i(t|k), \nu_i(t|k)) + \hat{\omega}_i(t|k), \tag{1.9b}$$

$$H_i^{\text{in}}(\xi_i(t|k), \nu(t|k)) \leq 0,\ t = 0, \ldots, N_p, \tag{1.9c}$$

$$H_i^{\text{eq}}(\xi(t|k), \nu(t|k)) = 0,\ t = 0, \ldots, N_p - 1, \tag{1.9d}$$

$$\xi_i(0|k) = \xi_i(k), \tag{1.9e}$$

Problem (1.9) is solved independently for each coalition $\mathcal{C}_i \in \mathcal{P}(\mathcal{N}, \mathcal{G}(k))$. At time k the first element of $\boldsymbol{\nu}_i(k)^*$ is applied to every subsystem involved in the coalition. Given (3.1b) and (1.8b) we have $\left\|w_j'\right\| \leq \|w_j\|$ for $j \in \mathcal{C}_i$; in words, since the effect of unmodeled interactions on the dynamics of any subsystem is reduced by its participation in a coalition, an improvement of the associated performance index is expected. Broadly speaking, provided the agents cost functions are linked, a prerequisite of cooperation is that the aggregate cost of the agents participating in a coalition outperforms the cost that the agents would have achieved through noncooperative optimization, that is, $\mathbf{J}_i^* < \sum_{j \in \mathcal{C}_i} J_j^*$ must hold. In case the cost function expresses economical quantities, this translates in the availability of a surplus that can be split among the members of the coalition.

1.2.2 Cost of cooperation

Cooperation may not come for free. First, as previously discussed, communication may be constrained: a clear example is given by wireless networks, where the use of the links can be restricted in bandwidth/duration to reduce the energy consumption. In order to stimulate an optimal use of the network, it is reasonable to associate a cost to any communication (including those performed for the obtainment of measures). In some contexts, where privacy concerns are preponderant, the cost may also depend on the identities of the transmitter and the receiver: some agents may be less prone to exchange information than others. Besides, the coordination of a large number of agents can become a problem itself because the computation and communication requirements grow with the number of cooperating controllers involved. Therefore, costs required for the cooperation of a given set of agents can be taken into account by means of ad hoc indices related with the composition of the coalition or the data links needed in order to establish communication between every member of the coalition. Further measures may be employed to evaluate cooperation costs, based on, for example, the number of decision variables and/or constraints of the aggregate problem, reflecting the computational requirements. For coalition $\mathcal{C}_i$, cooperation costs can be expressed as a function $\chi_i(\xi_i, \nu_i, \mathcal{C}_i, \mathcal{E}_i(k))$, where $\mathcal{E}_i(k) \subseteq \mathcal{E}(k)$ is the subset of edges of the graph $\mathcal{G}(k)$ connecting the nodes in $\mathcal{C}_i$. Such cooperation costs can be assumed comparable with the stage cost. We can thus modify what stated at the beginning of the previous section in "local controllers aggregate into a coalition with the aim of coordinating the effort and *achieving the best tradeoff* between the performance and the associated cooperation costs".

1.2.3 Global control problem

The overall control problem can be stated as

$$\min_{\nu,\mathcal{E}} \sum_{i\in\mathcal{S}_{\mathcal{P}}} \mathbf{J}_i(\xi_i(k), \nu_i) + \mathbf{J}_i^{\chi}(\mathcal{E}) \tag{1.10a}$$

s.t.

$$\xi_i(t+1|k) = F_{ii}(\xi_i(t|k), \nu_i(t|k)) + \hat{\omega}_i(t|k), \tag{1.10b}$$

$$H_i^{\text{in}}(\xi_i(t|k), \nu(t|k)) \leq 0\, t = 0, \dots, N_p, \tag{1.10c}$$

$$H_i^{\text{eq}}(\xi(t|k), \nu(t|k)) = 0,\ t = 0, \dots, N_p - 1, \tag{1.10d}$$

$$\xi_i(0|k) = \xi_i(k), \tag{1.10e}$$

$$\mathcal{E}(t) \subseteq \mathcal{N} \times \mathcal{N},\ t = 0, \dots, N_p, \tag{1.10f}$$

$$\mathcal{E}(t) = \mathcal{E}(0),\ t = 1, \dots, N_p, \tag{1.10g}$$

where $\mathcal{S}_{\mathcal{P}} = \{1, \dots, N_c\}$, and

$$\mathbf{J}_i^{\chi}(\mathcal{E}) = \sum_{t=0}^{N_p} \chi_i(t|k). \tag{1.11}$$

Notice that, according to constraints (1.10f) and (1.10g), we assume the set of edges $\mathcal{E}$—hence the system partition $\mathcal{P}(\mathcal{N}, \mathcal{G})$—constant during the prediction horizon $t \in [k, k+N_p]$. Problem (1.10) constitutes a dynamic optimization with mixed integer variables, which is generally not practical to solve. Since any given $\mathcal{E}$ corresponds to a partition of the global system, the composition of the resulting coalitions' state and input vectors and matrices will implicitly depend on it. The choice of the network topology is made within a discrete set whose size grows exponentially with the number of subsystems.

1.2.4 A game theoretical perspective

The role and properties of coalitions in multi-agent interactive decision problems have been studied in game theory for decades. Great interest has been directed on the fair allocation of benefit among the members of a coalition. Despite the intrinsic computational complexity, which hinders its use in real-time applications, some pioneering works explored the use of coalitional game theory in engineering applications. Being natural fields for the application of game theoretic analyses, wireless networks [48], the smart grid [49, 14] and the recharge market for plug-in electric vehicles [50] have received particular attention so far.

Formation of coalitions of controllers

The control agents can decide with whom to cooperate and under which conditions (namely, the allocation of the payoffs derived from the cooperation). Such situation can be modeled as a coalitional game, uniquely defined by the pair $(\mathcal{N}, v)$, where $\mathcal{N}$ is the set of players and v is the *value* of a given coalition.

Coalition-formation games consider scenarios in which the network topology and the cost for cooperation play a major role, such that the formation of a coalition is not necessarily beneficial. The theory about coalition formation games focuses on issues like: *Which coalitions will form? What is the optimal coalition size? Which methodologies can be employed to study the properties of the resulting structures?*

Unlike the canonical form of coalitional games, where the fundamental assumption is that *cooperation always brings benefit*, in coalition-formation games gains are limited by the costs of forming a coalition. Thus, the value of the merger of two disjoint coalitions can be worse than the sum of the coalitions' separate values, that is, the *superadditivity* property does not hold. Consequently, the *grand coalition* (the coalition containing all the players) is seldom the optimal arrangement. Environmental changes—such as variations in the number, relevance, or constraints of the players—can affect their distribution over the coalitions. Coalition formation games can be classified in *static* and *dynamic*. In the first case the objective is to study the structure imposed on the coalitions by some external factor; the second category concerns the analysis of the formation of coalitions arising by the *interaction* between the agents. The properties of the resulting dynamical structure and its adaptability to the environment are object of the research on dynamic coalition formation games. A monograph on this field can be found in [51]. Unfortunately, the availability of formal rules and analytical concepts is mostly limited to games in canonical form.

Coalition formation involves three main steps. The first two are *(i)* generation of the coalition structure and *(ii)* solution of the optimization problem for each coalition [52, 53]. Coalition formation is commonly studied in the form of *characteristic function* games, where a value is assigned to any possible coalition $\mathcal{C} \subseteq \mathcal{N}$ through a function $v : 2^{\mathcal{N}} \rightarrow \mathbb{R}$. Given the graph $\mathcal{G} = (\mathcal{N}, \mathcal{E})$ describing the associations among the control nodes of the system, the value of a coalition structure $\mathcal{P}(\mathcal{N}, \mathcal{G}) \equiv \{\mathcal{C}_1, \mathcal{C}_2, \ldots, \mathcal{C}_{N_c}\}$ is defined as its aggregate value

$$\mathcal{V}(\mathcal{P}) = \sum_{i \in \mathcal{S}_{\mathcal{P}}} v(\mathcal{C}_i), \tag{1.12}$$

where $\mathcal{S}_{\mathcal{P}} = \{1, \ldots, N_c\}$. The optimal coalition structure $\mathcal{P}^*$ is the one characterized by the highest value $\mathcal{V}^*$. However, the problem of finding the optimal coalition structure has been demonstrated to be NP-complete [52]. To overcome this issue, several solutions—resorting to heuristics, dynamic-programming, branch-and-bound algorithms—have been proposed in the literature (see [53, 9] and references therein). Particularly interesting for control applications is the analogy first proposed in [9] between (1.12) and (1.10), which serves as the foundation for a hierarchical scheme that manipulates the global controller structure (by decentralizing the feedback law over coalitions of local controllers) with regard to both the current state of the system and the communication cost. A similar architecture has been employed in the work of [10].

In characteristic form games, the value of a given coalition depends only on its members, with no regard to how the rest of the agents are organized. Such model does not apply to the vast majority of real life applications. Indeed, although games in characteristic form provide a means of modeling a wide spectrum of scenarios, it is natural in engineering applications to encounter problems in which the value of a given coalition cannot be determined regardless of how the rest of the agents are organized. Games in *partition form* can model this type of problems [54]. In these games, given a partition $\mathcal{P} = \{\mathcal{C}_1, \ldots, \mathcal{C}_l\}$ of $\mathcal{N}$, the value of any coalition $\mathcal{C}_i \in \mathcal{P}$ is expressed as $v(\mathcal{C}_i, \mathcal{P})$. However, it is not possible to derive a general closed-form allocation in the considered setting. Nevertheless, in some cases the partition function game can be approximated as a characteristic function game by assigning values to coalitions following an heuristic approach: for example, if a minmax approach is employed, the value of a given coalition will take into account the most unfavorable externalities produced by any coalitional setup of the rest of agents.

Particularly interesting when global objectives do not take over local ones, the third and final step consists in the *(iii)* distribution of the value of a coalition among its members. The *payoff* ϕ_i is the utility received by each agent $i \in \mathcal{C}$ by the division of $v(\mathcal{C})$; the vector of payoffs assigned to all the agents is referred to as the *allocation*. A variety of payoff rules have been proposed in the cooperative game theory, such as the *core* or the Shapley and Banzhaf values [55]. Of course, this third step is only possible if the real value $v(\mathcal{C})$ associated with coalition $\mathcal{C} \subseteq \mathcal{N}$ can be divided and transferred among its members (for instance, in the form of side-payments used to attract players). Let us define $\mathbf{J}_i^{(j)}$ as the quota relative to agent $j \in \mathcal{C}_i$ in the coalition cost (1.9a). Notice that the solution of (1.9) does not imply any relation between the cost J_j^* achievable *independently* by any $j \in \mathcal{C}_i$, and the cost $\mathbf{J}_i^{*(j)}$ incurred through its participation in the coalition. Provided a surplus is available, there exists a payoff assignment function such that $\mathbf{J}_i^{*(j)} \leq J_j^*$ is fulfilled for all $j \in \mathcal{C}_i$. As first pointed out in [56], the payoff allocation concepts developed for canonical games do not admit a straightforward implementation in presence of a coalitional structure different from the grand coalition. In the same work, the definitions of the core, the Shapley value and the *nucleolus* were extended to static coalition formation games, by redefining the *group rationality* concept with that analogous of *relative efficiency*. However, the results clearly showed that the complexity of the problem grows noticeably when dynamic coalition formation is considered, especially when the solution has to be computed in a distributed manner [48]. This fact motivates the application-oriented solutions found in the recent literature, such as [57, 51].

The essential steps of a coalitional control algorithm are summarized in Table 1.1. To handle the combinatorial explosion problem, Steps *3a* and *3b* can be executed at a lower rate as in [9]. Prior to the application of any change in the topology, theoretical properties such as stability or robustness can be checked [58, 59]. Once the structure of the coalitions is defined, local controllers belonging to a same coalition exchange information to calculate the control actions using a distributed control scheme [42].

Table 1.1: Steps of a coalitional control algorithm.

Step	Level	Function
1	Local	Measure the state $x_i(k)$.
2	Local	Evaluate performance J_i.
3a (*Top-down*)	Global	Supervisory layer gathers information of the controllers' performance and evaluates alternative network topologies. Changes in the topology are allowed only if the theoretical properties of interest (for example, stability) are retained after the switching.
3a (*Bottom-up*)	Coalition + neighbors	Collect information of the controllers involved in the coalition and its neighbors and decide whether to enable or disable links. Changes are allowed only if properties of interest are retained.
3b	Coalition	Update the information about the structure and members of the coalition.
4	Coalition	Exchange information with the rest of the members of the coalition and calculate the control actions $\nu_i(k)$. No communication takes place with other coalitions.
5	Local	Implement $u_i(k)$. Go to step 1.

1.3 Contributions of the thesis

An aspect so far rarely contemplated in distributed control problems is the explicit consideration of individual (local) interests of the components of a complex system [60]. Indeed, the focus of the majority of the literature about distributed control has been the overall system performance. While on one hand this permitted to address fundamental properties of centralized control, such as system-wide optimality and stability, one the other hand it implied assuming unrestricted cooperation across local controllers. However, when dealing with multi-agent systems with a strong heterogeneous character, cooperation between the agents cannot be taken for granted (due to, for example, logistics, market competition), and selfish interests may not be neglected. Another critical point that must be kept into consideration is the *diversity* characterizing systems of systems (SoS), yielding very complex interactions between the agents involved (one example of such system is the smart grid).

In order to tackle such inherent aspects of SoS, the research presented in this thesis has been concerned with the development of a novel framework, the *coalitional control*, that extends the scope of advanced control methods (in particular MPC) by drawing concepts from cooperative game theory that are suited for the inherent heterogeneity of SoS, providing as well an economical interpretation useful to explicitly take into account local selfish interests. Thus, coalitional control aims at governing the association/dissociation dynamics of the agents controlling the system, according to the expected benefits of their possible cooperation. From a control theoretical perspective, this framework is founded on the theory of switched systems and variable structure/topology networked systems, topics that are recently experiencing a renewed interest within the community. The main concepts and challenges in coalitional control, and the links with cooperative network game theory have been presented in [61], tracing a path from model partitioning to the control schemes whose principles delineate the idea of coalitional control. The work of this thesis focused on two basic architectures: a hierarchically supervised evolution of the coalitional structure [10], and a protocol for autonomous negotiation between the agents, with specific mechanisms for benefit redistribution, leading to the emergence of cooperating clusters [62].

The application of the hierarchical coalitional control architecture to an irrigation canal case study has been presented in [63, 10, 64]. Like most public infrastructures, water networks are geographically disperse systems, whose management requires a trade-off among sectors in direct competition (agricultural, municipal, and industrial), and whose different parts are often owned by independent entities. Permanent communication between the various control stations is impractical. Considering all these factors, the study focused on the design of an MPC control scheme featuring flexible structure. The approach relied on partitioning the global control law amongst a number of local control *agents*, a common starting point in distributed architectures. The aim was to adapt the partitioning to the varying coupling conditions between different parts of the system, in an online fashion, promoting cooperation among clusters of control nodes when clear benefits in the performance were foreseen. A two-layer architecture was developed, where the information flow is manipulated by disconnecting data links that do not yield a significant improvement of the control performance, compared with their relative cost of use. This feature is particularly interesting, for example, whenever battery-powered devices are used for decentralized sensing and control, or when such tasks are delegated to human-in-the-loop interventions. As a result, the system is partitioned into *coalitions* working in a decentralized fashion. The work was validated on a detailed model of a 45 km section of the Dez irrigation canal, implemented on the hydrodynamic simulator SOBEK [10].

While in [10] the cooperation in the achievement of the global objective is not questioned, in [65, 62] it is assumed instead that the agents controlling the system base their cooperation on the individual rationality criterion: they will be willing to cooperate only if the expected individual benefit derived through cooperation exceeds the one achieved through noncooperative control. Such individual rationality concerns have been addressed in an autonomous coalition formation framework, where coalitions are the outcome of an pairwise bargaining procedure, through which the structure of each agent's controller is adapted to the time-variant coupling conditions. Furthermore, the distribution of the value of a given coalition among its components is addressed in [62] by means of an iterative utility transfer scheme that compensates the dissatisfaction of subset of members with respect to their currently assigned payoff. Such method guarantees coalition-wise stability, provided that the set of stable allocations of the associated transferable-utility (TU) game is nonempty.

The last part of the thesis shows the application of coalitional control for the management of fast charging stations for plug-in electric vehicles (EV). Pricing strategies have been studied considering an open market scenario (analogous to common gas stations), with offers by several competing parties (charging managers). In such a scenario, the prices serve as incentive for EV drivers to deviate from their ideal route and seek for the best battery recharging alternative. The coalitional control framework has been employed to improve the performance of the charging managers on the market, by joint strategy planning and subsequent benefit redistribution [66].

1.4 Thesis outline

The thesis is organized in five chapters. After the introductory research outline presented before, chapters are described as follows.

- Chapter 2 addresses the hierarchical supervision of the cooperation structure among the agents of the system. A two-layer coalitional control architecture is presented: the cooperation structure is manipulated at the top layer according to given collective objectives, whereas the bottom layer handles the real-time control tasks, decentralized into the coalitions arising from the chosen cooperation structure. The discussion is directed on two case studies. The first regards the management of water distribution infrastructures, where the objectives of the local control agents align with those of the whole system. Coalitions are implemented as a means to change the cooperation topology to best fulfill an overall efficiency objective. The second illustrates a smart grid scenario involving a set of prosumers connected to the main grid and equipped with local generation and storage devices. Prosumers can establish a local energy market running in accordance to the coalitional control scheme, pursuing the minimization of the cost of buying energy from the main grid while minimizing losses due to transfers over the distribution lines. In this case, the prosumers are decoupled agents with autonomous objectives: therefore, the cooperation here aims at the energy loss reduction (collective goal) and at the maximization of individual economic objectives.

- In Chapter 3, the assumption of the availability of an omniscient supervisor is dropped. A protocol for autonomous negotiation between the agents is introduced, based on pairwise bargaining over coalition formation. This protocol provides a specific method for benefit redistribution, to specifically address individual rationality (agents cooperate only if the expected individual benefit derived through cooperation exceeds the one achieved through noncooperative control). This method consists in an iterative utility transfer scheme that compensates the dissatisfaction of subset of members with respect to their assigned payoff. Coalition-wise stability is subject to the nonemptiness of the set of stable allocations of the associated transferable-utility (TU) game. A wide-area control application for power grid, with the objective of minimizing frequency deviations and undesired inter-area power transfers, has been considered to demonstrate this second architecture.

- Chapter 4 shows the application of coalitional control for the management of fast charging stations for plug-in electric vehicles (EV). The use of coalitional control as a means to improve the performance of the charging managers on the market is shown. By modeling the interaction of charging managers in an open market scenario as a coalitional game, joint strategy planning and subsequent benefit redistribution are evaluated. Pricing strategies are optimized in order to incentivize EV drivers to deviate from their ideal route and seek for the best battery recharging alternative.

- The thesis is finally concluded in Chapter 5 by an overview of the results with last remarks about future developments and reserch challenges.

Chapter 2

Supervised coalition structure generation

2.1 Introduction

Often different parts of a networked system are owned and managed by independent entities (think about infrastructures), unwilling to coordinate their action unless strictly necessary. In addition, permanent communication across the entire system network can be impractical. Consequently, even when the whole system is owned and managed by a single entity, the use of a traditional centralized control approach is hampered. This motivates the two-layer hierarchical control scheme presented in this chapter. The basic setting, introduced in Chapter 1.1, is reported here for the linearized case specifically employed for the controller design. The proposed algorithm is an approximation of the global problem (1.10) formulated in Section 1.2.3, for the generation of the optimal coalitional structure according to (1.12).

The main goal of the supervisory layer is to find the best compromise between control performance and coordination effort by actively modifying the cooperation topology. The actions taken at the supervisory layer alter the control agents' knowledge of the complete system, and the set of agents with which each one of them can communicate. Each group of linked subsystems—a *coalition*—is independently controlled following a decentralized MPC scheme, constituting the bottom layer of the architecture [10].

The basic idea is to partition the centralized problem over a given number of local controllers or *agents* (see, e.g., [6]). The presence of a supervisor makes possible the global design of a feedback control law, that may be structured in accordance to any given partition. By a global design, the satisfaction of certain global properties can be guaranteed. Given such a feedback law, the cooperation of the agents can be realized in two ways: *(i)* it can turn into an explicit exchange of local information (such as interaction models, state measures, etc.) for the joint optimization of future input sequences, or *(ii)* it can remain at the implicit level dictated by the globally-designed control law.

A multi-agent control scheme based on the same basic idea is discussed in [9], where a design method with closed-loop stability guarantees is provided. The optimization of the data network topology, through which the agents establish cooperation links, is regarded as a cooperative game in order to study the relevance of the different links and agents (in view, e.g., of fault-tolerant policies) From this game-theoretical perspective, the sequence of optimal network topologies is interpreted as a set of coalitions of links that evolve in order to optimize the trajectory of the closed-loop system.

Among other related works is [33], addressing the formation of groups of cooperative agents according to the coupling constraints that are active at a given time. [19] describes a hierarchical framework where information is exchanged at each time step within clusters of strongly dynamically coupled subsystems, while a slower communication rate is required between different clusters. In [67], the complexity of the MPC control problem of the Barcelona drinking water network is reduced by means of a partitioning algorithm, controlling the resulting subnetworks in a hierarchical-distributed manner. In [44] a flexible hierarchical MPC scheme is proposed for a hydro-power valley, where the priority of the agents in optimizing their control actions can be rearranged according to the different operational conditions.

The scheme presented here focuses on how the coupling between subsystems varies with time [10, 61]. A cost on the coordination effort is considered according to several possible criteria, such as the data link usage, the total number of agents involved in the coalition, the number of decision variables and/or constraints of the aggregate problem, reflecting the computational requirements [65], etc. In this way, the overall structure of the controller evolves by trading off performance for savings on coordination costs. As a result, coordination between agents is promoted whenever the undesired effect of dynamic interaction between coupled subsystems (or the benefit of cooperative trajectory planning in case of uncoupled systems) exceeds the threshold dictated by the allowed cooperation costs.

2.2 System description

2.2.1 Model

Consider a set $\mathcal{N} = \{1, \ldots, N\}$ of interconnected systems. The dynamics of any subsystem $i \in \mathcal{N}$ are described by the linear model:

$$x_i(k+1) = A_{ii}x_i(k) + B_{ii}u_i(k) + D_i w_i(k), \tag{2.1a}$$

$$w_i(k) = \sum_{j \in \mathcal{M}_i} A_{ij}x_j(k) + B_{ij}u_j(k), \tag{2.1b}$$

where $x_i \in \mathbb{R}^{n_i}$ and $u_i \in \mathbb{R}^{q_i}$ are the state and input vectors respectively, and $w_i \in \mathbb{R}^{m_i}$ describes the influence on x_i of the neighbors' states and inputs. In (2.1b), $x_j \in \mathbb{R}^{n_j}$ and $u_j \in \mathbb{R}^{q_j}$ are the state and input vectors of each neighbor $j \in \mathcal{M}_i$ of subsystem i. The neighborhood set $\mathcal{M}_i$ is defined as:

$$\mathcal{M}_i = \{j \in \mathcal{N} | A_{ij} \neq \mathbf{0} \vee B_{ij} \neq \mathbf{0}, j \neq i\}, \tag{2.2}$$

i.e., it contains all the subsystems $j \neq i$ whose state and/or input produce some effect on the dynamics of subsystem i.

2.2.2 Exchange of information

The set of controllers can communicate through a network infrastructure described by the undirected graph $\mathcal{G}(k) = (\mathcal{N}, \mathcal{E}(k))$, where to each subsystem in $\mathcal{N}$ is assigned a node, and $\mathcal{E}(k) \subseteq \mathcal{N} \times \mathcal{N}$ is the set of edges. The time dependency of $\mathcal{E}(k)$ reflects the possibility to establish cooperation links at any given time step k. The description provided by $\mathcal{G}(k)$ delineates a partition $\mathcal{P}(\mathcal{N}, \mathcal{G}(k)) = \{\mathcal{C}_1, \ldots, \mathcal{C}_{N_c}\}$ of the the set of control agents into N_c connected components. As agents within the same communication component will benefit from cooperation—sharing information in order to aggregate their control tasks—we will refer to such components as coalitions, and the partition resulting by a given network topology $\mathcal{E}(k)$ will be denoted as $\mathcal{P}(\mathcal{N}, \mathcal{G}(k)) = \{\mathcal{C}_1, \mathcal{C}_2, \ldots, \mathcal{C}_{N_c}\}$. The set of indices $\mathcal{S}_{\mathcal{P}} = \{1, \ldots, N_c\}$ is defined as well.

2.2.3 Coalition dynamics

In order to describe the dynamics of each coalition $\mathcal{C}_i \in \mathcal{P}$, the following extension of (2.1a) holds:

$$\xi_i(k+1) = \mathbf{A}_{ii}\xi_i(k) + \mathbf{B}_{ii}\nu_i(k) + \mathbf{D}_i\omega_i(k), \tag{2.3}$$

where ξ_i and ν_i are respectively the state and input vectors of coalition $\mathcal{C}_i$, composed by stacking the vectors of all the subsystems in the coalition:

$$\xi_i = (x_j)_{j \in \mathcal{C}_i}, \quad \upsilon_i = (j_s)_{j \in \mathcal{C}_i}, \, i \in \mathcal{S}_{\mathcal{P}},$$

As an extension of (2.1b), ω_i expresses the influence on ξ_i of subsystems external to the coalition $\mathcal{C}_i$:

$$\omega_i = (w'_j)_{j \in \mathcal{C}_i}, \tag{2.4c}$$

where (2.4d) replaces (2.1b), since, for each $j \in \mathcal{C}_i$, the unknown coupling is that relative to the neighbors left out of the coalition:

$$w'_j = \sum_r A_{jr} x_r(k) + B_{jr} u_r(k), \text{ with } r \in \mathcal{M}_j \setminus (\mathcal{C}_i \cap \mathcal{M}_j)\,. \tag{2.4d}$$

That is, from the coalition standpoint, the uncertainty comes from any subsystems $r \in (\bigcup_{j \in \mathcal{C}_i} \mathcal{M}_j) \setminus \mathcal{C}_i$. Matrices $\mathbf{A}_{ii}$, $\mathbf{A}_{ij}$, $\mathbf{B}_{ii}$, $\mathbf{B}_{ij}$ and $\mathbf{D}_i$ are arranged in order to match the composition of the state and input vectors.[1]

2.3 Control objective

We assume in the remainder that the objective of the controller is to drive the system's state toward the origin of the state space. The performance of the controller in this task is measured by the MPC cost function

$$J = \sum_{t=0}^{N_p-1} \sum_{i \in \mathcal{S}_{\mathcal{P}}} \Big(\xi_i^{\intercal}(t|k) \mathbf{Q}_i \xi_i(t|k) + \nu_i^{\intercal}(t|k) \mathbf{R}_i \nu_i(t|k) + \xi_i^{\intercal}(N_p|k) \mathbf{P}_i \xi_i(N_p|k) \Big), \tag{2.5}$$

where $\mathbf{Q}_i \geq 0$, $\mathbf{R}_i > 0$ and $\mathbf{P}_i = \mathbf{P}_i^{\intercal} > 0$ are constant weighting matrices. Costs required for the cooperation of the coalition members are taken into account by means of ad hoc indices related with the composition of the coalition or the number of data links needed to share the feedback information. For coalition $\mathcal{C}_i$, cooperation costs are expressed as a function $\chi_i(\mathcal{C}_i, \mathcal{E}_i)$, where $\mathcal{E}_i \subseteq \mathcal{E}$ is the subset of edges of the graph $\mathcal{G} = (\mathcal{N}, \mathcal{E})$ connecting the nodes in $\mathcal{C}_i$. Such cooperation costs are assumed comparable with the cost (2.5). Hence, the optimal cooperation structure for the system at a given time step k, together with its associated global input, is obtained by the supervisor as

[1] In case of singleton coalition, i.e., $\mathcal{C} \equiv \{i\}$, the description given by (2.3) coincides with (2.1).

the solution of the following problem:

$$\min_{\boldsymbol{\nu},\mathcal{E}} J = \sum_{t=0}^{N_p-1} \sum_{i \in \mathcal{S}_\mathcal{P}} \Big(\xi_i^\intercal(t|k)\mathbf{Q}_i\xi_i(t|k) + \nu_i^\intercal(t|k)\mathbf{R}_i\nu_i(t|k) + \xi_i^\intercal(N_p|k)\mathbf{P}_i\xi_i(N_p|k)\Big) + \chi_i(\mathcal{C}_i, \mathcal{E}_i(k)) \tag{2.6a}$$

s.t.

$$\xi_i(t+1|k) = \mathbf{A}_{ii}\xi_i(t|k) + \mathbf{B}_{ii}\nu_i(t|k) + \mathbf{D}_i\omega_i(t|k), \tag{2.6b}$$

$$\xi_i(t|k) \in \Xi_i,\ t = 0, \dots, N_p, \tag{2.6c}$$

$$\nu_i(t|k) \in \Psi_i,\ t = 0, \dots, N_p - 1, \tag{2.6d}$$

$$\xi_i(0|k) = \xi_i(k), \tag{2.6e}$$

$$\omega_i(t|k) = \hat{\omega}_i(k+t),\ t = 0, \dots, N_p - 1, \tag{2.6f}$$

$$\mathcal{E}(t) \subseteq \mathcal{N} \times \mathcal{N},\ t = 0, \dots, N_p, \tag{2.6g}$$

where $\Xi_i = \mathcal{X}_1 \times \mathcal{X}_2 \times \dots \mathcal{X}_{N_i}$ is the Cartesian product of the local state constraints relative to each member of the coalition (an analogous definition holds for the input constraint set Ψ_i). Since any topology corresponds to a partition of the global system, the composition of the resulting coalitions' state and input vectors and matrices will implicitly depend on $\mathcal{E}$. The choice of the network topology is made within a discrete set whose size grows exponentially with the number of subsystems. As already mentioned in Section 1.2.3, Problem (2.6) constitutes a dynamic optimization problem with mixed integer variables (MINQP). Moreover, the predition model (2.6b) requires the knowledge of (2.4c), describing the effect of possible coupling between subsystems belonging to different coalitions. As previously motivated, one of the goals here is to avoid such communication requirement. Next, we present a hierarchical multi-agent control algorithm with lower computational and communicational requirements, though a suboptimal solution is provided.

2.4 The control algorithm

The architecture of the proposed approximation of Problem (2.6) is organized over two layers: the *top layer* takes charge of the choice of the network mode, whereas the *bottom layer* handles the estimation and the real-time control tasks. At the bottom layer, the control is decentralized into the coalitions arising from the optimal—according to (2.6)—partition $\mathcal{S}_\mathcal{P}^*$. With the term *decentralized* we designate the absence of communication among different coalitions; agents within a coalition share their information at each sample time. Coalitions still communicate with the supervisor whenever required for the choice of a new topology. As a consequence, the term ω_i in (2.6b), modeling the effect of neighboring coalitions, cannot be computed through (2.4c) and (2.4d), and coalitions may need to use an estimate $\hat{\omega}_i$. Issues related with such estimation are case-related. For instance, as shown in the example in Section 2.5, inter-coalition coupling can be viewed as a constant perturbation (so that suitable estimation techniques can be used) if it shows relatively slow dynamics and transient phenomena can be neglected. Next, details are given about the operation of the top layer.

The discrete part of Problem (2.6) regards the choice of the optimal controller topology. This constitutes the most computationally demanding part of the problem. For this reason it is handled at the top layer, and its solution can be computed on a coarser time frame (w.r.t. the sample time T_s required for the low-level control of the system), maintaining the resulting topology during the subsequent interval $T_{\mathcal{E}} \geq T_s$. In order to select the most appropriate global control structure, several network topologies are compared. Let $\mathfrak{E}^+ = \{\mathcal{E}_1, \mathcal{E}_2, \ldots, \mathcal{E}_{N_\mathcal{E}}\}$ be the set of candidate topologies. These are evaluated through the function $J : \mathbb{R}^n \times (\mathcal{N} \times \mathcal{N}) \mapsto \mathbb{R}$ defined as follows [9]:

$$J(\xi, \mathcal{E}) = \sum_{i \in \mathcal{S}_\mathcal{P}} \xi_i^\intercal \mathbf{P}_i \xi_i + T_\mathcal{E} \chi_i(\mathcal{C}_i), \tag{2.7}$$

for each $\mathcal{E} \in \mathfrak{E}^+$. $\mathbf{P}_i = \mathbf{P}_i^\intercal > 0$, derived as the solution of (2.8) described in the following, and $\chi_i(coal_i)$ expresses the cost of coordinating the members of $\mathcal{C}_i$, considered over the interval $T_\mathcal{E}$. In the following, It is not pragmatic to see $\mathfrak{E}^+$ as the set containing every possible configuration of links. Because the number of all possible topologies grows exponentially with the number of subsystems, the set $\mathfrak{E}^+$ should be defined as a reasonably sized set of *relevant* topologies for the system to be controlled. The composition of $\mathfrak{E}^+$ may either be static or evolving in relation with, e.g., the current state of the system, the network constraints, or the willingness to cooperate among the agents. Of all the configurations considered at a given moment, the one providing the minimum value of (2.7), denoted as $\mathcal{E}^* \in \mathfrak{E}^+$, is applied during the subsequent interval $T_\mathcal{E}$.

According to any given topology $\mathcal{E}$, the set of agents is partitioned into a given set of coalitions $\mathcal{P}(\mathcal{N}, \mathcal{G}(k)) = \{\mathcal{C}_1, \mathcal{C}_2, \ldots, \mathcal{C}_{N_c}\}$. To attain the optimal performance objective (2.5), a feedback gain $\mathbb{K}$ for the whole system is computed at the top layer. In conformity with the partition $\mathcal{P}(\mathcal{N}, \mathcal{G}(k))$, $\mathbb{K}$ will be composed of a set of decentralized feedback gains, each one associated to a coalition, i.e., $\mathbb{K} = \text{diag}(\mathbf{K}_1, \ldots, \mathbf{K}_{N_c})$.[2] Given

[2]For the grand coalition, the feedback law $\mathbb{K}$ will coincide with the LQR gain.

the block-diagonal matrix $\mathbb{P} = \operatorname{diag}(\mathbf{P}_1, \ldots, \mathbf{P}_{N_c}) > 0$, consider the Lyapunov function $V(\xi) = \xi^\intercal \mathbb{P} \xi$, where $\xi \triangleq (\xi_i)_{i \in \mathcal{S}_\mathcal{P}}$ is the global state vector, permuted according to the partition $\mathcal{P}$. $V(\xi)$ will constitute an upper bound of the infinite-horizon performance objective if the constraints of the following LMI problem are satisfied (see, e.g., [68]):

$$\max_{\mathbb{K},\mathbb{P}} \mathbf{Tr}\, \mathbb{P}^{-1} \tag{2.8a}$$

s.t.

$$\mathbb{P} = \mathbb{P}^\intercal > 0, \tag{2.8b}$$

$$(\mathbf{A} + \mathbf{B}\mathbb{K})^\intercal \mathbb{P} (\mathbf{A} + \mathbf{B}\mathbb{K}) - \mathbb{P} \leq -\mathbf{Q} - \mathbb{K}^\intercal \mathbf{R} \mathbb{K}, \tag{2.8c}$$

where $\mathbf{A}$ and $\mathbf{B}$ are respectively the global state and input matrices, rearranged to match ξ and $\nu \triangleq (\nu_i)_{i \in \mathcal{S}_\mathcal{P}}$. Similarly, $\mathbf{Q} = \operatorname{diag}(\mathbf{Q}_i)_{i \in \mathcal{S}_\mathcal{P}} \geq 0$ and $\mathbf{R} = \operatorname{diag}(\mathbf{R}_i)_{i \in \mathcal{S}_\mathcal{P}} > 0$ are the global weighting matrices.

By the solution of (2.8), a set of feedback control laws $\nu_i = \mathbf{K}_i \xi_i$ that minimize $V(\xi)$ is obtained for all $\mathcal{C}_i \in \mathcal{P}$, along with the set of associated matrices $\{\mathbf{P}_i\}_{i \in \mathcal{S}_\mathcal{P}}$. These matrices are then used at the bottom layer in the formulation of the "local" MPC controller associated to each coalition. The set of matrices $\{\mathbf{P}_i\}_{i \in \mathcal{S}_\mathcal{P}}$ is used to determine the cost-to-go associated to a given topology in the computation of (2.7).

Remark 2.1. *The evaluation of different network topologies is independent and can be executed in parallel on a multi-processor platform. Also, the set of control laws associated with any network topology can be stored and reused whenever the same topology is considered again, without the need of solving more than once the relative LMI problem.*

Next, two study cases are used to illustrate the deployment of a top-down coalitional architecture. The first one is an irrigation canal application (Section 2.5), where the objective is to keep at a minimum the need for information exchange between sensors and actuators located at different reaches. The second case study regards the formation of coalitions among prosumers in a power microgrid (Section 2.6): there the objective is to enable local energy transfers, allowing the grid users to access energy at more competitive prices. From the grid operator's standpoint, such a scheme allows to prioritize the satisfaction of demand with locally available resources, thus reducing long-distance transfer losses over the distribution lines.

2.5 Illustrative case I: Coalitional MPC control of an irrigation canal

This case study addresses water management in irrigation canals, a demanding task which entails finding the right trade-off among different sectors in direct competition (agricultural, municipal, and industrial) [10]. Since irrigated agriculture constitutes the largest consumer of freshwater resources, the modernization of canal operation management can drastically improve water conservation efficiency and supply flexibility. Moving in this direction, several advanced control strategies have been proposed over the last decades (see, e.g., the survey [69] and references therein). In [70], an optimal quadratic criteria is used to adjust the parameters of downstream level feedback controllers. Different classes of controllers are considered, ranging from proportional-integral (PI) controllers at each gate to centralized control. The improvement derived from the communication of control actions among neighboring pools is also investigated. In [71], the effectiveness of model predictive control in water systems is studied and compared to classical feedback and feedforward strategies.

Among several challenging aspects regarding irrigation systems, geographical distance is one of the most interesting. Water networks are generally very disperse, and often different parts of the system are owned by independent entities, expectedly unwilling to coordinate their control actions unless strictly necessary. Moreover, permanent communication between the various parts of the network can be impractical. Consequently, the traditional centralized control approach is hampered, even when the water network is owned and managed by a single entity. All these factors considered, distributed control schemes can provide satisfactory solutions to the problem. Thus, irrigation canals have become a popular benchmark to assess the performance of hierarchical and distributed control schemes.

A survey of centralized and distributed MPC schemes for water systems is provided in [72]. Moreover, the control of an irrigation canal by means of a distributed MPC scheme based on an augmented Lagrangian formulation is investigated therein. The work of [73] describes a receding-horizon optimal control problem for heterogeneous irrigation systems, where the costs associated to water pumping and water losses and the profits from power generation are considered. To reduce the computational complexity and to conform to the system topology, the problem is decomposed following an augmented Lagrangian formulation. A two-layer control scheme is proposed in [74], where the top layer follows a risk management strategy to cope with unexpected changes in the demand, failures or additional maintenance costs, and the bottom layer optimizes

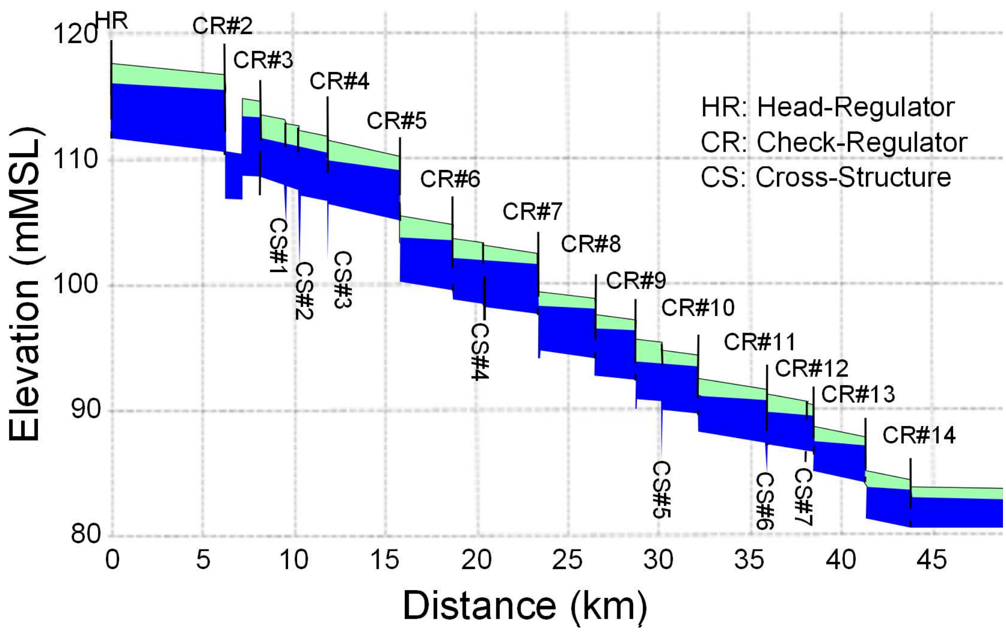

Figure 2.1: Longitudinal layout of the first 44 km of the west main canal of the Dez irrigation network.

the values of water flows by means of a distributed MPC technique. A section of an irrigation canal located in Spain is considered as case study.

Here we consider the control of water levels in a 44 km section (corresponding to 13 pools) of the west main Dez irrigation. Its longitudinal profile is shown in Figure 2.1. Located in the south-west of Iran, near the city of Dezful, the Dez canal was designed for the conveyance of irrigation water from a large dam on the Dez river to the irrigated areas in the north of Khuzestan province. Constraints on both states and inputs are considered, and local Kalman filters are used to estimate the dynamic coupling between different coalitions, viewed as perturbations. The top-down coalitional control scheme is tested on a detailed model of canal, implemented on the SOBEK hydrodynamic simulator [75]. The results are compared to those obtained using a centralized MPC controller.

2.5.1 Modeling the canal

Following the work of [71], where the implementation of model-based control techniques on water systems has been examined, a discrete-time linear approximation of the dynamics of the irrigation canal—namely the integrator-delay (ID) model [76]—is considered here. The ID model [76] is commonly adopted in studies regarding the application of advanced control strategies on water systems (e.g., [72, 77, 78, 79]) where a

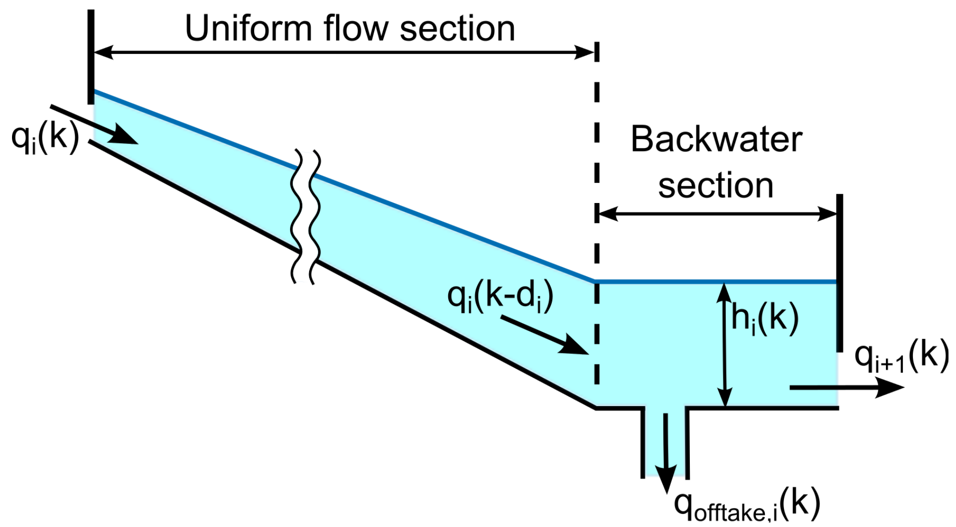

Figure 2.2: Simplified profile of a reach. The inflow $q_i(k)$ crosses the uniform flow section in a time d_i. The flow $q_i(k-d_i)$ enters the backwater section inducing a change in the water level $h_i(k)$. The water demand is $q_{\text{offtake},i}(k)$, while $q_{i+1}(k)$ is the flow passing to the downstream reach.

minimal order characterization of the response is critical for limiting the computational complexity. According to this model, each canal reach is characterized as a transport delay (uniform flow section) in series with an integrator (backwater section), where the water accumulates maintaining an almost horizontal surface [80]. The scheme in Figure 2.2 illustrates this idea. A change Δq_i of the inflow is regarded as a kinematic wave traveling along the uniform flow section in downstream direction. The delay d_i is the discretized time interval before Δq_i induces a variation in the water level h_i in the backwater section. This is considered as the reservoir of the reach, and constitutes the integrator part of the model, characterized by its average storage area $A_{\text{s},i}$. The offtakes are usually scheduled in advance by the authorities in charge of the canal. Nevertheless, in the controller formulation we consider the offtake flow as a measurable disturbance $q_{\text{offtake},i}(k)$. This allows us to show the effectiveness of the proposed control scheme in an "on demand" operation, in which users can take water anytime without any previous agreement with canal authorities.

The nonlinear dynamics of the system are not covered by this model. When resonance waves play a dominant role—which is usual in short or flat pools at low discharge rates—the closed loop system can become unstable. Common ways to deal with this issue are, e.g., low-pass filtering, time-variant linear models, higher order models [81, 77]. For this study, the safety of operation regarding the amplification of resonance waves has been studied beforehand. The considered canal section consists of long and steep pools; also, the two scenarios presented in the simulations feature high discharge rates.

Assumption 2.1. *The gates are equipped with a local flow controller that manipulates the opening of the gate in order to maintain the water flow at a reference value. If the response of these local control loops is sufficiently fast, the only cause of unintended coupling among adjacent reaches is the manipulation of the flow through a gate, that will affect the water level in the upstream reach [76].*

The most common technique used in primary irrigation canals, and considered in this case study as well, is the distant downstream control. Following this technique, the water level in the backwater section of a reach is controlled by manipulating the opening of the upstream gate, physically located at the end of the upstream reach. For example, in response to a decrease of the water level in reach i, the gate upstream will open in order to restore it. From Assumption 2.1 it follows that this will produce a *direct* unintended effect on the water level of reach $i-1$. Notice that the water discharge at the downstream gate in reach 13 (denoted as CR14 in Fig. 2.1) cannot be manipulated by the controller.

For every reach, the following variables are considered:

- $e_i \triangleq h_i - \bar{h}_i$, the error w.r.t. the desired water level in the backwater section of reach i;

- q_i, the input flow to reach i.

In order to take into account the delay d_i along the uniform flow section, an augmented state representation is used. From the ID model the following discrete linear time-invariant model is obtained for each reach:

$$\begin{aligned} e_i(k+1) &= e_i(k) + \frac{T_\mathrm{c}}{A_{\mathrm{s},i}}\big[q_i(k-d_i) - q_{\mathrm{out},i}(k)\big], \\ q_i(k) &= q_i(k-1) + \Delta q_i(k), \end{aligned} \tag{2.9}$$

with

$$q_{\mathrm{out},i}(k) = q_{i+1}(k-1) + \Delta q_{i+1}(k) + q_{\mathrm{offtake},i}(k),$$

where Δq_i is a component of the control action computed through (2.19), representing the increment in the target flow of the local gate controller; $A_{\mathrm{s},i}$ is the backwater surface area, d_i is the discretized value of the transport delay and T_c is the sampling time.

The water levels are subject to an offset caused by the offtake flows and the disturbance due to downstream reaches. The purpose of the proposed control scheme is to maintain the water level of each reach around a fixed value ($\bar{h}_i$), that is, to regulate the level errors e_i to zero, while minimizing the control effort and the number of active network links.

For the description of the controller design, we restate the system model (2.9) as

$$x_i(k+1) = A_{ii}x_i(k) + B_{ii}u_i(k) + D_i^w w_i(k) + D_i^p p_i(k), \tag{2.10a}$$
$$w_i(k) = \sum_{j\in\mathcal{M}_i} A_{ij}x_j(k) + B_{ij}u_j(k), \tag{2.10b}$$

where $x_i \in \mathbb{R}^{n_i}$ and $u_i \in \mathbb{R}^{q_i}$ are the state and input vectors respectively, $p_i \in \mathbb{R}^{l_i}$ is a measurable perturbation due to the offtake flow, and $w_i \in \mathbb{R}^{m_i}$ describes the influence on x_i of the neighbors' states and inputs. In (2.10b), $x_j \in \mathbb{R}^{n_j}$ and $u_j \in \mathbb{R}^{q_j}$ are the state and input vectors of each neighbor $j \in \mathcal{M}_i$ of subsystem i. The augmented state vector

$$x_i(k) \triangleq [q_i(k-1), \dots, q_i(k-d_i), e_i(k)]^\intercal$$

is used in order to take into account the flow transport delay d_i. The measure of the water level deviation $e_i(k)$ in the backwater section of the reach is available; the rest of the state variables (water flow in different sections of the reach) are observable. The variation of the flow entering the reach i, controlled at its upstream gate, is the input $u_i(k) \triangleq \Delta q_i(k)$.

2.5.2 Coalition dynamics

The network topology reflecting the data links enabled between the control agents is modeled by the graph $\mathcal{G}(k) = (\mathcal{N}, \mathcal{E}(k))$. The coalition structure $\mathcal{P}(k) = \{\mathcal{C}_1, \dots, \mathcal{C}_{N_c}\}$ identifies the connected components—the coalitions—in $\mathcal{G}(k)$ (see Section 2.2.2). Following (2.3), the dynamics of each coalition $\mathcal{C}_i \in \mathcal{P}$ are described as

$$\xi_i(k+1) = \mathbf{A}_{ii}\xi_i(k) + \mathbf{B}_{ii}\upsilon_i(k) + \mathbf{D}_i^p\rho_i(k) + \mathbf{D}_i^w\omega_i(k) \tag{2.11}$$

where ξ_i and υ_i are composed by stacking the state and input vectors of all subsystems in coalition $\mathcal{C}_i$; similarly, $\rho_i = (p_j)_{j\in\mathcal{C}_i}$ gathers all the offtakes relative to $\mathcal{C}_i$. As in (2.4), ω_i expresses the coupling with subsystems external to the coalition. Matrices $\mathbf{A}_{ii}$, $\mathbf{A}_{ij}$, $\mathbf{B}_{ii}$, $\mathbf{B}_{ij}$, $\mathbf{D}_i^p$ and $\mathbf{D}_i^w$ are composed accordingly.

2.5.3 Control objective

The control objective is to regulate the water level error of all the reaches to zero while minimizing a cost that depends on the state and input trajectories. An additional term in the cost function will take into account the use of network resources.

In order to meet the objective, the offset caused by the offtake flows is canceled by steering each coalition's state to a suitable setpoint $(\bar{\xi}_i, \bar{\upsilon}_i)$. By imposing the steady state condition for all the coalitions, and setting the water level errors to zero, the following system of equations is obtained:

$$\begin{bmatrix} I - \mathbf{A} & -\mathbf{B} \\ \mathbf{\Gamma} & 0 \end{bmatrix} \begin{bmatrix} \bar{\boldsymbol{\xi}} \\ \bar{\boldsymbol{\upsilon}} \end{bmatrix} = \begin{bmatrix} \mathbf{D}^p \boldsymbol{\rho}(k) \\ 0 \end{bmatrix} \tag{2.12}$$

where $\boldsymbol{\xi} = (\xi_i)_{i \in \mathcal{S}_\mathcal{P}}$ and $\boldsymbol{\upsilon} = (\upsilon_i)_{i \in \mathcal{S}_\mathcal{P}}$, i.e., the global state and input vectors permuted according to the partition $\mathcal{P}(\mathcal{N}, \mathcal{G}(k))$. Similarly, $\mathbf{A} \in \mathbb{R}^{n \times n}$ and $\mathbf{B} \in \mathbb{R}^{n \times q}$ are the permuted global state and input matrices. The offtake vector $\boldsymbol{\rho} = (\rho_i)_{i \in \mathcal{S}_\mathcal{P}}$ and $\mathbf{D}^p$ are composed likewise. The matrix $\mathbf{\Gamma} \in \mathbb{R}^{N \times n}$ is determined such that $\mathbf{\Gamma}\boldsymbol{\xi}$ is the stacked vector of the water level errors of all the coalitions, i.e.:

$$\mathbf{\Gamma}\boldsymbol{\xi} = (e_j)_{j \in \mathcal{C}_i}, \ \forall i \in \mathcal{S}_\mathcal{P}.$$

For each coalition $\mathcal{C}_i$, the cost function is divided into a term $\mathbf{J}_i$, $i \in \mathcal{S}_\mathcal{P}$, representing the optimal performance objective and a term $\mathbf{J}_i^\mathcal{X}$, expressing the network-related cost:

$$\mathbf{J}_i = \sum_{t=0}^{N_p-1} (\zeta_i^\intercal(t|k)\mathbf{Q}_i\zeta_i(t|k) + \nu_i^\intercal(t|k)\mathbf{R}_i\nu_i(t|k)) + \zeta_i^\intercal(N_p|k)\mathbf{P}_i\zeta_i(N_p|k), \tag{2.13a}$$

$$\mathbf{J}_i^\mathcal{X} = \sum_{j \in \mathcal{C}_i} N_p \frac{c_l}{2} n_{l,j}(\mathcal{E}), \tag{2.13b}$$

where $\zeta_i = \xi_i - \bar{\xi}_i$ and $\nu_i = \upsilon_i - \bar{\upsilon}_i$ denote respectively the shifted state and input of coalition $\mathcal{C}_i$, and $\mathbf{Q}_i \triangleq \operatorname{diag}(Q_j)_{j \in \mathcal{C}_i}$, $\mathbf{R}_i \triangleq \operatorname{diag}(R_j)_{j \in \mathcal{C}_i}$ and $\mathbf{P}_i = \mathbf{P}_i^\intercal > 0$ are constant weighting matrices.[3] In (2.13b), $n_{l,j}(\mathcal{E})$ is the number of active links *directly* connecting agent j to other agents according to the network topology $\mathcal{E}$. Note that each agent shares the cost of a link with the agent located at the other side of that link. Given the serial topology of the considered canal section, each agent is responsible of two active links at most. The overall control problem can be posed as the following receding-horizon optimization:

$$\min_{\boldsymbol{\upsilon}, \mathcal{E}} \sum_{i \in \mathcal{S}_\mathcal{P}} \mathbf{J}_i(\xi_i(k), \upsilon_i, \mathcal{E}) + \mathbf{J}_i^\mathcal{X}(\mathcal{E}) \tag{2.14a}$$

[3] In this example, the weighting matrix Q_i only penalizes deviations of the water level.

s.t.

$$\xi_i(t+1|k) = \mathbf{A}_{ii}\xi_i(t|k) + \mathbf{B}_{ii}\upsilon_i(t|k) + \mathbf{D}_i^p\rho_i(k) + \mathbf{D}_i^w\hat{\omega}_i(k), \tag{2.14b}$$

and (2.6c)–(2.6g). Since coalition $\mathcal{C}_i$ has no knowledge of the states and inputs of external subsystems, an estimate $\hat{\omega}_i$ of the perturbation they cause on ξ_i is performed at each time step k, and its value is assumed constant along the prediction horizon in (2.14b). Details are given in Section 2.5.4.

Remark 2.2. *In typical canal operation, the offtake planning is typically made in advance, and the perturbation $\rho_i(k+t)$ can be known for the entire prediction horizon. In this example, however, forecasts are not considered, so as to simulate an "on-demand" operation. Therefore, a constant value of the offtake flow, corresponding to the current measure, is maintained along the horizon.*

2.5.4 The control algorithm

The hierarchical multi-agent architecture introduced in this chapter is proposed as an approximation of problem (2.14), with the intent of reducing the computational and communicational requirements of (2.14). Hence, problem (2.14) is split into two layers: a top layer, taking charge of the choice of the network mode (see Section 2.4), and a bottom layer handling the estimation and the real-time control tasks. A conceptual diagram of the resulting coalitional MPC strategy is shown in Figure 2.3.

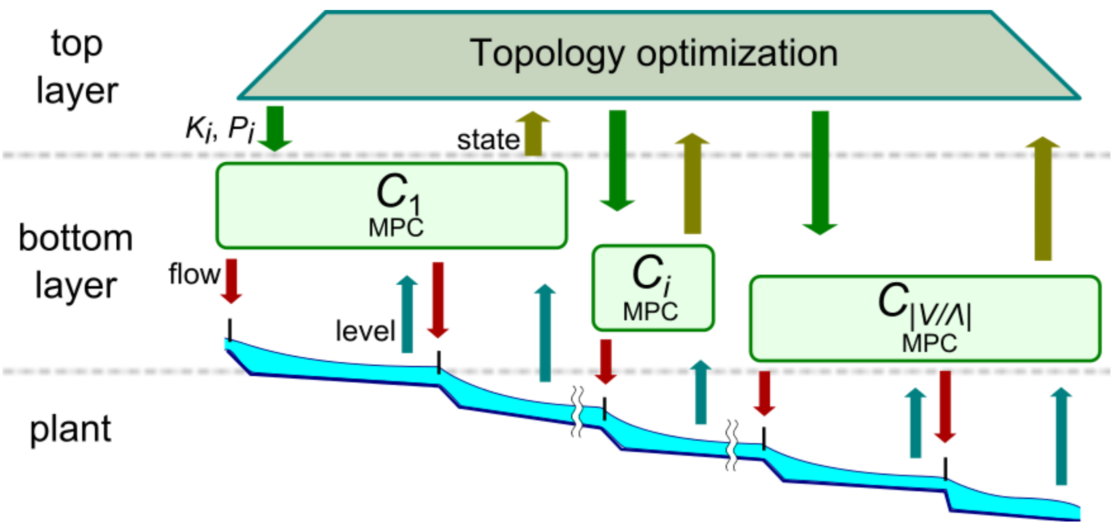

Figure 2.3: Functional diagram of the hierarchical coalitional MPC architecture applied to the irrigation canal case.

Top layer

The discrete part of Problem (2.14), namely the topology optimization, is computed on a coarse time scale at the top layer. A set $\mathfrak{E}^+ = \{\mathcal{E}_1, \mathcal{E}_2, \ldots, \mathcal{E}_{N_\mathcal{E}}\}$ of candidate network topologies are compared, by defining their value as $J : \mathbb{R}^n \times \mathcal{N} \times \mathcal{N} \mapsto \mathbb{R}$ (see also [82]):

$$J(\boldsymbol{\xi}, \mathcal{E}) = \sum_{i \in \mathcal{S}_\mathcal{P}} \zeta_i^\intercal \mathbf{P}_i \zeta_i + c_l |\mathcal{E}| T_\mathcal{E}, \; \mathcal{E} \in \mathfrak{E}^+, \tag{2.15}$$

where $\mathbf{P}_i = \mathbf{P}_i^\intercal > 0$, $|\mathcal{E}|$ is the number of enabled links and c_l is the cost of use of one link, considered over the interval $T_\mathcal{E}$. In this particular case, at a given time k, the set of topologies candidate for the interval $[k + T_s, k + T_\mathcal{E}]$ is formed by considering the topologies derived by switching the current state of (at most) one of the links.[4] To compute the value of (2.15), Problem (2.8) is solved and the block-diagonal matrix $\mathbb{P} = \text{diag}(\mathbf{P}_i)_{i \in \mathcal{S}_\mathcal{P}}$, defining a global Lyapunov function $V(\boldsymbol{\xi}, \mathcal{E}^*) = \boldsymbol{\xi}^\intercal \mathbb{P} \boldsymbol{\xi}$ for the (unconstrained) system is obtained. Of all the topologies considered, the one giving the minimum value of (2.15), denoted as $\mathcal{E}^* \in \mathfrak{E}^+$, will be applied during the next interval $T_\mathcal{E}$. As a consequence of the chosen cooperation graph $\mathcal{G}(k) = (\mathcal{N}, \mathcal{E}^*)$, the set of agents is partitioned into a specific set of coalitions $\mathcal{P}(\mathcal{E}^*) = \{\mathcal{C}_1, \mathcal{C}_2, \ldots, \mathcal{C}_{|N_c|}\}$. To each coalition is associated the feedback law $\upsilon_i = \mathbf{K}_i \xi_i$, obtained as the minimizer of $V(\boldsymbol{\xi}, \mathcal{E}^*)$ by the solution of Problem (2.8).

Bottom layer

As schematized in Figure 2.3, the control is decentralized at the bottom layer into the coalitions arising from the partition $\mathcal{P}(\mathcal{E}^*)$, whose choice is carried out at the top layer. Agents within the same coalition share their information at each sample time k. The term ω_i is related with the water demand in neighboring coalitions. Every coalition gets an estimate $\hat{\omega}_i$ by a local Kalman filter, based on the available measures of water level errors and current offtake flows. Given the slow dynamics of the system and the steady nature of the offtake flows, transient dynamics can be neglected.

Remark 2.3. *In general, inter-pool transient dynamics are not negligible. However,* (i) *the system examined in the case study is inherently stable, and* (ii) *local flow controllers are present at each gate. If the response of these local control loops is sufficiently fast, the interaction between two adjacent pools reduces to a one-way perturbation [76].*

Therefore, $\hat{\omega}_i$ is viewed as a constant integrating disturbance, included in the model by an augmented state vector. Then, implementing a standard offset-free scheme for

[4] The new topology will be active starting from the next sample time.

regulation [83], the agents steer their subsystems to an appropriate setpoint in order to compensate for both the estimated disturbance and the offset caused by the measurable offtake flows. Notice that any offset due to mismatches between the linear model and the actual system will be also included in $\hat{\omega}_i$. The Kalman filter also serves as an observer for the values of water flows.

For any coalition $\mathcal{C}_i$, the setpoint $(\bar{\xi}_i, \bar{\upsilon}_i)$ is obtained by the solution of the linear system:

$$\begin{bmatrix} I - \mathbf{A}_{ii} & -\mathbf{B}_{ii} \\ \Gamma_i & 0 \end{bmatrix} \begin{bmatrix} \bar{\xi}_i \\ \bar{\upsilon}_i \end{bmatrix} = \begin{bmatrix} \mathbf{D}_i^p \rho_i(k) + \mathbf{D}_i^w \hat{\omega}_i(k) \\ 0 \end{bmatrix} \tag{2.16}$$

where Γ_i is an output matrix defined such that $\Gamma_i \xi_i = (e_j)_{j \in \mathcal{C}_i}$, i.e., the water level deviations of all the subsystems in coalition $\mathcal{C}_i$. Because of the estimation of $\hat{\omega}_i$, the setpoint computed through (2.16) is expected to change at each time step. Note that when the topology is changed the Kalman filters structure changes as well, according to the composition of the new set of coalitions. To avoid undesired drifts on the computed value of the setpoint, a good initial guess of the state and the covariance matrix is needed for each new coalition's local filter. Past data, communicated by the members of the coalition, can be used to initialize the Kalman filter.

The setpoint obtained by (2.16) may not satisfy the constraints. Therefore, Problem (2.17)—featuring the slack variable σ_i in the equality constraint—is solved to obtain the nearest feasible setpoint (ξ_i^s, υ_i^s) to $(\bar{\xi}_i, \bar{\upsilon}_i)$

$$\min_{\xi_i^s, \upsilon_i^s, \sigma_i} (\upsilon_i^s - \bar{\upsilon}_i)^\intercal \mathbf{R}_i (\upsilon_i^s - \bar{\upsilon}_i) + \xi_i^{s\intercal} \mathbf{Q}_i \xi_i^s + \sigma_i^\intercal \mathbf{G}_i \sigma_i \tag{2.17a}$$

s.t.

$$(I - \mathbf{A}_{ii})\xi_i^s - \mathbf{B}_{ii}\upsilon_i^s - \sigma_i = \mathbf{D}_i^p \rho_i(k) + \mathbf{D}_i^w \hat{\omega}_i(k) \tag{2.17b}$$

$$H_i \xi_i^s > 0 \tag{2.17c}$$

$$K_i(\xi_i(k) - \xi_i^s) + \upsilon_i^s \in \mathcal{U}_i. \tag{2.17d}$$

In (2.17), the input reference $\bar{\upsilon}_i$ is the one obtained from (2.16); $\mathbf{Q}_i$ and $\mathbf{R}_i$ are the submatrices relative to coalition $\mathcal{C}_i$ (the same used for the optimal performance specification in the top layer); $\mathbf{G}_i > 0$ is a constant weighting matrix, whose value has been chosen such that the magnitude of the term $\sigma_i^\intercal \mathbf{G}_i \sigma_i$ in (2.17) is comparable with the rest of the cost function. Hard constraints are imposed on the water flows with (2.17c): the product $H_i \xi_i^s$ is the vector composed of the flow values at each section of any reach controlled by coalition $\mathcal{C}_i$.

From the solution of Problem (2.8) (top layer) and Problem (2.17), the following controller is available for each coalition to regulate the subsystems to the desired setpoint:

$$\upsilon_i(k) = \mathbf{K}_i\zeta_i(k) + \upsilon_i^s(k), \tag{2.18}$$

where the shifted state is redefined as $\zeta_i = \xi_i - \xi_i^s$. However, feasibility cannot be guaranteed with (2.18). Thus, the value given by (2.18) is "rectified" through the solution of MPC problem (2.21), obtaining an additional input term:

$$\upsilon_i(k) = \mathbf{K}_i\zeta_i(k) + \upsilon_i^s(k) + \upsilon_i'(k). \tag{2.19}$$

Possible issues related with the loss of feasibility are dealt with by considering physical limits on the water flows as soft constraints. Restrictions on the input change rate are formulated as hard constraints. By redefining the shifted input as $\nu_i = \upsilon_i - \upsilon_i^s$, the cost function of the MPC problem solved at the bottom layer is derived from (2.13a) as follows:

$$\begin{aligned}\mathbf{J}_i' = \sum_{t=0}^{N_p-1} &\Big(\zeta_i^\intercal(t|k)\mathbf{Q}_i\zeta_i(t|k) + \nu_i^\intercal(t|k)\mathbf{R}_i\nu_i(t|k)\Big) \\ &+ \zeta_i^\intercal(N_p|k)\mathbf{P}_i\zeta_i(N_p|k) + \sum_{t=1}^{N_p}\epsilon_i^\intercal(t)S_i\epsilon_i(t)\end{aligned} \tag{2.20}$$

where $S_i > 0$ is a constant weighting matrix for the slack variable ϵ_i, used to relax the constraints on the flows. The optimization problem to be solved by coalition $\mathcal{C}_i$ at each time step k is:

$$\min_{\upsilon_i',\epsilon_i} \mathbf{J}_i'(\zeta_i(k), \nu_i) \tag{2.21a}$$

s.t.

$$\zeta_i(t+1|k) = (\mathbf{A}_{ii} + \mathbf{B}_{ii}\mathbf{K}_i)\zeta_i(t|k) + \mathbf{B}_{ii}\upsilon_i'(t|k) \tag{2.21b}$$

$$H_i\Big(\zeta_i(t|k) + \xi_i^s(k)\Big) + \epsilon_i(t) > 0,\ \forall t \in [0, N_p] \tag{2.21c}$$

$$K_i\zeta_i(t|k) + \upsilon_i'(t|k) + \upsilon_i^s(k) \in \mathcal{U}_i,\ \forall t \in [0, N_p] \tag{2.21d}$$

$$\zeta_i(0|k) = \xi_i(k) - \xi_i^s(k) \tag{2.21e}$$

where the product $H_i\left(\zeta_i + \xi_i^s\right) = H_i\xi_i$ gives the vector composed of the stacked water flows at each section of any reach considered within coalition $\mathcal{C}_i$.

A description of the proposed algorithm is provided below.

Algorithm 2.1. ***Coalitional MPC***

Step 1. *Prepare a set* $\mathfrak{E}^+$ *of suitable network topologies to be evaluated for their use during the next interval* $T_{\mathcal{E}}$*, defined as a multiple of the sampling time at the bottom layer.*

Step 2. *For each* $\mathcal{E} \in \mathfrak{E}^+$ *compute* $\mathbb{K}(\mathcal{E})$ *and* $\mathbb{P}(\mathcal{E})$*.*

Step 3. *For each* $\mathcal{E} \in \mathfrak{E}^+$*, estimate the steady-state effect due to neighbor coalitions as:*

$$\hat{\omega}_i(k) = \sum_{j \in \mathcal{M}_i} \mathbf{A}_{ij} \hat{\xi}_j^s + \mathbf{B}_{ij} \hat{\upsilon}_j^s, \; \forall i \in \mathcal{S}_{\mathcal{P}},$$

where each pair $(\hat{\xi}_j^s, \hat{\upsilon}_j^s)$ *is the most updated setpoint available from coalition* $\mathcal{C}_j$*.*

Step 4. *For each* $\mathcal{E} \in \mathfrak{E}^+$*, solve* (2.16) *to obtain the setpoints* $(\bar{\xi}_i(k), \bar{\upsilon}_i(k))$*,* $\forall i \in \mathcal{S}_{\mathcal{P}}$*, using the value of* $\hat{\omega}_i(k)$ *computed at Step 3.*

Step 5. *Compute an estimate of the global cost with* (2.7) *and pick the network mode* $\mathcal{E}^*$ *that would give the minimum cost.*

Step 6. *Communicate each local feedback law* $\mathbf{K}_i(\mathcal{E}^*)$ *and* $\mathbf{P}_i(\mathcal{E}^*)$ *to the corresponding coalition.*

Step 7. *Each coalition computes a setpoint* $(\xi_i^s(k), \upsilon_i^s(k))$ *by solving* (2.16) *and* (2.17)*.*

Step 8. *Each coalition solves* (2.21) *for* $\upsilon_i'(k)$*, and the control action* (2.19) *is applied to the subsystems in coalition* $\mathcal{C}_i$*.*

Step 9. *By means of the local Kalman filter, each coalition obtains the estimate* $\hat{\omega}_i(k+1) \equiv \hat{\omega}_i(k+1|k)$ *to be used during the following time step.*

Step 10. *Repeat Steps 7–9 during the interval* $T_{\mathcal{E}}$*, then go to Step 1.*

2.5.5 Simulation model

A detailed simulation of the physics of the west main canal of the Dez irrigation network has been performed using the SOBEK modeling suite for water systems. Based on the WL|Delft Hydraulics implicit finite difference scheme [75], this software package is currently developed at the Deltares research institute in the Netherlands. Design parameters have been specified in order to accurately reproduce the canal dynamics: path, cross-sections, layout of the canal network, type and width of gate, crest levels and discharge coefficients, upstream and downstream boundary conditions. All the necessary information about the geometry of the canal and the hydraulic structures has been obtained from the water authority of Khuzestan province. The boundary condition at the head gate is a constant water level at its upstream side, while its maximum discharge capacity is 157 m^3/s. The model has been calibrated and validated using real data relative to six months of operation [84], and has been further employed in [79, 85].

2.5.6 Identification of the control model

The parameters of the ID model for the 13 reaches have been identified through simulations on the SOBEK validated model, and are given in Table 2.1. The transport delay and the average storage area have been characterized while considering the canal at steady state with an input amounting to 80% of the maximum inflow, and all the offtakes at 80% of the maximum discharge capacity. The values in Table 2.1 refer to the canal in this operational conditions. An additional identification of the model parameters has been carried out for a medium discharge setting, namely 50% of the maximum inflow and 50% of the maximum offtake. Since the parameters have demonstrated little sensitivity to the change in the discharge regime, the dependence of the parameters on the flow has been neglected. Furthermore, the implementation of an offset-free method, together with the inherent robustness of the MPC, contributes to the compensation of model-plant mismatches. The values in Table 2.1 have been used throughout the scenarios presented in the next section.

2.5.7 Results

Two scenarios are analyzed in the following, reflecting the canal operation at medium–high discharge regimes. In the first one, the water levels and flows are initially settled for the supply of constant nonzero offtakes along the canal until four of the reaches undergo a step decrease in their offtake flows, 360 minutes past the beginning of the simulation ($k = 72$). The same situation is considered in the second scenario, with the addition of a second step change—360 minutes after the first one ($k = 144$)—restoring the offtakes to their former values. The variation of the offtake flows amounts to 10 m^3/s at reaches 4 and 13, and to 5 m^3/s at reaches 9 and 10, ranging from 20% to 100% of their initial magnitude. The simulation is meant to test the performance of the proposed control scheme in rejecting the simultaneous changes in the offtakes, keeping the water level at each reach around its corresponding reference. The exchange

Reach	Length [m]	Width (bottom) [m]	Backwater surface ($\cdot 10^5$) [m^2]	Delay steps
1	6219	12	0.9318	3
2	1933	12	1.0952	1
3	3718	10	0.8554	2
4	3906	10	3.7060	2
5	2934	5	1.7095	2
6	4670	5	0.7786	3
7	3110	5	0.6661	2
8	2240	5	0.8904	1
9	3405	5	0.8671	2
10	3820	5	0.4897	2
11	2520	4	0.4032	2
12	2874	4	0.3820	2
13	2468	5	0.3884	2

Table 2.1: Parameters of the first 13 reaches of the west main Dez canal, identified at 80% of the maximum discharge rate.

Symbol	Description	Value
N_p	Prediction horizon	10
N_c	Control horizon	3
Q_i	Weight on the errors	250
R_i	Weight on the flow increments	2800
S_i	Weight on flows < 0 (soft constr.)	10^4
c_ℓ	Cost of an active link	0.6
T_c	Sampling time [s]	300

Table 2.2: Parameters of the controller.

of information between different agents is enabled by the chosen network topology, according to how the dynamic coupling between the reaches evolves with time (see Section 2.5.4). In the simulations, the state of only one of the links is allowed to change between any two subsequent choices of topology. Hard constraints are imposed on the water flow increment at each gate, $|\Delta q_i(k)| \leq 1$ m^3/s. Constraints on the direction of the water flows, i.e., $q_i(k) > 0$, are imposed as soft constraints. Table 2.2 lists the values of the controller's parameters used for both scenarios. These values have been tuned by trial and error, balancing the performance improvement with the computational requirements (an initial guess for matrices Q_i and R_i has been obtained following the inverse-variance weighting method). The plots in Figure 2.4 refer to Scenario 1. In the upper plot, the evolution of water level errors is shown. It can be seen how the sudden decrease in the offtake flows at time $k = 72$ causes the water levels to rise above the desired setpoint, reaching in some pools a peak of 0.5 m. In the bottom plot of Figure 2.4, bold segments indicate active links between the corresponding agents. The agents in charge of the first four upstream reaches act jointly when the disturbance occurs. This coordination allow to minimize the perturbation on reach 3 (and consequently on reach 2 and 1) due to the recovery maneuver of the agent in charge of reach 4.

During the transient response of the local flow controllers, the sudden variation of the offtake flows produces an immediate perturbation in downstream direction. Therefore, in order to improve the performance of the overall system, the agents are organized into bigger coalitions while the effect of the offtakes' variation is perceived. As the disturbance is rejected, the data links are disabled and most of the agents continue to control their reaches in a decentralized way. It can be seen that the coalition among upstream agents is profitable and thus does not eventually disappear. One reason to this might be the fact that, in the system under study, an accurate decentralized estimation of neighbor's state is not possible, and water levels at upstream reaches tend to deviate from the setpoint as soon as their agents stop to communicate. This may suggest that in an optimal partition of the overall system the upstream agents would be part of the same coalition. Figure 2.5 shows the inflows $q_i(k)$ to the reaches. Starting from time $k = 72$, the flows are reduced in response to the decreased offtakes in order to bring the water levels back to their setpoints.

The results relative to Scenario 2 are shown in Figure 2.6. Before the offtakes variation at time $k = 72$, the network topology changes to a decentralized configuration while the water levels are kept at their setpoints. When the decrease in the offtakes occurs, the system reacts by reducing the inflows (Fig. 2.7), while data links are enabled in order to coordinate the operations along the canal. At time $k = 144$ the offtake flows are restored, which is matched with an increase in the input flows. As the error in the water levels is attenuated, downstream data links are disabled. Notice in the last part of the simulation the persistence of the coalition among the upstream agents, and also the coalition formed by agents 5 and 6, since the water level in reach 5 does not converge to its setpoint. It can be seen in Figures 2.5 and 2.7 that the constraints on the water flows are satisfied in both scenarios. Moreover, even without taking into account any offtake forecast, the results achieved with the proposed distributed control scheme are within the admitted range of canal operation.

For comparison, the performance of a centralized MPC controller in the same scenarios is shown in Figures 2.8 and 2.9. The centralized control law is computed as

		Coal. ($\cdot 10^3$)	Centr. ($\cdot 10^3$)
Scn. 1	$c_\ell = 0$	5.62	2.06
	$c_\ell = 0.6$	10.44	14.06
Scn. 2	$c_\ell = 0$	9.36	3.89
	$c_\ell = 0.6$	14.80	15.89

Table 2.3: Comparison of the average costs of the proposed coalitional scheme and centralized MPC for the two scenarios.

	n° dec. var.	n° coal.
Scn. 1	5.6	8.2
Scn. 2	6.3	7.6
Centr. MPC	39	1

Table 2.4: Average number of decision variables for the decentralized MPC controllers at the bottom layer, relative to both scenarios.

in (2.19), using the same parameters of Table 2.2 (except for the cost of active links, which is null). The centralized controller can coordinate the response of the entire canal to provide a faster reaction to the disturbance, which yields about 30% reduction in the level error peaks.[5] As expected, due to the absence of network topology switching with centralized control, a smoother response of the system is obtained. Table 2.3 displays a comparison of the average control costs of the coalitional and centralized MPC schemes, for both scenarios. In Figure 2.10 the accumulated costs relative to Scenario 1 are represented, evidencing the impact of communication-related costs in a centralized framework. The average number of decision variables for the decentralized MPC problems solved by the coalitions at the bottom layer is shown in Table 2.4, along with the average number of coalitions.

[5] An exception to this is the water level in reach 13, as no further downstream reaches can be employed to improve its response (the water discharge at the downstream gate in reach 13 cannot be manipulated by the controller).

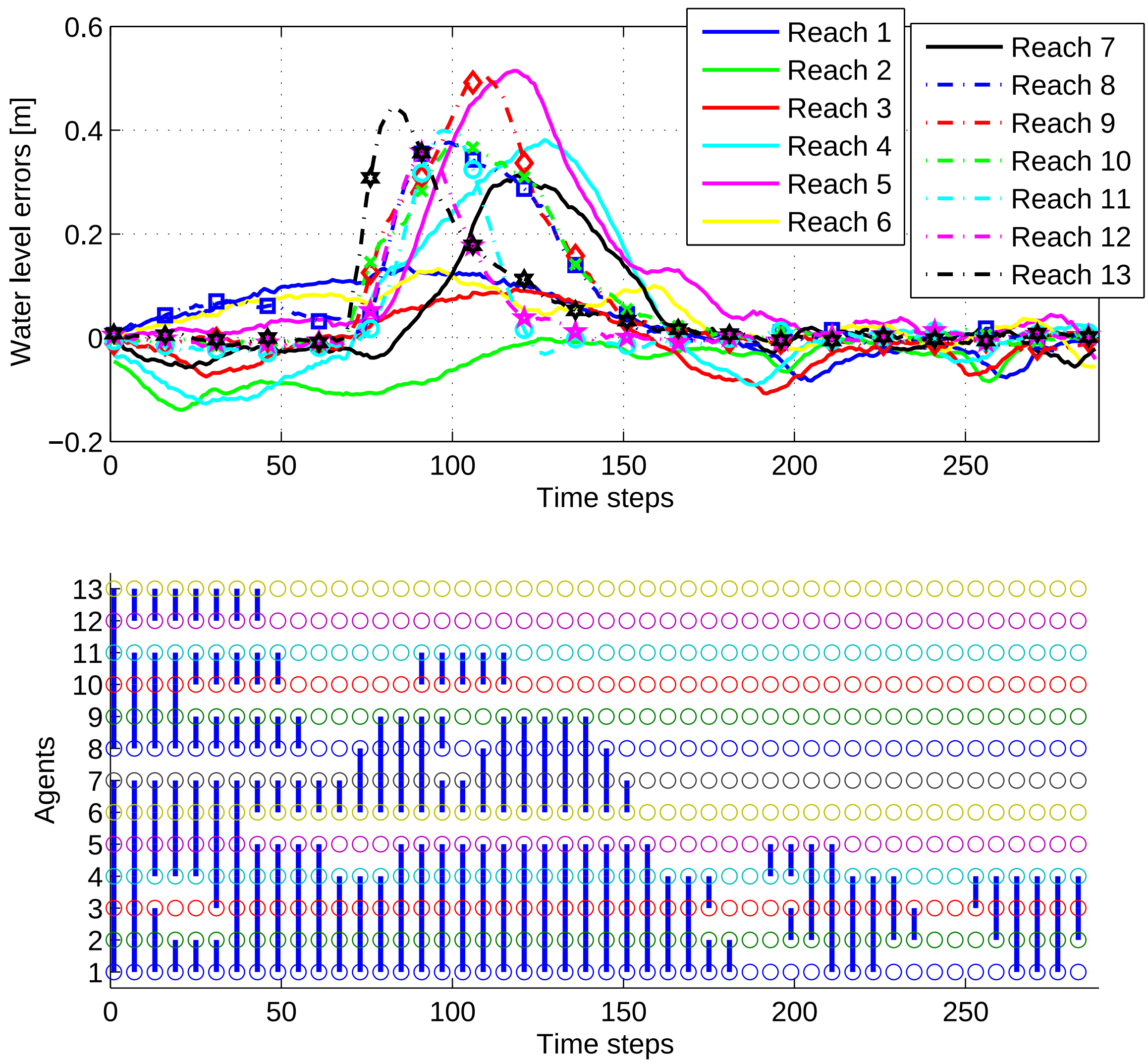

Figure 2.4: Scenario 1: At $k = 72$ reaches 4, 9, 10 and 13 undergo a step decrease in the offtake flows. The upper plot shows how the controller regulates the water level errors along the canal. Each bold segment in the bottom plot represents an active data link between two control agents. Starting from a centralized configuration, links are deactivated one at a time until the variation in the offtakes is sensed. Then links are enabled to form coalitions among the most concerned control agents, until the disturbance is eventually rejected.

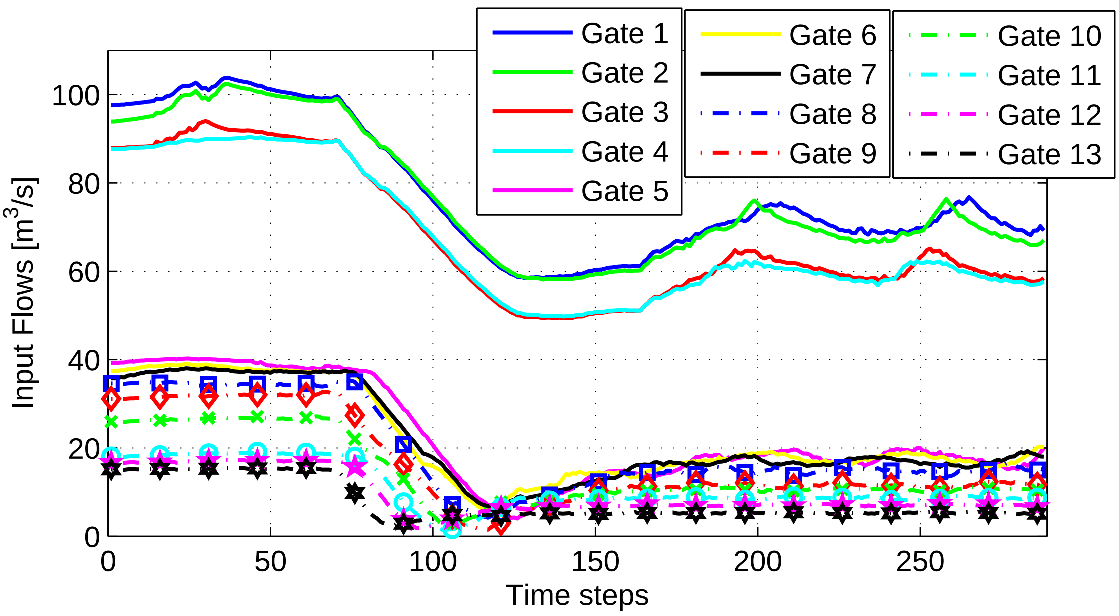

Figure 2.5: Scenario 1: Water flows in input to each reach.

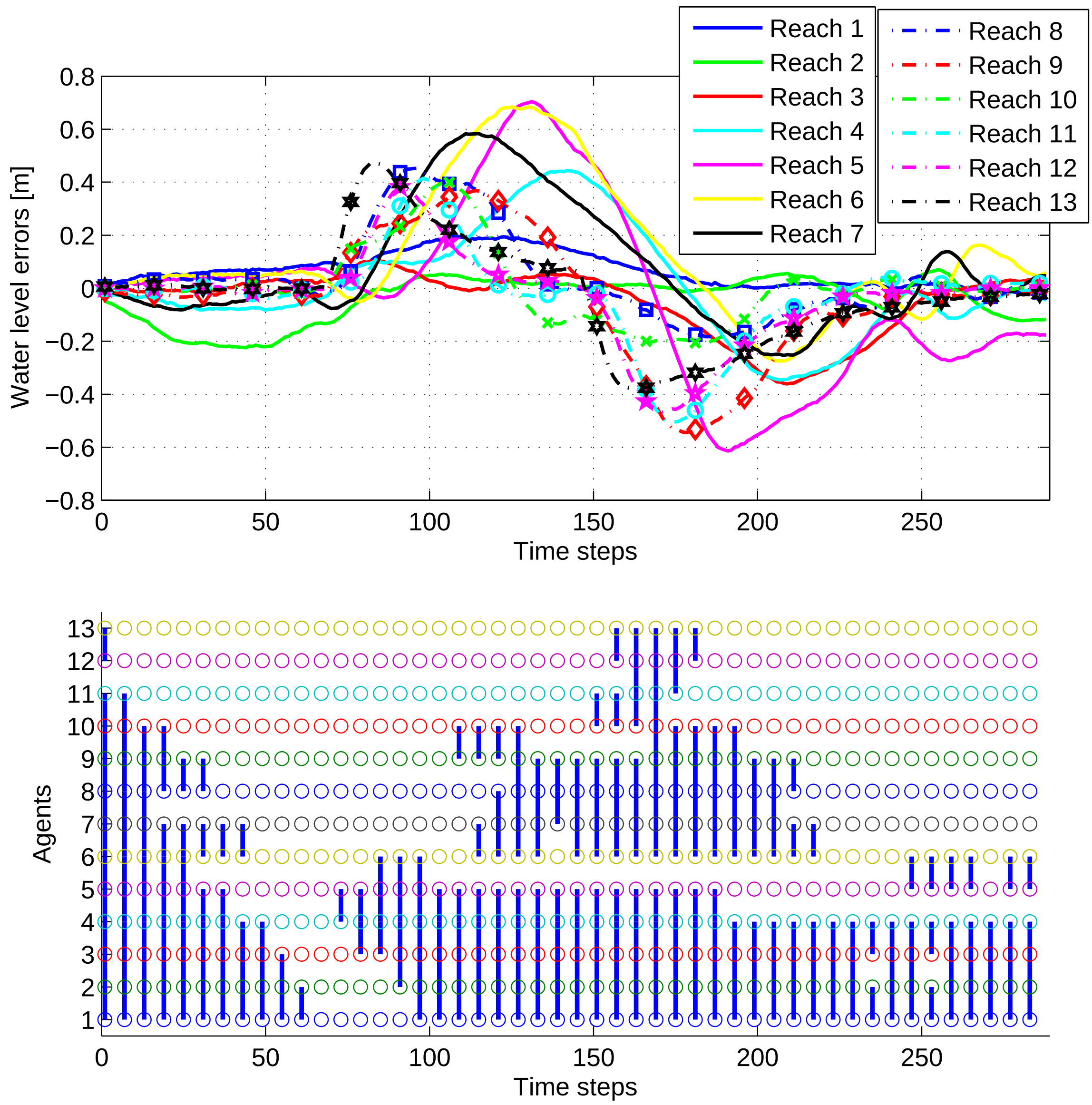

Figure 2.6: Scenario 2: The offtake flows in reaches 4, 9, 10 and 13 undergo a step decrease at $k = 72$, and are restored at $k = 144$. The upper plot shows the water level errors in all the reaches. The use of data links between the control agents is represented by the bold segments in the bottom plot. With the water levels at their setpoints, the network changes toward a decentralized topology. In reaction to the offtake change, the control agents are organized into coalitions to improve the overall response.

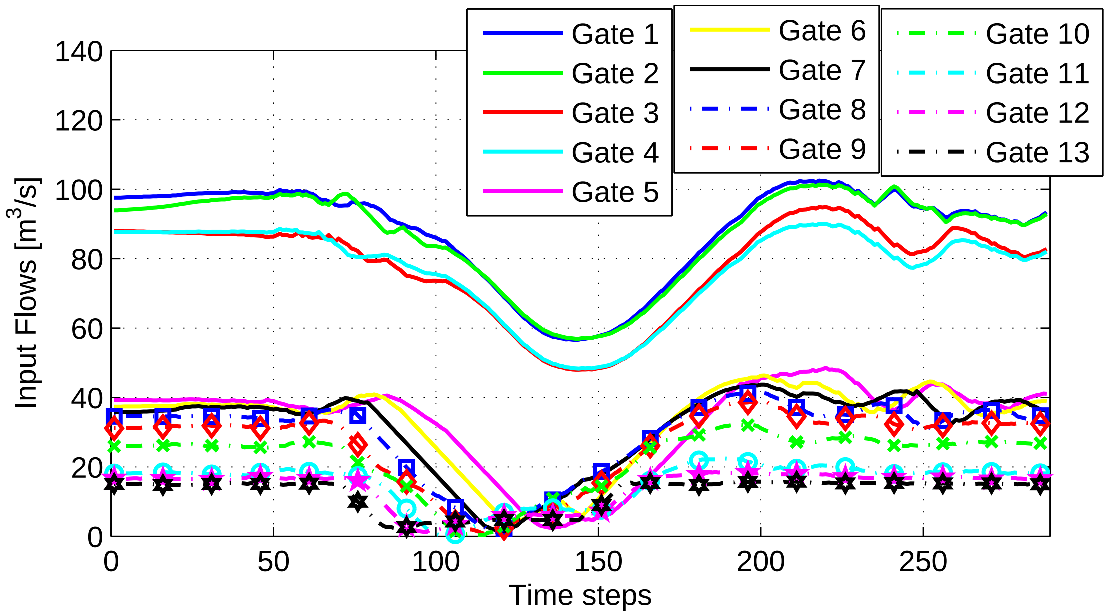

Figure 2.7: Scenario 2: Water flows in input to each reach.

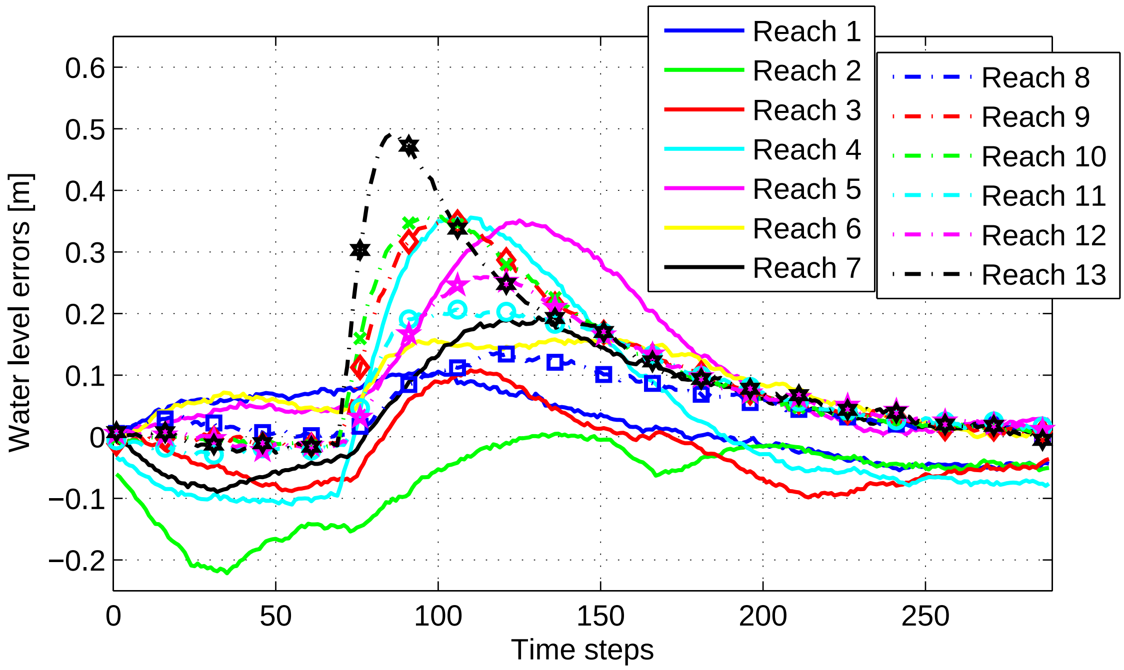

Figure 2.8: Scenario 1: Water level errors with centralized MPC controller.

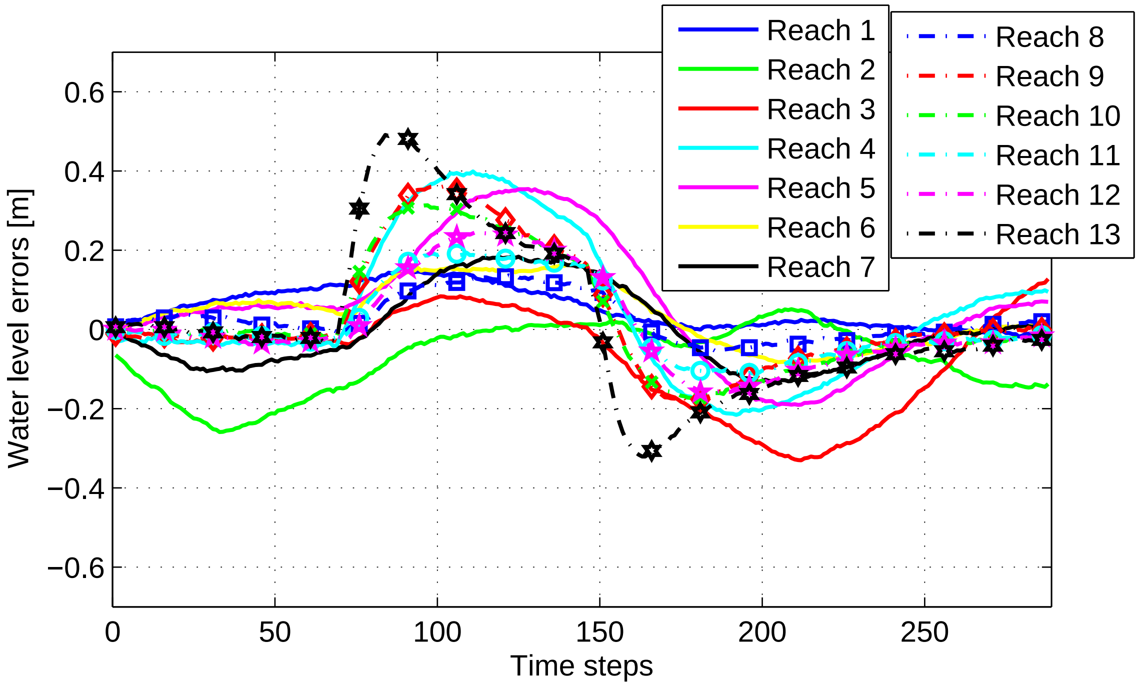

Figure 2.9: Scenario 2: Water level errors with centralized MPC controller.

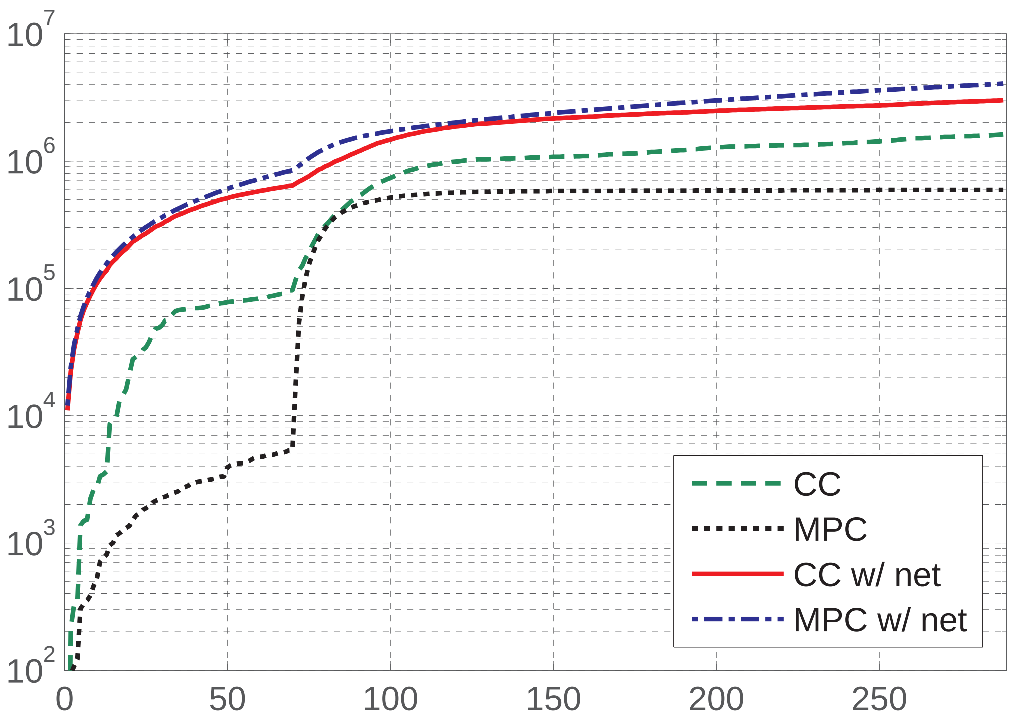

Figure 2.10: Scenario 1: Accumulated costs comparison between the proposed coalitional control strategy and a centralized MPC, w/ and w/o network costs.

2.6 Illustrative case II: Microgrid

Smart grids constitute an exhaustive example of complex large-scale system. They encompass advanced power, communication, control and computing technologies. In such a heterogeneous domain the game theory finds natural applications, such as energy markets and dynamic pricing. The potential of the integration of game theoretical tools in the control of smart grids is discussed in [14].

In existing power systems, consumers are serviced by a main electricity grid that delivers the power over the transmission lines to a substation which, in turn, delivers the power over the low-voltage distribution network. One of the building blocks of the smart grid is the microgrid, a network of distributed energy sources located at the *distribution side* of the grid that can provide energy to a restricted geographical area. It may operate either together with the main grid or in an autonomous fashion. Power supply within microgrids is mainly based on small production from renewable sources or combined heat and electricity generation. Microgrids can count storage facilities (including electric vehicles' batteries) and flexible demand among their resources as well.

The service capacity of microgrids can be exploited to relieve the demand on the main grid. However, the intermittent generation coupled with the unpredictable nature of the demand implies that customers serviced by a microgrid may come to need extra energy from other sources. Of course, this extra energy can be provided by the main power grid. Nevertheless, the future smart grid is envisioned to encompass a large number of microgrid elements. Whenever some microgrids have an excess of production while others incur in a power shortage, a mutual exchange of energy can be beneficial for both parties, instead of relying on the main grid. The advantage of a local exchange is not limited to this: indeed, the energy transfer between nearby microgrids can significantly reduce the amount of power wasted for long-distance transmission over the distribution lines.

The aggregation of renewable-energy plants for their participation in the electricity market is analyzed as a canonical coalitional game in [49]. The main objective is the reduction of the variability in the production due to the unpredictability of renewable energy sources, exploiting the decorrelation of wind speeds at separated geographic locations. The focus is then on finding a fair mechanism for the allocation of the benefit among the producers, which can alleviate the risk associated with market participation. Intuitively, those individuals who contribute to a larger reduction in the production's variability should receive a greater share of the benefit achieved through the cooperation. The problem is solved in [49] through an approximated computation of the *nucleolus* of the associated game, carried out as a single LP optimization that minimizes the *worst-case* dissatisfaction for all possible coalitions.

In [86], a cooperative energy exchange game among micro-grids, with the objective of minimizing line power losses, is formulated. The formulation involves the solution of two subproblems: an auction matching game to find the pairs of suppliers and consumers minimizing power losses, and a coalition formation game to establish the coalitions. The rules proposed in [57], based on the Pareto order, are used to decide whether to form or break coalitions. The results show that such cooperative energy exchange mechanism has the advantage of improving the autonomy of microgrids with respect to the main grid, as well as reducing the losses over the distribution lines by promoting local energy trade among neighboring microgrids. The coalition structure can be adjusted to meet variations in the demand/supply.

The coordination of demand and supply among communicating prosumers is addressed in [87] with the objective of alleviating the load on substations' transformers. The focus is on the routing of information about individual demand/supply availability used for the estimation of the aggregate imbalance. The minimization of the energy imbalance of the cooperating nodes—which translates in less energy required from the main grid—is the objective of the control problem, whose distributed solution is coordinated by means of Lagrangian multipliers.

2.6.1 Problem formulation: coalitions among prosumers in a microgrid

Here we consider a set $\mathcal{N} = \{1, \ldots, N\}$ of consumer nodes equipped with domestic production systems such as solar panels and storage devices (see Figure 2.11). These nodes, situated within a small area as shown in Figure 2.12, pertain to the distribution layer of the grid, and are connected to the main grid through a substation. According to the coalitional control algorithm described in the remainder, the nodes can aggregate into coalitions. Inside each coalition, the power transfer is the result of an optimal control problem, formulated such as to minimize the cost of buying energy from the main grid *for the entire coalition.* Power losses over the distribution lines due to the energy transfer between members of the coalition are added to the incurred costs (costs of power losses from the main grid are not considered separately from the spot price). It is interesting to see how, as a result of the application of the coalitional control algorithm, the associations of nodes are reorganized according to the variations in the

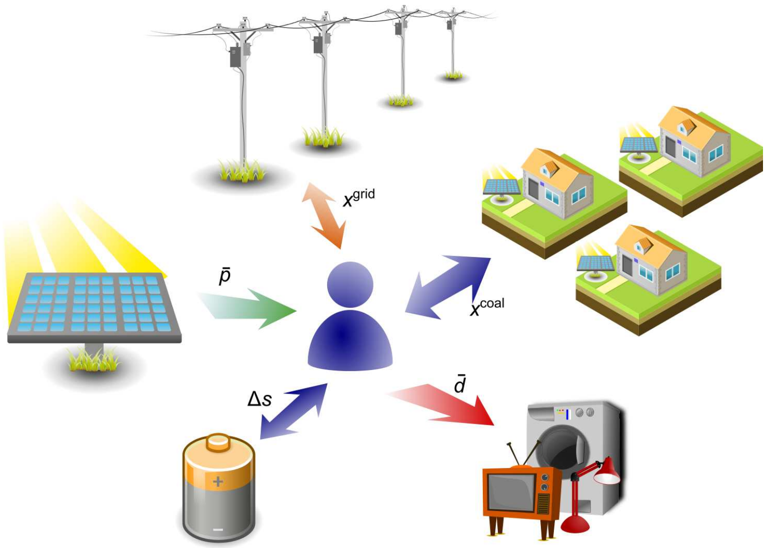

Figure 2.11: We consider a set of nodes connected to the main grid, equipped as well with local generation and storage devices. These prosumers can establish a local energy market by aggregating into coalitions, so as to minimize the cost of buying energy from the main grid. Power losses over the distribution lines are added to the incurred costs. As a result of the application of the coalitional control algorithm, nodes associate according to variations in the local demand and supply, as well as to changes in the energy prices. The figure shows the energy balance at each node.

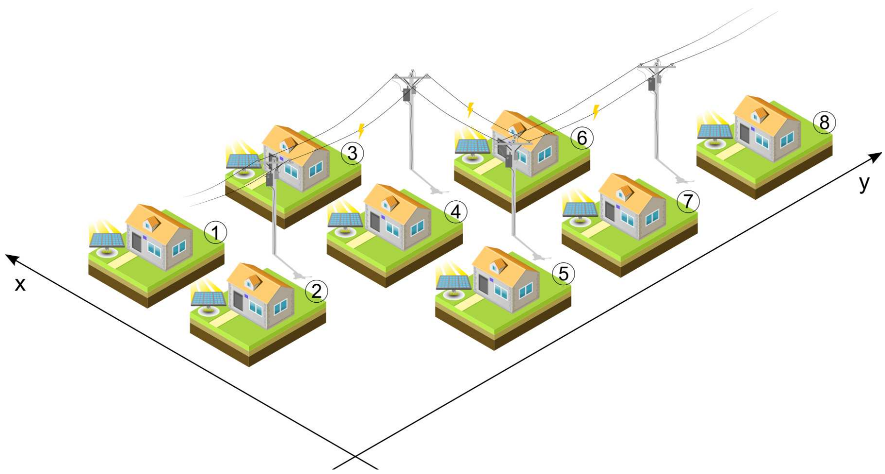

Figure 2.12: Reciprocal location of the 8 prosumers considered in the example: the distance between rows of houses is 0.5 km. This distance is taken into account for the losses in the distribution lines resulting from the local energy transfer.

Table 2.5: List of symbols employed in the description of the example.

Symbol	Description	Unit
$\bar{d}$	Demand	[kWh]
$\bar{p}$	Generation output	[kWh]
d^{grid}	Energy bought from the grid	[kWh]
p^{grid}	Energy sold to the grid	[kWh]
c^{grid}	Grid spot price	[CU]
v^{grid}	Feed-in tariff	[CU]
d^{coal}	Energy bought from the coalition	[kWh]
p^{coal}	Energy sold to the coalition	[kWh]
c^{coal}	Coalition spot price	[CU]
v^{coal}	Coalition feed-in tariff	[CU]
s	State of charge of the storage	[kWh]
Δs	Increment in the storage level	[kWh]

local demand and production, as well as to the changes in the energy prices.

Let us consider first the case in which the consumer nodes only rely on the main grid. For any node $i \in \mathcal{N}$, the energy exchange with the main grid is quantified by the variable x_i^{grid}, representing the difference $\bar{d}_i - \bar{p}_i$ between local demand and generation. Whenever $x_i^{\text{grid}} > 0$, node i buys energy $d_i^{\text{grid}} = x_i^{\text{grid}}$ from the grid—to fulfill the residual demand that cannot be matched by its local production—at the spot price c_i^{grid}. In case of local energy surplus instead, that is $x_i^{\text{grid}} < 0$, node i can sell energy p_i^{grid} to the grid at the feed-in tariff v_i^{grid}. We assume that both generation and demand profiles are deterministic, known beforehand within a 5-hour horizon. We also assume that the tariff scheme implemented by utility companies is always such that $c_i^{\text{grid}}(k) > v_i^{\text{grid}}(k)$. The local availability of a storage device allows the agent some flexibility when facing the spot prices imposed by the grid: the purchase and the sale of energy can be shifted in order to benefit from more convenient prices. At this point, the control problem individually addressed by each node would be (symbols are defined in Table 2.5)

$$\min_{\mathbf{u}_i} \sum_{t=0}^{N_p-1} c_i^{\text{grid}}(t|k) d_i^{\text{grid}}(t|k) - v_i^{\text{grid}}(t|k) p_i^{\text{grid}}(t|k), \tag{2.22a}$$

s.t.

$$s_i(t+1|k) = s_i(t|k) + \Delta s_i(t|k), \tag{2.22b}$$

$$\bar{d}_i(t|k) + \Delta s_i(t|k) + p_i^{\text{grid}}(t|k) = \bar{p}_i(t|k) + d_i^{\text{grid}}(t|k), \tag{2.22c}$$

$$d_i^{\text{grid}}(t|k), p_i^{\text{grid}}(t|k) \geq 0, \tag{2.22d}$$

$$s_i(t|k) \in [0, s_{i,\max}],\ t = 0, \ldots, N_p, \tag{2.22e}$$

$$s_i(0|k) = s_i(k). \tag{2.22f}$$

The manipulable inputs are $\mathbf{u}_i \triangleq [\Delta\mathbf{s}_i^\intercal, \mathbf{d}_i^\intercal, \mathbf{p}_i^\intercal]^\intercal$, where the bold notation indicates a vector containing the values along the prediction horizon. The monetary amount expressed by (2.22a) is the local balance of the energy exchange with the grid. Since the problem is formulated as a minimization, a positive balance indicates the expense required to buy energy from the grid, whereas a negative balance is the revenue from feeding energy to the grid. Constraints (2.22b)–(2.22f) represent, respectively, the dynamics of the storage, the energy balance at the node, the admitted values of inputs and storage level, and the initial state of charge.

Problem (2.22) is now modified taking into account the possibility for two or more nodes to agree over mutual exchange of energy, establishing a common pool of resources. The local variable $x_i^{\mathrm{coal}} \triangleq d_i^{\mathrm{coal}} - p_i^{\mathrm{coal}}$, whose components are the demand of energy to the coalition and the energy transferred to its members, describes such exchange. The objective function of the coalitional problem involves a component for the minimization of the costs of energy exchange with the main grid, and an additional component concerning the minimization of power losses due to transfers between members of the coalition.

$$\min_{\boldsymbol{\nu},\mathcal{C}} \rho_{\mathrm{coal}} \sum_{i,j\in\mathcal{C}} \sum_{t=0}^{N_p-1} r_{ij} \left(\frac{x_{ij}^{\mathrm{coal}}(t|k)}{2} \right)^2 + \sum_{i\in\mathcal{C}} \sum_{t=0}^{N_p-1} c_i^{\mathrm{grid}}(t|k) d_i^{\mathrm{grid}}(t|k) - v_i^{\mathrm{grid}}(t|k) p_i^{\mathrm{grid}}(t|k), \tag{2.23a}$$

s.t.

$$s_i(t+1|k) = s_i(t|k) + \Delta s_i(t|k),\ i \in \mathcal{C} \tag{2.23b}$$

$$\bar{d}_i(t|k) + \Delta s_i(t|k) + p_i^{\mathrm{grid}}(t|k) + p_i^{\mathrm{coal}}(t|k) = \bar{p}_i(t|k) + d_i^{\mathrm{grid}}(t|k) + d_i^{\mathrm{coal}}(t|k),\ i \in \mathcal{C}, \tag{2.23c}$$

$$\sum_{i\in\mathcal{C}} p_i^{\mathrm{coal}}(t|k) = \sum_{i\in\mathcal{C}} d_i^{\mathrm{coal}}(t|k), \tag{2.23d}$$

$$d_i^{\mathrm{grid}}(t|k), p_i^{\mathrm{grid}}(t|k) \geq 0,\ i \in \mathcal{C}, \tag{2.23e}$$

$$s_i(t|k) \in [0, s_{i,\max}],\ t = 0, \ldots, N_p,\ i \in \mathcal{C} \tag{2.23f}$$

$$s_i(0|k) = s_i(k),\ i \in \mathcal{C}, \tag{2.23g}$$

$$\mathcal{C} \subseteq \mathcal{N}, \tag{2.23h}$$

where x_{ij}^{coal} is the interchange of energy among the pair of agents $i, j \in \mathcal{C}$, and r_{ij} is their relative Euclidean distance. The coalitional energy transfer $d_i^{\mathrm{coal}} - p_i^{\mathrm{coal}}$ is taken into account in the balance constraints (2.23c). Constraint (2.23d) expresses the zero sum energy balance of the coalition.

Given its complexity, problem (2.23) is approximated here by splitting it in two subproblems, each one concerning one of the two components of the objective function. So, for any $\mathcal{C} \subseteq \mathcal{N}$, the first subproblem is formulated as:

$$\min_{\boldsymbol{\nu}} \mathbf{J} = \sum_{i \in \mathcal{C}} \sum_{t=0}^{N_p-1} c_i^{\text{grid}}(t|k) d_i^{\text{grid}}(t|k) - v_i^{\text{grid}}(t|k) p_i^{\text{grid}}(t|k), \tag{2.24}$$

subject to (2.23b)–(2.23g). The resulting energy transfers are accompanied by energy losses over the distribution lines. An approximation of their value is added to $\mathbf{J}$ as

$$\mathbf{J}^{\chi} = \rho_{\text{coal}} \hat{r} \sum_{i \in \mathcal{C}} (d_i^{\text{coal}})^2, \tag{2.25}$$

where $\hat{r}$ is a representative mean distance between every pair of coalition members, and d_i^{coal} is the energy demanded to the coalition by agent i. Finally, the value $v(\mathcal{C})$ of any given coalition $\mathcal{C} \subseteq \mathcal{N}$ (recall that $v : 2^{\mathcal{N}} \mapsto \mathbb{R}$ is the function mapping any possible coalition of agents into a real value) is defined as $v(\mathcal{C}) \triangleq \mathbf{J} + \mathbf{J}^{\chi}$, where (2.25) represents the cost of forming the coalition.

Now, the second subproblem consists in finding the partition $\mathcal{P} = \{\mathcal{C}_1, \ldots, \mathcal{C}_{N_c}\}$ of $\mathcal{N}$ such that the preference of every agent is satisfied according to the Pareto order. In order to do this, individual payoffs within each possible subset of agents $\mathcal{S} \subseteq \mathcal{N}$ are first calculated as those defined by the Shapley value $\phi^{\mathcal{S}} : \mathbb{R}^{2^{|\mathcal{S}|}} \mapsto \mathbb{R}^{|\mathcal{S}|}$. Thus, for $i \in \mathcal{S}$:

$$\phi_i^{\mathcal{S}}(v) = \sum_{\mathcal{C} \subseteq \mathcal{S} \setminus \{i\}} \frac{|\mathcal{C}|!(|\mathcal{S}| - |\mathcal{C}| - 1)!}{|\mathcal{S}|!} \left[v(\mathcal{C} \cup \{i\}) - v(\mathcal{C}) \right]. \tag{2.26}$$

Note how the marginal contribution $v(\mathcal{C} \cup \{i\}) - v(\mathcal{C})$ is weighted by the probability for any agent i of joining the coalition $\mathcal{C} \subseteq \mathcal{S} \setminus \{i\}$, in case the agents form the coalition $\mathcal{S}$ in a random order: in this way, the value assigned by Shapley's criterion corresponds to the individual *expected* marginal contribution.

Once this step is accomplished, a mapping $\Phi : \mathcal{N} \times 2^{\mathcal{N}} \mapsto \mathbb{R}$ of the individual payoff for each possible coalition the agent $i \in \mathcal{N}$ can participate in is available. At time step k, $\Phi(i, \mathcal{C}, k)$ defines the cost (or the benefit) incurred by agent i by participating in the coalition $\mathcal{C} \subseteq \mathcal{N}$. Note that such payoff will coincide with the cost of energy exchange with the main grid ($\Phi(i, \{i\}, k) \equiv c_i^{\text{grid}}(k) d_i^{\text{grid}}(k) - v_i^{\text{grid}}(k) p_i^{\text{grid}}(k)$) in case the agent does not participate in any coalition. On the other hand, if the agent is member of a coalition, the *equivalent* price payed/earned on the coalition's internal market can be

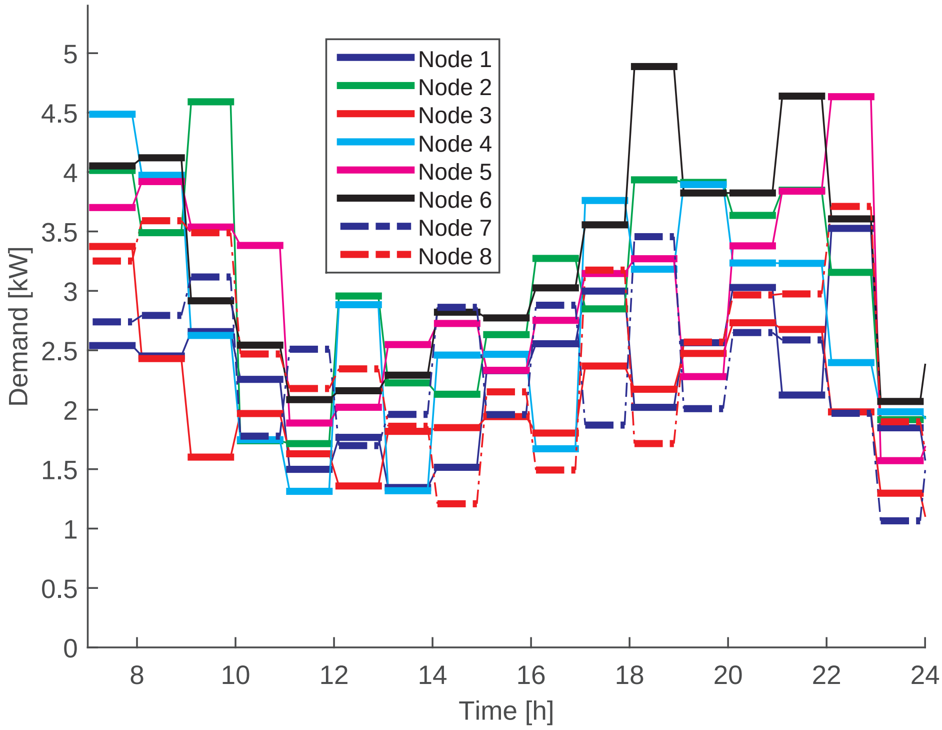

Figure 2.13: Daily demand patterns considered in the simulations for the 8 nodes.

derived as:

$$c_i^{\text{eq}}(k) \triangleq \frac{\Phi(i, \mathcal{C}, k)}{x_i^{\text{grid}}(k) + x_i^{\text{coal}}(k)} \left[\frac{\text{CU}}{\text{kWh}}\right], \tag{2.27}$$

where CU stands for currency unit. Such mapping provides each agent with a preference order over the coalitions he wishes to join. Since any agent can be in one coalition at a time (coalitions do not overlap), the agents will organize themselves into a partition $\mathcal{P}^*$ *following the preference order dictated by* Φ.

2.6.2 Results

The demand and generation patterns considered in the simulation are depicted in Figures 2.13 and 2.14. Grid spot prices are shown in Figure 2.15, relative to the purchase (top) and feed-in (bottom). The interval 7 a.m.–24 p.m. is considered in the simulations. A time step of 1 h and a prediction horizon $N_p = 5$ h are employed in the optimization problem. We assume the possibility for each node to access the grid with different prices, to emulate the presence of multiple utility companies. Notice that this means that coalitions do not merely consist of a combination of nodes with a surplus of power and nodes that are in need of additional power to meet their demand.

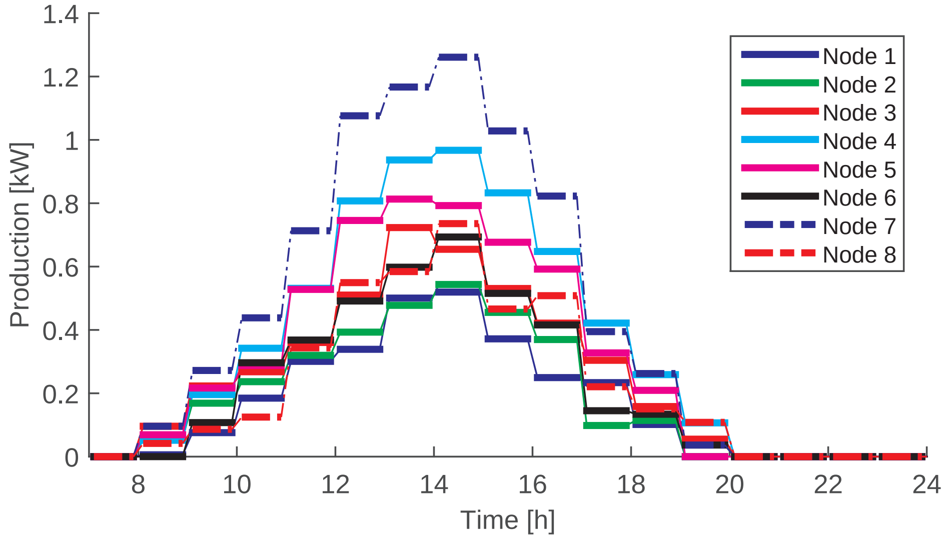

Figure 2.14: Generation profiles considered in the simulations for the 8 nodes.

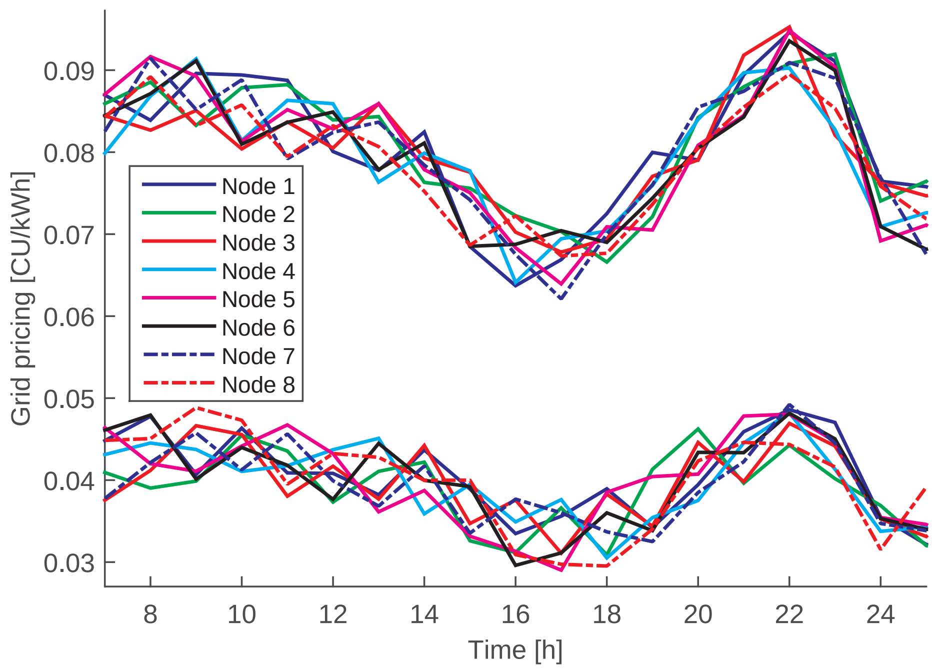

Figure 2.15: Grid spot prices relative to the energy purchase (top) and excess of production sale (bottom).

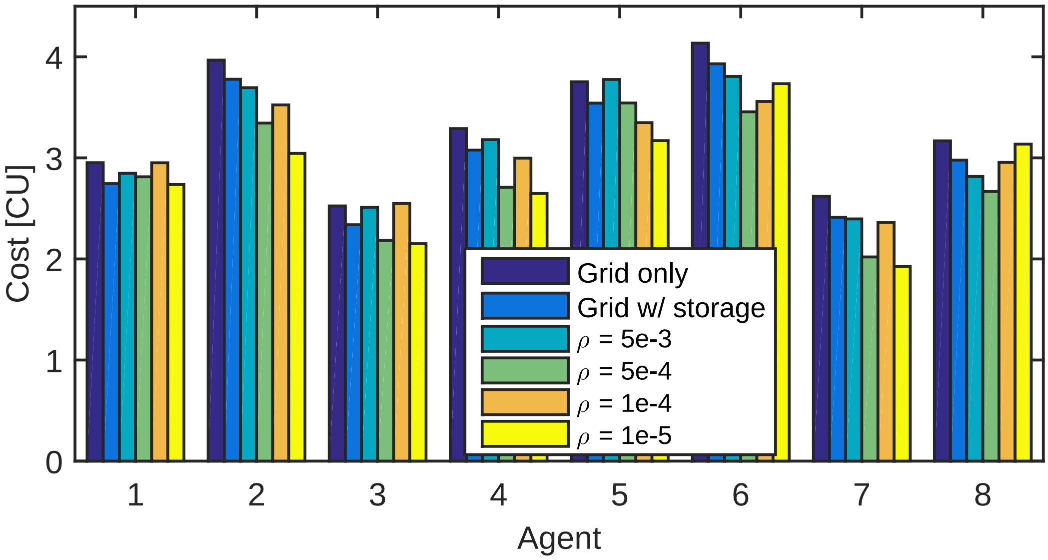

Figure 2.16: Comparison of the accumulated costs incurred by each agent during the entire simulated interval, over different scenarios: *Grid only* no coalitions, no storage; *Grid w/ storage* local storage available; $10^{-5} \leq \rho_{\text{coal}} \leq 5 \cdot 10^{-3}$ coalitions with different costs for power losses. The choice over which coalition to form is made on performances predicted over an horizon N_p of several time steps. In particular, the aggregate performance is evaluated, and predictions are not required to be favorable at all time steps. However, nodes can change their affiliation at each time step. This may lead to the accumulation of monetary losses. This phenomenon becomes more visible as the penalty for energy losses ρ_{coal} increases, since it implies less stability of coalitions in time.

Indeed, nodes can make agreements to get access to the main grid through the more advantageous tariff of another node. The evolution of the coalitions, under different penalties ρ_{coal} for energy losses, is shown in Figure 2.17. By recomputing the mapping $\Phi(i, \cdot, k)$, agents can reconsider their affiliation at each time step. When costs for local energy transfers are significant, coalitions typically involve a restricted number of neighboring agents. On the other hand, big cooperating clusters form when penalties for power losses are low. The costs incurred by the agents for the whole simulated interval are shown in Figure 2.16. As expected, internal transfers' power losses affects the final result. The high costs for agents 6 and 8 with $\rho_{\text{coal}} = 10^{-5}$ can be ascribed to the fact that they are mostly left out of coalitions, as can be seen in Figure 2.17d. Furthermore, recall that the payoff mapping, and thus the decision whether to join a coalition, is based on a forecast along the horizon $N_p = 5$ h (see (2.24)). However, since agents are allowed to join/leave coalitions every time step, possible monetary losses taking place in the short term may accumulate (this issue is pointed out in [49] as well). The realizations of the equivalent prices during the simulations are shown in

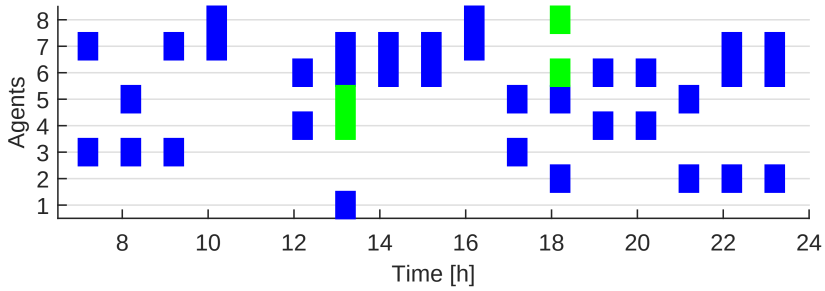

(a) $\rho_{\text{coal}} = 5 \cdot 10^{-3}$

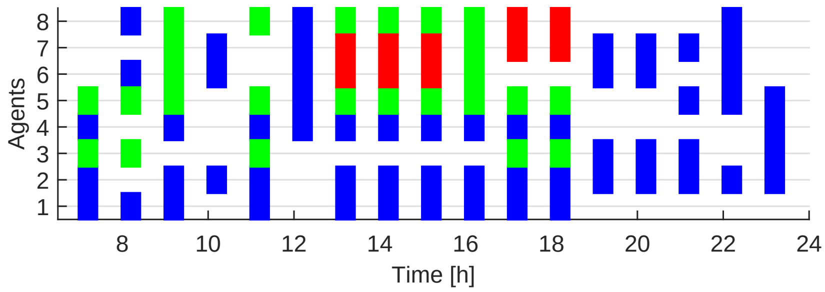

(b) $\rho_{\text{coal}} = 5 \cdot 10^{-4}$

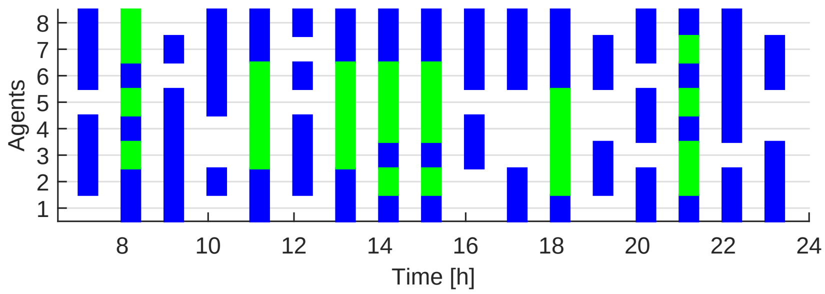

(c) $\rho_{\text{coal}} = 10^{-4}$

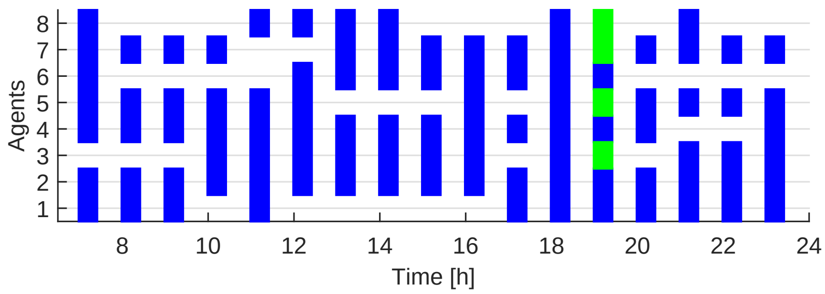

(d) $\rho_{\text{coal}} = 10^{-5}$

Figure 2.17: Evolution of the coalitions among the nodes, under different penalties ρ_{coal} for energy losses. Nodes marked with the same color belong to the same coalition. Agents are allowed to reevaluate their affiliation at each time step, by updating the preference mapping $\Phi(i, \cdot, k)$. When costs for local energy transfers are significant, coalitions typically involve a restricted number of neighboring agents. Conversely, big cooperating clusters form when penalties for power losses are low.

Table 2.6: Comparison of the average prices (in [CU/kWh]) paid by each agent. The figures in the third column are the equivalent average prices relative to the coalitions' internal market. See how, in reference to the tariffs in Figure 2.15, both buyers and sellers are benefited by the local energy market. Demand can be satisfied at prices lower than those offered by the main grid, and supply gets better value on the local market.

Agent	Grid only no storage	Grid only w/ storage	Coalitions ($\rho = 10^{-5}$)
1	0.0817	0.0787	0.0784
2	0.0813	0.0795	0.0603
3	0.0810	0.0782	0.0653
4	0.0812	0.0784	0.0620
5	0.0822	0.0797	0.0714
6	0.0805	0.0784	0.0745
7	0.0810	0.0776	0.0620
8	0.0810	0.0786	0.0798

Table 2.6. Comparing the average prices resulting by the coalitions' internal market with the grid tariffs in Figure 2.15, it is clear that the Shapley allocation benefits both buyers and sellers. Buyers can access energy at prices more affordable than those offered by the main grid, while sellers can achieve a higher profit on the local market.

In conclusion, local energy trade has been induced among consumers within a small geographical areas through the implementation of a coalitional control scheme. Power losses over the distribution lines can be taken into account in the coalition formation mechanism. Naturally, the larger the number of agents participating in such scheme, the higher the chance to match demand and supply among them, resulting in a higher profitability of the coalitions.

CHAPTER 3

Autonomous coalition formation

3.1 Introduction

Major challenges in control are in dealing with the increasing heterogeneity of networked systems—possibly characterized by decentralized management, a certain degree of autonomy of the parts and dynamic structure reconfiguration possibilities [88]. In such setting selfish interests may assume a dominant role, significantly influencing the way systems are managed, and their resulting performance. This issue is especially evident in public infrastructures, often co-owned by independent entities, and whose management requires a trade-off among sectors in direct competition [2, 15].

This constitutes an impulse to new approaches to distributed control problems, where the cooperation between networked controllers is actively fostered and adapted in real-time to the state of the system, by characterizing the improvement provided by a broader feedback information [89, 90].

Methods for the analysis of the relevance of the agents and data links involved in the distributed control of a complex network system have been recently studied by [91, 27, 26]. The structural information about the system provided by these methods allows the available control resources to be efficiently allocated, promoting sparsity in order to minimize computational and communicational requirements [92]. A step further is the *online* identification of the optimal controller structure: besides accommodating the controller requirements in real-time [93], such flexibility grants the possibility of reconfiguring the system for improving robustness or fault-tolerance [94], or even for featuring plug-and-play capabilities [95]. The notion of *cooperating sets* of controllers is employed in [33, 39]. At each time step, one controller locally computes the optimal control actions for all the controllers belonging to the same cooperating set. Although only the local input sequence is broadcast, the individual strategy is optimized considering what others may be able to achieve, so cooperation is indirectly promoted by favoring the best plans for everyone within the cooperating set. The composition of such sets is updated according to a graph representing the active coupling constraints.

The work of [10] investigates the design of a hierarchical model predictive control (MPC) scheme characterized by flexibility over the use of the data network through which the local control agents exchange information. In particular, the sparsity pattern of the overall MPC problem is dynamically adjusted so as to optimize the requirements over the data link usage.

A cooperative distributed MPC scheme considering local objectives is presented in [43]: the cost incurred by each local controller is dynamically adjusted to fulfill minimum local requirements—through an online adaptation of the local objectives priority along the Pareto front—on the basis of situational altruism criteria. In [44] the hierarchy of the agents can be rearranged, adapting the order followed in the optimization of the control actions to different operational conditions.

While in the aforementioned works the cooperation in the achievement of the global objective is not questioned, we assume that the agents controlling the system base their cooperation on the *individual rationality* criterion: they will be willing to cooperate only if the expected individual benefit derived through cooperation exceeds the one achieved by following a unilateral strategy (local control). To address such individual rationality concerns we propose a new approach to *coalitional control* [61]. Coalitional control extends the scope of advanced control methods (in particular model predictive control) by drawing concepts from cooperative game theory that are suited for heterogeneous, competitive environments, also providing an economical interpretation useful to explicitly take into account possible selfish interests.

In particular, a bottom-up approach to coalitional control is proposed here: coalitions are the outcome of an autonomous pairwise bargaining procedure, through which the structure of each agent's controller can be adapted to the time-variant coupling conditions. This procedure follows ad-hoc criteria, formulated on the basis of both cooperative control and game-theoretical fundamentals [8, 55]. We address the distribution of the value of a given coalition among its components by means of a method guaranteeing coalition-wise stability, provided that the *core*, i.e., the set of stable allocations, of the associated transferable-utility (TU) game is nonempty. More specifically, we formulate an iterative transfer scheme, local to each coalition, that redistributes the benefit to compensate the dissatisfaction of subset of members over their assigned payoff [96, 97]. If the value allocated in excess to the complementary subset of players is not sufficient to compensate the demanded amount, the coalition divides.

Other recent works are contributing to bringing dynamical aspects into the coalitional TU games framework, conventionally developed for static decision environments. A decentralized algorithm for benefit redistribution among cooperating agents is proposed in [98]. The bargaining protocol is run on a time-varying communication graph, and the resulting allocation is proven to converge to a stable one, that is, satisfying all players. The work of [45] provides a cooperative MPC formulation where cooperation is subject to bargaining. The satisfaction of a minimum individual performance is imposed by a *disagreement point*, defined as the threshold of maximum allowed loss of performance in case of cooperation.

The use of incentive mechanisms from game theory is being studied for traffic or service demand reshaping [99], also in competing markets like electric vehicles (EVs) recharge [50, 100]. In [53], self-organizing coalitions among EVs are considered as a means to enhance the predictability of the vehicle-to-grid offer, by presenting a wider energetic portfolio to the grid operator. Analogously, the work of [49] studies the formation of coalitions among wind energy producers with the objective of reducing the output variability in the aggregate offer, and so improve their expected profit. The authors of [15] investigate how the equilibrium can be reached in an EV recharging market whose actors are (coalitions of) charging stations and EV users.

The rest of this chapter is organized as follows: in Section 3.2.1 the control problem is stated, while the ingredients employed for autonomous coalition formation are described in Section 3.3. Then, the bargaining protocol is presented in Section 3.4, and its associated utility transfer scheme is discussed in 3.5. Finally, in Section 3.6, this coalitional control architecture is demonstrated on a wide-area control application for a power grid, with the objective of minimizing frequency deviations and undesired inter-area power transfers.

3.2 Problem statement

3.2.1 System description

Consider a system that can be described as a set $\mathcal{N}$ of dynamically coupled linear processes, each modeled by the following discrete-time state-space equation:

$$x_i(k+1) = A_{ii}x_i(k) + B_{ii}u_i(k) + w_i(k), \tag{3.1a}$$

$$w_i(k) = \sum_{j\in\mathcal{M}_i} A_{ij}x_j(k) + B_{ij}u_j(k), \tag{3.1b}$$

where $x_i \in \mathbb{R}^{n_i}$ and $u_i \in \mathbb{R}^{q_i}$ are respectively the state and input vectors of subsystem $i \in \mathcal{N}$, constrained in the sets $\mathcal{X}_i$ and $\mathcal{U}_i$ respectively. Indices $j \in \mathcal{M}_i$ designate *neighbor* subsystems, i.e., those whose state and/or inputs influence the trajectory of x_i. The neighborhood set is defined as

$$\mathcal{M}_i = \{j \in \mathcal{N} \setminus \{i\} |\, A_{ij} \neq \mathbf{0} \vee B_{ij} \neq \mathbf{0}\}\,. \tag{3.2}$$

Models analogous to (3.1) have been employed for the control of real large-scale systems such as drinking water networks composed of interconnected water tanks [67], irrigation canals, modeled as integrator-delay cascades [76, 10, 72], supply chains [101, 38], traffic networks and power grids [102].

Denoting the global state as $x = (x_i)_{i\in\mathcal{N}} \in \mathbb{R}^n$ and the global input as $u = (u_i)_{i\in\mathcal{N}} \in \mathbb{R}^q$, the state evolution of the whole system of systems is governed by the following equation

$$x(k+1) = Ax(k) + Bu(k), \tag{3.3}$$

where $A = [A_{ij}]_{i,j\in\mathcal{N}} \in \mathbb{R}^{n\times n}$ and $B = [B_{ij}]_{i,j\in\mathcal{N}} \in \mathbb{R}^{n\times q}$.

3.2.2 Exchange of information

Each subsystem is governed by a control agent. Controllers can communicate through a network infrastructure schematized by the graph $\mathcal{G}(k) = (\mathcal{N}, \mathcal{E}(k))$, where $\mathcal{E}(k) \subseteq \mathcal{N} \times \mathcal{N}$ is the set of links. The time dependence of $\mathcal{E}(k)$ reflects the possibility of establishing cooperation links at any given time step k. From a global standpoint, the description provided by $\mathcal{G}(k)$ delineates a partition $\mathcal{P}(\mathcal{N}, \mathcal{G}(k)) = \{\mathcal{C}_1, \ldots, \mathcal{C}_{N_c}\}$ of the set of controllers into N_c connected components, referred to as coalitions, such that $\mathcal{C}_i \subseteq \mathcal{N}$, $\mathcal{C}_i \cap \mathcal{C}_j = \varnothing$, $\forall i, j \in \{1, \ldots, N_c\}, i \neq j$, and $\bigcup_{i=1}^{N_c} \mathcal{C}_i = \mathcal{N}$ [46, 103]. The number of coalitions N_c pertains to the interval $[1, |\mathcal{N}|]$, whose extremes correspond to the centralized control case, and the case where each subsystem "forms a coalition" on its own ($|\cdot|$ denotes the cardinality of a set). For the sake of readability, let us define the set $\mathcal{S}_{\mathcal{P}} = \{1, \ldots, N_c\}$ indexing the coalitions characterizing the current partition of the system. The dynamics (3.1) of all subsystems relative to a given connected component $r \in \mathcal{S}_{\mathcal{P}}$ can be aggregated as

$$\xi_r(k+1) = \mathbf{A}_{rr}\xi_r(k) + \mathbf{B}_{rr}\nu_r(k) + \varpi_r(k), \tag{3.4}$$

with $\xi_r = (x_i)_{i\in\mathcal{C}_r}$ the aggregate state vector, and $\mathbf{A}_{rr} = [A_{ij}]_{i,j\in\mathcal{C}_r}$ the relative state transition matrix, describing the state coupling between members of the same coalition. The vector ν_r and the matrix $\mathbf{B}_{rr}$ are derived analogously. Finally, the vector

$$\varpi_r = \{w_i\}_{i\in\mathcal{C}_r} \tag{3.5e}$$

gathers the disturbances due to the coupling with subsystems external to $\mathcal{C}_r$.[1] Following (3.1b) it holds that

$$w_i = \sum_j A_{ij}x_j(k) + B_{ij}u_j(k), \text{with } j \in \mathcal{M}_i \setminus \mathcal{C}_r, \tag{3.5f}$$

pointing out how, for each $i \in \mathcal{C}_r$, the set of unknown coupling from neighboring subsystems is reduced to the neighbors left out of the coalition. That is, from the coalition standpoint, the uncertainty comes from subsystems $j \in (\bigcup_{i\in\mathcal{C}_r} \mathcal{M}_i) \setminus \mathcal{C}_r$.

3.2.3 Control objective

A central point in this discussion is the assumption that the control agents act in order to minimize their local stage cost (3.6) over a decentralized noncooperative MPC architecture. In a game-theoretical perspective, this translates in considering *rational* and *selfish* agents. The performance of each controller $j \in \mathcal{N}$ is measured through the following stage cost:

$$\begin{aligned}\ell_j(k) = (x_j(k) - \bar{x}_j)^\intercal Q_j(x_j(k) - \bar{x}_j)\\ + (u_j(k) - \bar{u}_j)^\intercal R_j(u_j(k) - \bar{u}_j),\end{aligned} \tag{3.6}$$

where the matrices $Q_j \geq 0$ and $R_j > 0$ weight the deviation of state and input from their reference $\bar{x}_j$ and $\bar{u}_j$, respectively.

[1] In case of singleton coalition, i.e., $\mathcal{C} \equiv \{i\}$, the description given by (3.4) coincides with (3.1).

Cooperation is introduced within each connected component $i \in \mathcal{S}_{\mathcal{P}}$ through the definition of the coalitional stage cost (3.7). The cooperation carried out by coalition members $j \in \mathcal{C}_i$ may vary from a mere sum of local costs to a different cooperative objective (as seen in the example in Section 3.6).

$$\boldsymbol{\ell}_i(k) = (\xi_i(k) - \bar{\xi}_i)^\intercal \mathbf{Q}_i(\xi_i(k) - \bar{\xi}_i) + (\nu_i(k) - \bar{\nu}_i)^\intercal \mathbf{R}_i(\nu_i(k) - \bar{\nu}_i), \tag{3.7}$$

where $\mathbf{Q}_i$ and $\mathbf{R}_i$ are properly sized weighting positive (semi-)definite matrices. At time k, a control sequence for $\mathcal{C}_i$ is derived from the (joint) solution of the MPC problem[2]

$$\min_{\boldsymbol{\nu}_i} J_i = \sum_{t=0}^{N_p-1} \boldsymbol{\ell}_i(t|k) + \boldsymbol{\ell}_i^{\mathrm{f}}(N_p|k) \tag{3.8a}$$

s.t.

$$\xi_i(t+1|k) = \mathbf{A}_{ii}\xi_i(t|k) + \mathbf{B}_{ii}\nu_i(t|k) + \varpi_i(t|k), \tag{3.8b}$$

$$\xi_i(t|k) \in \Xi_i,\ t = 0, \dots, N_p, \tag{3.8c}$$

$$\nu_i(t|k) \in \Psi_i,\ t = 0, \dots, N_p - 1, \tag{3.8d}$$

$$\xi_i(0|k) \equiv \xi_i(k), \tag{3.8e}$$

$$\varpi_i(t|k) = \hat{\varpi}_i(k+t),\ t = 0, \dots, N_p - 1, \tag{3.8f}$$

where $\boldsymbol{\ell}_i^{\mathrm{f}}(N_p|k)$ denotes the terminal cost, and $\Xi_i = \mathcal{X}_1 \times \mathcal{X}_2 \times \dots \mathcal{X}_{|\mathcal{C}_i|}$ is the Cartesian product of the local state constraints relative to each member of the coalition (an analogous definition holds for the input constraint set Ψ_i). The problem is solved independently for each coalition $\mathcal{C}_i \in \mathcal{P}(\mathcal{N}, \mathcal{G}(k))$: in case of absent/partial information exchange, the inputs and the state of neighboring agents are unknown and problem (1.9) has to be solved over an estimated $\hat{\varpi}_i$.

Remark 3.1. *Notice that the estimation of ϖ_i may not be mandatory for local control purposes. However, our algorithm for autonomous coalition formation is based on predicted outcomes. For this reason, an estimate of the influence of neighboring subsystems is needed. In this work, in order to improve the reliability of the decisions on coalition formation/split, the knowledge of the interaction model—exchanged by the agents for the evaluation of a merger—is exploited in the algorithm. Details are given in Section 3.3.2.*

The minimizer of $\mathbf{J}_i$ over the prediction horizon of length N_p in (3.8a) is the column

[2]Several algorithms are available for the distributed solution of (3.8), see e.g. [42].

vector

$$\boldsymbol{\nu}_i \triangleq [\nu_i(0|k) \ \dots \ \nu_i(N_p - 1|k)].$$

At time k the first element of the minimizing sequence is applied to every subsystem involved in the coalition, i.e., $\nu_i(k) \triangleq \nu_i^*(0|k) \equiv (u_j(0|k)^*)_{j\in\mathcal{C}_i}$, and (1.9) is solved again at subsequent time instants in a receding horizon fashion [104, 105].

Assumption 3.1. *The triple* $(A_{ii}, B_{ii}, Q_i^{1/2})$, $\forall i \in \mathcal{N}$, *is stabilizable and detectable. Moreover, we assume that the dynamic interaction between subsystems is bounded such as to allow the system to be globally stabilized through the solution of the decentralized MPC problem defined by* (1.9), *with* $\mathcal{C}_i \equiv \{i\}$, $\forall i \in \mathcal{N}$.

By means of the autonomous coalition generation framework considered in the remainder, agents will be able to expand their knowledge of the rest of the system and to jointly agree on the value assigned to the inputs.

3.3 Coalitional control

The scenario introduced in the previous section admits the establishment of a flexible degree of cooperation over coalitions of agents. Cooperation within a controlled system translates into better performances [8], at the expense of higher communicational and computational requirements. In many cases, constraints on the use of such resources have to be taken into account. For instance, the size of the control problem—also related to the level of detail of the subsystems' interactions model—may not be manageable at some point because of, e.g., timing requirements imposed by the system dynamics, constraints on the communication channel and/or on the available computation resources. It is expected that the effort required for the coordination increases with the number of agents involved in a coalition. Costs incurred for cooperation can be taken into account by means of ad-hoc indices related to, e.g., the size of the coalition, the number of data links needed to establish communication between every member [9, 10], their distance [61]. Whenever such costs are comparable with the stage cost (3.7), the evolution of the overall controller architecture can be steered by trading off control performance for savings on coordination costs.

The presence of an omniscient supervisor is not assumed here, and the cooperation between two given parts is established *autonomously*, according to the dynamic behavior of the system and to given agreements on the redistribution of the benefit achieved. Two parties that commit to acting coordinately can at any time revert to the previous state or extend the cooperation to other agents, allowing for a *dynamically evolving* *coalitional structure.*

From now on, the term *player* may refer to either a single control agent or a group of agents that, as a consequence of their participation in the same coalition, act as a single entity. In order to keep the notation simple, indices $\{1, 2\}$ will be used to designate the parties of the bargaining process for the formation of a (bigger) coalition;[3] furthermore, the notation $\{1{\cup}2\}$ will refer to their merger. The subsystems involved in either part of a given bargaining process are identified by the sets $\mathcal{P}_1 \in \mathcal{P}(\mathcal{N}, \mathcal{G}(k))$ and $\mathcal{P}_2 \in \mathcal{P}(\mathcal{N}, \mathcal{G}(k)) \setminus \mathcal{P}_1$. The set of merging subsystems will be designated as $\mathcal{P}_{1\cup 2} \triangleq \mathcal{P}_1 \cup \mathcal{P}_2$.

Following the notation introduced in Section 3.2.2, the states and inputs of every subsystem taking part in the bargaining process are gathered into the player's state and input vectors, defined as $\xi_i \triangleq (x_i)_{j\in\mathcal{P}_i}$, $\nu_i \triangleq (u_j)_{j\in\mathcal{P}_i}$, where $\xi_i \in \mathbb{R}^{\mathbf{n}_i}$, $\mathbf{n}_i = \sum_{j\in\mathcal{P}_i} n_j$ and $\upsilon_i \in \mathbb{R}^{\mathbf{q}_i}$, $\mathbf{q}_i = \sum_{j\in\mathcal{P}_i} q_j$, $i \in \{1, 2\}$. Finally, the merger state and input vectors are composed as $\xi_{1\cup 2} = (\xi_1, \xi_2)$, $\nu_{1\cup 2} = (\nu_1, \nu_2)$.

Next, the objective is to establish a possible criterion for endogenous coalition formation, oriented at dynamically-coupled networks of systems, featuring the redistribution of the benefits derived from cooperation. Starting from a discussion of the performance improvement offered by cooperative control, viewed as coalitional benefit, we point out the issues of the absence of redistribution of such benefit from the individual control agent's standpoint. Then, we propose a solution based on the equal division of the benefit between the players.

3.3.1 Evaluation of coalitional benefit

As mentioned earlier, the structure of each agent's MPC controller is allowed to evolve according to the time-variant coupling conditions of the system. Such evolution is the outcome of a bargaining procedure over the formation of a coalition between any two players. The bargaining is based on an index accounting for both control performance and cooperation-related costs:

$$J_i = \sum_{t=0}^{N_b} \boldsymbol{\ell}_i(t|k) + N_b \chi_i(k), \quad i \in \{1, 2, 1{\cup}2\}. \tag{3.9}$$

The first term evaluates the stage cost (3.7) associated with either the merger or the individual players' over a *bargaining horizon* of length N_b. Since we assume the agents free to switch their membership between coalitions at any given time step (coalition is

[3] The case of split will be considered later in this document.

not binding for the entire horizon length N_p), the possible outcomes of the bargaining procedure can be evaluated over a shorter time slot, i.e., $N_b \leq N_p$. In the second term, $\chi_i(k) = f(|\mathcal{P}_i|, |\mathcal{E}_i(k)|)$ expresses the cooperation costs for coalition $\mathcal{P}_i$—assumed comparable with the stage cost (3.7)—where $\mathcal{E}_i(k) \subseteq \mathcal{E}(k)$ is the subset of edges of the graph $\mathcal{G}(\mathcal{N}, \mathcal{E}(k))$ connecting the nodes in $\mathcal{P}_i$. Notice that for $i \in \{1, 2\}$ the costs expressed by χ_i involve only player i internal connections.

The predicted state and input sequences used in the computation of (3.9) are obtained as solution of the MPC problem (1.9) for the three possible cost functions associated to $i \in \{1, 2, 1{\cup}2\}$, where $\boldsymbol{\ell}_i(t|k)$ is the stage cost (see Section 3.2.3) predicted on the basis of the knowledge available within either set of agents $\mathcal{P}_i$ if $i \in \{1, 2\}$ or, in case of merger, the joint knowledge provided by $\mathcal{P}_1 \cup \mathcal{P}_2$.

3.3.2 Joint benefit through cooperation

A necessary condition for the coalition $\mathcal{P}_1 \cup \mathcal{P}_2$ to form is that its predicted cost (3.9) outperforms the aggregate cost resulting from unilateral strategies:

$$J_{1\cup 2} \leq J_1 + J_2. \tag{3.10}$$

Remark 3.2. *Any new coalition will be product of the union of two players,* and thus of all agents they involve*. The present approach is based on the performance of the player as a whole and not on that of its individual components. This approximation avoids the combinatorial explosion of the possible configurations that would arise otherwise. Local performance concerns are addressed later in this document.*

Example 3.1. *The procedure presented so far is illustrated on a simple example, which will be utilized to set the point for further discussion as well. Consider a pair of agents controlling two input-coupled unidimensional linear systems whose dynamics conform to* (3.1)*. In particular, the state trajectory $x_i \in \mathbb{R}$ of the ith system responds to*

$$x_i(k+1) = A_{ii}x_i(k) + B_{ii}u_i(k) + B_{ij}u_j(k), \tag{3.11}$$

for $i, j \in \{1, 2\}$, $i \neq j$. $A_{11} = A_{22} = 0.99$, $B_{11} = 0.2$, $B_{12} = 0.4$, $B_{21} = 0.15$ and $B_{22} = 0.3$; weights are chosen as $Q_i = 1$ and $R_i = 10$, $i \in \{1, 2\}$. Inputs are constrained to the interval $\mathcal{U}_i = [-0.2, 0.2]$. The matrices relative to the merger correspond to $\mathbf{A}_{1\cup 2} = \mathrm{diag}(A_{11}, A_{22})$, $\mathbf{B}_{1\cup 2} = [B_{ij}]_{i,j\in\{1,2\}}$, and $\mathbf{Q}_{1\cup 2} = \mathrm{diag}(\{Q_i\})$, $\mathbf{R}_{1\cup 2} = \mathrm{diag}(\{R_i\})$, $i \in \{1, 2\}$. Cooperation costs are considered null.

We assume that both agents base their decisions over the unilateral strategies on

Table 3.1: Example 3.1. Expected and actual costs.

	J_1	J_2	$J_1 + J_2$	$J_{1\cup 2}$
$\hat{u}_j \leftarrow \min\max$	25.200	24.579	49.779	**48.975**
$\hat{u}_j = 0$	24.405	24.284	**48.689**	48.975
actual	*24.992*	*24.432*	*49.424*	**48.975**

the worst-case MPC cost, with prediction horizon $N_p = 1$. Hence, the performance of the merger ($i = 1\cup 2$) is evaluated through the solution of (1.9)*, whereas the following problem is solved for $i \in \{1, 2\}$ in order to evaluate the expected performance of the unilateral strategies.*

$$\min_{\mathbf{u}_i} \max_{\mathbf{u}_j} \sum_{t=0}^{N_p-1} \ell_i(t|k) + \ell_i^{\mathrm{f}}(N_p|k),\ j \in \{1, 2\} \setminus \{i\}, \tag{3.12a}$$

s.t.

$$x_i(t+1|k) = A_{ii}x_i(t|k) + B_{ii}u_i(t|k) + B_{ij}u_j(t|k), \tag{3.12b}$$

$$u_i(t|k) \in \mathcal{U}_i,\ t = 0, \dots, N_p - 1, \tag{3.12c}$$

$$u_j(t|k) \in \mathcal{U}_j,\ t = 0, \dots, N_p - 1, \tag{3.12d}$$

$$x_i(0|k) = x_i(k). \tag{3.12e}$$

The figures in Table 3.1 are obtained from an initial condition $x^0 = (5, -5)$. The first row reports the expected values, whereas the last row the costs actually achieved by implementing the control inputs relative to each strategy. Since condition (3.10) *is fulfilled for the values in the first row of Table 3.1, the merger is formed.*

Neglecting other players' actions is generally not a reasonable option in such coupled systems, since it means completely ignoring their effect—either beneficial or detrimental—on the actual performance of the unilateral strategies. This may lead to mistakenly considering these as the most profitable to implement. For instance, the second row of Table 3.1 shows that condition (3.10) *is not verified and the merger is rejected.*■

At this point, it is clear that useful predictions can only be achieved if some knowledge about the unilateral strategies is available to both parties. Different techniques can be applied for their estimation (e.g., worst-case predictions, as in the example above): this point, however, goes beyond the scope of the present work. Here, we propose exploiting the knowledge of the interaction model—communicated by the players in order to perform the evaluation of their merger—in the optimization of unilateral strategies.[4] Thus, unilateral strategies ($\boldsymbol{\nu}_i$, $i \in \{1,2\}$) are evaluated by assuming that the tails of previously obtained input sequences will be applied by the other player. This means solving (1.9) over $\boldsymbol{\nu}_i$, for $i \in \{1,2\}$, by replacing constraints (3.8b) with

$$\begin{aligned} \hat{\xi}_{1\cup 2}(t+1|k) &= \mathbf{A}_{1\cup 2}\hat{\xi}_{1\cup 2}(t|k) + \mathbf{B}_{1\cup 2,i}\nu_i(t|k) \\ &\quad + \mathbf{B}_{1\cup 2,j}\tilde{\nu}_j(t|k) + \varpi_{1\cup 2}(t|k), && (3.13a) \\ \tilde{\nu}_j(t|k) &\triangleq \nu_j^*(t+1|k-1), && (3.13b) \\ \tilde{\nu}_j(N_p-1|k) &\triangleq \mathbf{0}, && (3.13c) \end{aligned}$$

with $j \in \{1,2\} \setminus \{i\}$. Then, recalling that $\xi_{1\cup 2} \triangleq (\xi_1, \xi_2)$, the predicted evolution can be separated into the components corresponding to either player.

3.3.3 Individual rationality

So far we have assumed that if an agreement is beneficial for the coalition then it is beneficial for its members too. However, the premise here is that agents are rational and selfish. Let

$$J_{1\cup 2}^{(j)} \triangleq \sum_{t=k}^{k+N_b} \boldsymbol{\ell}_{1\cup 2}^{(j)}(t) + N_b \chi_{1\cup 2}^{(j)},\ j \in \{1,2\}, \tag{3.14}$$

be the quota relative to player j in the merger cost $J_{1\cup 2}$. The stage cost $\ell_{1\cup 2}^{(j)}(t)$ in (3.14) is the component of (3.7) relative to player j within the merger (i.e., relative to the state and input trajectories obtained by solving the MPC problem (1.9) for $i = 1\cup 2$). The value of $\chi_{1\cup 2}^{(j)}$ is a proper share of the cooperation costs. Notice that $J_{1\cup 2} = J_{1\cup 2}^{(1)} + J_{1\cup 2}^{(2)}$.

It can be verified (by assuming, for simplicity, $\chi = 0$) that

$$J_{1\cup 2} \leq J_1 + J_2 \;\not\Longrightarrow\; J_{1\cup 2}^{(j)} \leq J_j, \quad \forall j \in \{1,2\}, \tag{3.15}$$

which can be shown by referring again to the same couple of systems considered in Example 3.1. The components of the merger costs therein are:

$$J_{1\cup 2}^{(1)} = 24.271 < J_1, \quad J_{1\cup 2}^{(2)} = 24.704 \not< J_2.$$

Indeed, condition (3.10) is not sufficient to guarantee lower *individual* costs to both players. On the grounds of individual rationality, a new coalition is formed if and only if a secure benefit can be granted to their future members. In other words, the

[4] An analogous problem has to be addressed for the correct evaluation of the performance derived from leaving a coalition. This issue is further discussed in Section 3.4.2.

individual player's payoff in the merger has to be at least equal to the one obtained through a unilateral strategy. In particular, player j will accept participating in the merger $\mathcal{P}_1 \cup \mathcal{P}_2$ if and only if the following individual rationality requirement is fulfilled:

$$J_{1\cup 2}^{(j)} \leq J_j, \ j \in \{1, 2\}. \tag{3.16}$$

Notice that (3.15) can be extended to the individual members of any coalition. Thus, even if cooperation allows the aggregate cost to be decreased, it can indeed be unfavorable for some agents from the point of view of the locally incurred costs. Hence, there is not a straightforward relationship between cooperation and *individual rationality*—unless some means of transferring the value between (sets of) agents is provided. In Section 3.3.4, starting from the assumption of transferable utility (TU), specific criteria for the bargaining are given to provide the possibility of coalition formation whenever individual rationality does not directly follow condition (3.10) for both players. In Sections 3.4 and 3.5 we get at the individual agent's level, addressing the redistribution of the value of a coalition among its members.

3.3.4 Transferable utility

In the remainder we assume that (3.9) is defined so as to express an economic index. Then, we consider the possibilities opened whenever a value equivalent to the surplus achieved through the merger, i.e.,

$$\Pi = J_1 + J_2 - J_{1\cup 2}, \tag{3.17}$$

can be transferred between the players. The surplus expressed by (3.17) is defined as a positive quantity, representing savings on control-associated costs. Essentially, the recompense has to be valuable for the players, so its nature may vary. For example, it may consist of a monetary amount, or a flow of (shared) resources across the system. In such a scenario it is possible to fulfill condition (3.16) for both players by means of a proper *a posteriori* redistribution of the utility between the players. We refer to this as a *transferable utility* (TU) scenario.

Here we take a more abstract approach, and aim at reallocating the individual control costs. It is worth emphasizing that such compensation is an *a posteriori* procedure: first, the bargaining players agree on a given reallocation—based on the expected performance—before incurring the actual control-associated costs; then, these actual costs are balanced out on the basis of the prior agreement.[5]

Remark 3.3. *Only a prediction of the quantity expressed by* (3.17) *can be computed in practice: following the outcome of the bargaining, either the realization of the merger performance or that of the unilateral strategies can be measured. Value transfers calculated over expected costs will be eventually converted into feasible ones, based on the actual merger performance.*

Let $p_j \in \mathbb{R}$ designate the payoff assigned to agent $j \in \mathcal{P}_i$, $i \in \{1,2\}$, and $\mathbf{p}_i = \sum_{j\in\mathcal{P}_i} p_j$ denote the aggregate payoff for a given player. If rational players come to an agreement, they will agree on achieving the largest possible payoff, subject to $\sum_i \mathbf{p}_i = J_{1\cup 2}$. Such joint agreement—referred to as *cooperative strategy*—will belong to the Pareto front (where no allocation can make a player better off without making another player worse off) [51, 106]. The values achieved with unilateral strategies, i.e., (J_1, J_2), constitute the *disagreement point*: players would not accept an *aggregate* payoff $\mathbf{p}_i = \sum_{j\in\mathcal{P}_i} p_j$ worse than their own disagreement point. It is worth to point out that the following discussion addresses the problem at the level of the pair of bargaining players. The final problem is to find a vector $p \in \mathbb{R}^{|\mathcal{P}_1\cup\mathcal{P}_2|} \triangleq (p_j)_{j\in\mathcal{P}_1\cup\mathcal{P}_2}$, $\sum_j p_j = J_{1\cup 2}$, i.e., a reallocation of the control costs such that all agents *in the merger* are satisfied w.r.t. individual and group (i.e., taking into account the outcome of possible subcoalitions) rationalities.

A natural and straightforward solution for the allocation of the surplus between two cooperating entities is the *egalitarian* redistribution. In particular, we assign to each player an *equal* share of the surplus Π obtained by the merger, w.r.t. the disagreement point, i.e.,

$$\mathbf{p}_i = J_i - \frac{1}{2}\Pi. \tag{3.18}$$

Geometrically, the allocation $(\mathbf{p}_1^*, \mathbf{p}_2^*)$ corresponds to the midpoint of the line segment connecting $(J_1, J_{1\cup 2} - J_1)$ and $(J_{1\cup 2} - J_2, J_2)$:

$$\mathbf{p}_i = \frac{1}{2}\left(J_{1\cup 2} + J_i - J_j\right), \tag{3.19}$$

for $i \in \{1,2\}$ and $j \in \{1,2\}\setminus\{i\}$.[6] Since the formation of any coalition is conditional on the subadditivity requirement (3.10), an efficient and individually rational allocation is guaranteed to exist for the two-player case: $\Pi > 0$ if (3.10) is strictly satisfied, and

[5] Analogous to an *a priori* compensation can be considered, e.g., the distributed MPC scheme proposed in [43] where, on the basis of situational altruism criteria, the cost incurred by each controller is dynamically adjusted so as to fulfill minimum local requirements.

[6] Notice that (3.19) coincides with the Shapley value formula for a two-player game.

the allocation computed through (3.19) always fulfills the following condition

$$\mathbf{p}_i^* < J_i^*, \quad \forall i \in \{1, 2\}, \tag{3.20}$$

which corresponds to the individual rationality property for the player.[7] It is easy to see that the cost allocated over each player depends on the difference between the expected performances of unilateral strategies (centered about a half of the merger cost), and

$$J_i > J_j \implies \mathbf{p}_i > \mathbf{p}_j,\ i, j \in \{1, 2\},\ j \neq i.$$

Finally, consider the situation prior to the utility transfer. Let $\check{J}_{1\cup 2}^{(i)}$ be the cost actually incurred by player $i \in \{1, 2\}$ within the merger. Note that $\sum_i \check{J}_{1\cup 2}^{(i)} = \check{J}_{1\cup 2}$. The expected payoff (4.6) is used to derive the quota of each player in the realization of the compound cost $J_{1\cup 2}$: once the merger performance is measured, *feasible* payoffs are defined by assigning to each player a share $\mathbf{p}_i / J_{1\cup 2}$ of $\check{J}_{1\cup 2}$

$$\mathbf{p}_i = \frac{\mathbf{p}_i}{J_{1\cup 2}} \check{J}_{1\cup 2},\ i \in \{1, 2\}. \tag{3.21}$$

Now consider the quantity $\mathbf{p}_i - \check{J}_{1\cup 2}^{(i)}$, i.e., the gap between the feasible payoff (3.21) and the cost the player actually incurs. Recall that by efficiency of the allocation, we have $\sum \mathbf{p}_i = J_{1\cup 2}$. Also, by definition $\sum_i \check{J}_{1\cup 2}^{(i)} = \check{J}_{1\cup 2}$. By subtracting these two equalities we have

$$\mathbf{p}_i - \check{J}_{1\cup 2}^{(i)} = -\left[\mathbf{p}_j - \check{J}_{1\cup 2}^{(j)}\right],\ i, j \in \{1, 2\},\ j \neq i \tag{3.22}$$

revealing that one of the players is excessively benefited—according to the surplus distribution dictated by (4.6)—following its participation in the coalition, whereas the other player experiences the opposite situation. Thus, we can define a unique value for the gap $\epsilon \triangleq |\mathbf{p}_i - \check{J}_{1\cup 2}^{(i)}|$.

By the transferable utility assumption, we aim at compensating this gap in order to incentivize the formation of a coalition between individually rational players. The cost distribution dictated by (3.21) can be established by transferring a value $\tau_{\mathrm{TU}} = \epsilon$ from one player to the other, i.e., $J_{1\cup 2}^{(1)} \pm \tau_{\mathrm{TU}} = \mathbf{p}_1$ and $J_{1\cup 2}^{(2)} \mp \tau_{\mathrm{TU}} = \mathbf{p}_2$.

Example 3.2. *Consider the system defined in Example 3.1. The payoffs obtained by applying* (4.6) *are displayed in Table 3.2. The costs incurred by the players are shown in the first column of Table 3.2. The gap amounts to* $\epsilon = 0.496$ *(predicted* 0.527*), meaning that player 2 is penalized—prior to any value transfer—by participating in the coalition*

[7]Recall that here we refer the term *individual* to the entire player coalition.

Table 3.2: Example 3.2. Individual costs with merging and unilateral strategies.

		$J_{1\cup 2}^{(i)}$	$\mathbf{p}_i$	J_i
$\mathcal{P}_1$	predicted	24.271	24.798	25.200
	actual	*24.271*	*24.767*	*24.992*
$\mathcal{P}_2$	predicted	24.704	24.177	24.579
	actual	*24.704*	*24.208*	*24.432*

with player 1. Therefore, player 1 compensates player 2 by a transfer $\tau_{TU} = \epsilon$. *Final perceived costs are shown in the second column of Table 3.2. Costs incurred through unilateral strategies are shown for comparison in the last column.*■

So far, we have presented the TU framework for two-player bargaining, without explicitly dealing with the case $|\mathcal{P}_i| > 1$, i.e., with the redistribution of a player's payoff over the multiple agents composing its corresponding coalition. Next, we address the coalition structure evolution due to the autonomous coalition formation within the whole set of agents whenever $|\mathcal{N}| > 2$.

3.4 Bargaining procedure

All players *in pairs* will perform, at given time intervals, a one-shot bargaining whose outcome will decide the generation of new coalitions. At each round, all players available for bargaining have to be paired. It is worth to remark that the way the pairs are selected may influence the final outcome of the coalition formation process [107].

3.4.1 Coalition formation

At time k, let the global set of agents $\mathcal{N} = \{1, \dots, N\}$ be partitioned into $N_c \in \{2, \dots, N\}$ coalitions as defined by $\mathcal{P}(\mathcal{N}, \mathcal{G}(k)) = \{\mathcal{C}_1, \dots, \mathcal{C}_{N_c}\}$. A pair of coalitions $\mathcal{P}_1, \mathcal{P}_2 \in \mathcal{P}(\mathcal{N}, \mathcal{G}(k))$ is randomly selected. This procedure is performed over the remaining coalitions until all possible pairs of players are selected.[8] It may occur that the total number of coalitions N_c available for bargaining is not even: in this case, the unpaired coalition will not participate in the bargaining (i.e., it will skip the round).

Assumption 3.2. *The bargaining is carried on simultaneously by all players. Each pair of bargaining players assumes that no further coalitions are being formed or disrupted among the rest of players.*

[8]Different methods can be employed, e.g., favoring big (or small) coalitions.

Therefore, when evaluating the possible formation of coalition $\mathcal{P}_1 \cup \mathcal{P}_2$, each pair assumes that the rest of agents remain organized as they were at the previous time step. Each pair of players verifies (3.10) before stipulating the agreement, following Assumption 3.2 in the computation of (1.9). This means that potential changes of configuration concerning subsystems external to $\mathcal{P}_1 \cup \mathcal{P}_2$ are not taken into account on the estimate of the unknown coupling $\hat{\omega}_i$. As pointed out at the end of Section 3.3.2, in order to correctly ponder the outcome of unilateral strategies, tails of previous input sequence are used in the bargaining.

In case the merger yielding $(\mathbf{p}_1, \mathbf{p}_2)$ is approved, an initial payoff is assigned to each agent $j \in \mathcal{P}_i$, $i \in \{1, 2\}$, by equally splitting $\mathbf{p}_j$:

$$p_j = \frac{1}{|\mathcal{P}_i|} J_{1\cup 2},\ j \in \mathcal{P}_i, \tag{3.23}$$

Notice that the payoff allocation given by (3.23) is not necessarily stable in the coalitional sense: some agents may estimate more profitable to leave (or modify) the current agreement. Requests for utility transfer within $\mathcal{P}_1 \cup \mathcal{P}_2$ are checked over a number N_s of randomly sampled subsets $\mathcal{C}_r \subset \mathcal{P}_1 \cup \mathcal{P}_2$, $r \in \{1, \ldots, N_s\}$. If some subset $\mathcal{C}_r$ of agents is dissatisfied with the initial allocation, the iterative utility transfer scheme described in Section 3.5 is performed in order to adjust (if possible) the allocation according to their request.

3.4.2 Coalition disruption

While any coalition is formed through a bilateral agreement, an agent can leave it unilaterally. If for a given pair the bargaining does not result into a merger, the possibility of some subset of agents wanting to leave coalition $\mathcal{P}_i$, $i = \{1, 2\}$, is checked. The same is done when the current configuration corresponds to the grand coalition as well, in that case the only (unpaired) player available.

Remark 3.4. *In cooperative game theory, the coalition is viewed as a binding agreement. In this work, the agreement is not binding over the prediction horizon. In order to adapt to the time-varying system state, agents are free to change their affiliation at any time step.*

More specifically, over each one of the selected players, (i) a subset of agents $\mathcal{C} \subset \mathcal{P}_i$ is randomly chosen and (ii) the conditions for the unilateral exit of either $\mathcal{C}$ or its complementary subset $\mathcal{P}_i \setminus \mathcal{C}$ are checked. Keeping the same notation as before, we refer to the above subsets of $\mathcal{P}_i$ by the indices $\{1, 2\}$. In particular, we define $\mathcal{S}_1 = \mathcal{C}$, and $\mathcal{S}_2 = \mathcal{P}_i \setminus \mathcal{C}$. The whole coalition $\mathcal{P}_i$ will be designated by $\{1\cup 2\}$.

Either of the above subsets will want to leave the coalition if condition (3.20) is not fulfilled. Consider, for instance, the case where $J_1 < \mathbf{p}_1$: in order to reestablish the individual rationality of $\mathbf{p}_1$, it may be possible to reallocate part of the benefit from $\mathcal{S}_2$. However, since the agents in $\mathcal{S}_2$ have the option of leaving the coalition and achieve an expected payoff $\mathbf{p}_2 = J_2$, they will not accept to get past this value (the disagreement point, as defined in Section 3.3.4). Hence, if $J^{(1)}_{1\cup 2} - J_1 > -(J^{(2)}_{1\cup 2} - J_2)$, $\mathcal{P}_i$ will split into two coalitions $\mathcal{S}_1$ and $\mathcal{S}_2$. As with merging, the process is simultaneous over all players, so it is assumed that the exit of one or more members of a coalition does not affect the decisions of other agents.

The split of $\mathcal{P}_i$ would result in a modification of the coalition structure (and of the associated communication graph) such that $\mathcal{P}_i$ is replaced in $\mathcal{P}(\mathcal{N}, \mathcal{G}(k+1))$ by $\mathcal{S}_1$and $\mathcal{S}_2$. Once the new coalitions are formed, the payoff allocation among the members of $\mathcal{S}_i$, $i \in \{1, 2\}$ is updated so that $\sum_{j\in\mathcal{S}_i} p_j = \mathbf{p}_i = J_i$. This is done as in (3.23). After the initial allocation is set, requests for utility transfer within $\mathcal{S}_i$, $i \in \{1, 2\}$ are checked over a random sample of subsets $\mathcal{C}_r \subset \mathcal{S}_i$, $r \in \{1, \dots, N_s\}$. If some subset $\mathcal{C}_r$ is found dissatisfied with the initial allocation, the iterative utility transfer scheme described in Section 3.5 is performed on the player $\mathcal{S}_i \supset \mathcal{C}_r$.

In contrast, if

$$J^{(1)}_{1\cup 2} - J_1 \leq -(J^{(2)}_{1\cup 2} - J_2), \tag{3.24}$$

it is possible for $\mathcal{S}_2$ to compensate the dissatisfaction while maintaining some benefit in participating in the coalition $\mathcal{P}_i = \mathcal{S}_1 \cup \mathcal{S}_2$. The utility transfer protocol aimed at achieving a stable allocation of the coalitional benefit is discussed in the following section.

Remark 3.5. *Notice that either the randomly chosen* $\mathcal{C}$ *or* $\mathcal{P}_i \setminus \mathcal{C}$ *might not be included among the allowed coalitions (for instance, they might not be significant due to the topology of the system*[9]*). Given a feasible* $\mathcal{C}$*, then the complementary subset may consist of several feasible coalitions. If this is the case, the procedure described in this section does not change, except the above conditions are verified for each of these coalitions.*

Remark 3.6. *As for coalition formation, the veracity of the unilateral strategies used to evaluate the possible exit from a coalition is critically important. However, in this case previous input sequence result from a joint optimization. For this reason, they are not useful for correctly pondering the outcome of coalition split as done in* (3.13)*. Therefore, problem* (1.9) *is solved over several iterations—with constraints* (3.13) *re-*

[9] One such example is considered in Section 3.6.

placing (3.8b)*—using the solution from the previous iteration as unilateral strategy for the other player. In this way, the optimized inputs converge to realistic unilateral actions.*

3.5 Coalitional stability

For presentation simplicity, we refer in the remainder to the case where agents aim at their individual payoff maximization. On grounds of rationality, any agent $i \in \mathcal{N}$ will choose an allocation p_i (associated to a coalition $\mathcal{C} \subseteq \mathcal{N}$) over p'_i (associated to a different coalition $\mathcal{C}' \subseteq \mathcal{N}$) if $p_i > p'_i$. As introduced in Section 3.4, a subset of agents $\mathcal{S} \subset \mathcal{C}_i \in \mathcal{P}(\mathcal{N}, \mathcal{G}(k))$ may estimate that the benefit allocation $\sum_{j \in \mathcal{S}} p_j$ they are achieving while being part of $\mathcal{C}_i$ is worse than the overall value $\sum_{j \in \mathcal{S}} p'_j$ they could achieve by playing as a standalone coalition. In this case, the agents in $\mathcal{S}$ will claim a better individual payoff. If the required improvement can be provided by the rest of the coalition $\mathcal{C}_i \setminus \mathcal{S}$, i.e., if condition (3.24) is fulfilled, then a proper utility transfer can be computed.

The joint benefit of coalition $\mathcal{C}_i$ has to be redistributed in order to satisfy such claims: all agents external to the claiming subset, i.e., all $j \in \mathcal{C}_i \setminus \mathcal{S}$, must support the demanded amount. After such an amount is transferred and the claim is satisfied, a new demand may arise by a different subset $\mathcal{S}' \subset \mathcal{C}_i$ of agents, giving rise to an iterative process, that may be finite or not. We want the outcome of such a process to be a stable allocation of the value of coalition $\mathcal{C}_i$, i.e., an allocation such that all agents $j \in \mathcal{C}_i$ have no incentive to leave the coalition. The set of such stable allocations is designated as the *core* of the associated cooperative game. We begin by defining a cooperative TU game restricted to the members of the coalition $\mathcal{C}_i$, defined by the pair $(\mathcal{C}_i, v)$, where $v(\cdot)$ is a *characteristic function* $v : 2^{\mathcal{C}_i} \mapsto \mathbb{R}$ mapping each coalition $\mathcal{S} \subseteq \mathcal{C}_i$ to a real value. This value can be derived through the procedure described in Section 3.3.

Remark 3.7. *The reason for restricting the game to the members of $\mathcal{C}_i$ is the impracticability of computing values for the whole set $\mathcal{N}$ of agents, since that would require a substantial exchange of information in order to compute the values of all $2^{\mathcal{N}}$ possible coalitions through* (1.9). *For similar reasons, the value $v(\mathcal{S})$ of any coalition $\mathcal{S} \subset \mathcal{C}_i$ is not computed unless the corresponding subset is selected as a player (see description of the algorithm in Section 3.4).*

The value of a coalition $\mathcal{C}_i \in \mathcal{P}$ is divided among its members through a set of vector payoffs such that:

$$\mathcal{V}_i \triangleq \left\{ \pi_i = (p_j)_{j\in\mathcal{C}_i} \in \mathbb{R}^{|\mathcal{C}_i|} \middle| \sum_{j\in\mathcal{C}_i} p_j = v(\mathcal{C}_i) \right\}, \tag{3.25}$$

satisfying the *efficiency* property w.r.t. the game $(\mathcal{C}_i, v)$. Now, a formal statement of (3.22) is provided. Given a payoff $\pi_i \in \mathcal{V}_i$, the *excess* for any subset of agents $\mathcal{S} \subseteq \mathcal{C}_i$ is defined as

$$e(\mathcal{S}, \pi_i) = v(\mathcal{S}) - \sum_{j\in\mathcal{S}} p_j, \tag{3.26}$$

with $e(\varnothing, \pi_i) = 0$. That is to say, the excess represents the difference between the value the members of $\mathcal{S} \subseteq \mathcal{C}_i$ can obtain by playing as the coalition $\mathcal{S}$ and the aggregate payoff they achieve by participating in $\mathcal{C}_i$, characterized by the allocation π_i.

The set of allocations able to guarantee that no agent has an incentive to leave $\mathcal{C}_i$ to form a coalition $\mathcal{S} \subset \mathcal{C}_i$ is called the *core*. It can be defined with reference to the excess as:

$$\mathcal{O}_i = \{\pi_i \in \mathcal{V}_i |\, e(\mathcal{S}, \pi_i) \leq 0, \forall \mathcal{S} \subseteq \mathcal{C}_i\}. \tag{3.27}$$

In other words, the core represents the set of allocations that cannot be improved by any coalition $\mathcal{S} \subset \mathcal{C}_i$. Notice that all $\pi_i \in \mathcal{O}_i$ fulfill individual rationality, i.e., $p_j \geq v(\{j\})$, $\forall j \in \mathcal{C}_i$, as well as group rationality, i.e., $\sum_{j\in\mathcal{S}} p_j \geq v(\mathcal{S})$, $\forall \mathcal{S} \subseteq \mathcal{C}_i$. For the purpose of the transfer scheme that will be presented next, we restate (3.27) in terms of the *demand* made by the set of players $\mathcal{S}$ against an allocation π_i [97].

Definition 3.1 (Demand). *A demand against $\pi_i \in \mathcal{V}_i$ is a pair $(\mathcal{S}, \delta_i)$ where $\varnothing \neq \mathcal{S} \subset \mathcal{C}_i$,[10] and $\delta_i \triangleq (d_j)_{j\in\mathcal{S}}$ is a vector satisfying*

$$d_j > 0, \, \forall j \in \mathcal{S}, \tag{3.28a}$$

$$\sum_{j\in\mathcal{S}} d_j = e(\mathcal{S}, \pi_i). \tag{3.28b}$$

A *satisfaction* to a demand $(\mathcal{S}, \delta_i)$ against $\pi_i \in \mathcal{V}_i$ is an allocation $\sigma_i = (s_j)_{j\in\mathcal{C}_i}$ such that the agents in $\mathcal{S} \subset \mathcal{C}_i$ get the same value $v(\mathcal{S})$ that they expect to achieve as a standalone coalition.[11] The satisfaction of such demand requires an equivalent amount—drawn from the rest of agents in $\mathcal{C}_i \setminus \mathcal{S}$—to be transferred.

Remark 3.8. *Such utility transfer can be made by the rest of agents while keeping $e(\mathcal{C}_i \setminus \mathcal{S}, \pi_i) \leq 0$ if the game is* superadditive, *i.e., $v(\mathcal{S}) + v(\mathcal{C}_i \setminus \mathcal{S}) \leq v(\mathcal{C}_i)$ for any*

[10]Note that the demand for the grand coalition $\mathcal{C}_i$ is null by definition (since the excess is null).

[11]$v(\mathcal{S})$ can be computed as described in Section 3.3.1.

$\mathcal{S} \subseteq \mathcal{C}_i$ *(*subadditive *if referred to* (3.24)*).*

We consider here that the value of the demand is equally shared over the demanding set of agents, and that such demand is equally supported by the rest of the agents. More formally, for every agent $j \in \mathcal{C}_i$,

$$s_j = \begin{cases} p_j + \frac{e(\mathcal{S},\pi_i)}{|\mathcal{S}|}, & \text{if } j \in \mathcal{S}, \\ p_j - \frac{e(\mathcal{S},\pi_i)}{|\mathcal{C}_i \setminus \mathcal{S}|}, & \text{if } j \in \mathcal{C}_i \setminus \mathcal{S}, \end{cases} \tag{3.29}$$

where p_j is the payoff assigned to agent j within coalition $\mathcal{C}_i$ by the allocation π_i.

A transfer scheme is a sequence of allocation proposals $\pi_i^{(t)}$, $k \in \mathbb{N}$, such that $\pi_i^{(t+1)} \triangleq \sigma_i^{(t)}$ is a satisfaction to a demand against $\pi_i^{(t)}$. Moreover, if there exists a $\hat{t}$ such that for all $t \geq \hat{t}$ we have $\pi_i^{(t)} = \pi_i^{(\hat{t})}$, the transfer scheme is finite, i.e., $e(\mathcal{S}, \pi_i^{(t)}) \leq 0$ for all $t \geq \hat{t}$ and all $\mathcal{S} \subseteq \mathcal{C}_i$. As discussed in [97], a transfer sequence based on (3.29) guarantees convergence to $\mathcal{O}_i$, provided it is not empty. Different transfer schemes are possible [96].

Remark 3.9. *Allocations produced in any intermediate iteration of the transfer scheme may not satisfy individual rationality for the agents in the supporting set* $\mathcal{C}_i \setminus \mathcal{S}$*. We assume that this is not an issue, as this constitutes a base for a new demand. Nonetheless, the distance to the core of any vector payoff* σ_i *produced by a transfer is bounded and, under given circumstances detailed in the following, decreasing.*

In order to clarify the convergence properties of a given transfer sequence, notice that (3.29) can be stated in vector form as

$$\sigma_i = \pi_i + e(\mathcal{S}, \pi_i)\zeta(\mathcal{S}, \mathcal{C}_i), \tag{3.30}$$

where $\zeta(\mathcal{S}, \mathcal{C}_i) \in \mathbb{R}^{|\mathcal{C}_i|}$ is defined as

$$\zeta_j = \begin{cases} \frac{1}{|\mathcal{S}|}, & \text{if } j \in \mathcal{S}, \\ -\frac{1}{|\mathcal{C}_i \setminus \mathcal{S}|}, & \text{if } j \in \mathcal{C}_i \setminus \mathcal{S}. \end{cases} \tag{3.31}$$

Then, for any $\mathcal{C}_i \subseteq \mathcal{N}$ and $\mathcal{S} \subseteq \mathcal{C}_i$, there exists $\underline{\zeta}(|\mathcal{C}_i|), \overline{\zeta}(|\mathcal{C}_i|) \in \mathbb{R}$ such that $\underline{\zeta}(|\mathcal{C}_i|) \leq \|\zeta(\mathcal{S}, \mathcal{C}_i)\|_2 \leq \overline{\zeta}(|\mathcal{C}_i|)$. Let $\mathcal{S}^{(t)} \subset \mathcal{C}_i$ be a subset demanding towards the allocation $\pi_i^{(t)}$ at iteration t. According to the transfer scheme described above, $v(\mathcal{C}_i)$ is reallocated as $\pi_i^{(t+1)} = \pi_i^{(t)} + e(\mathcal{S}^{(t)}, \pi_i^{(t)})\zeta(\mathcal{S}^{(t)}, \mathcal{C}_i)$. Then, there exists $\epsilon > 0$ such that

$$e(\mathcal{S}^{(t)}, \pi_i^{(t)})\|\zeta(\mathcal{S}^{(t)}, \mathcal{C}_i)\| = \|\pi_i^{(t+1)} - \pi_i^{(t)}\| \leq \epsilon, \tag{3.32}$$

since any allocation obtained along the transfer sequence belongs to $\mathcal{V}_i$, which is a closed set. Taking into account the boundedness of $\|\zeta(\mathcal{S}, \mathcal{C}_i)\|_2$,

$$e(\mathcal{S}^{(t)}, \pi_i^{(t)}) \leq \frac{\epsilon}{\underline{\zeta}(|\mathcal{C}_i|)}. \tag{3.33}$$

At this point, if at all steps

$$e(\mathcal{S}^{(t)}, \pi_i^{(t)}) = \max_{\mathcal{S} \subset \mathcal{C}_i} e(\mathcal{S}, \pi_i^{(t)}), \tag{3.34}$$

there exists $\hat{t}$ such that, for all $t \geq \hat{t}$, (3.32) holds. By making ϵ arbitrarily small, it can be concluded that $e(\mathcal{S}, \pi_i) \leq 0$, i.e., $\pi_i \in \mathcal{O}_i$. However, due to the reasons detailed in Remark 3.7, it is not viable to look for the $\mathcal{S} \subset \mathcal{C}_i$ characterized by the maximum excess in the considered framework.

So far we have shown the boundedness of the allocations computed in order to satisfy demands from a given subset. A result from [108] allows us to demonstrate that, if the core of the game is not empty, the distance of the allocations obtained by the transfer scheme gets smaller at each iteration, relaxing (3.34) as

$$0 \leq e(\mathcal{S}^{(t)}, \pi_i^{(t)}) \leq \max_{\mathcal{S} \subset \mathcal{C}_i} e(\mathcal{S}, \pi_i^{(t)}), \tag{3.35}$$

which is always the case in the procedure described in Section 3.4. More formally, let $\mathcal{O}_i \neq \varnothing$, $\pi_i \in \mathcal{V}_i$ and $\mathcal{S} \subset \mathcal{C}_i$ a coalition such that $e(\mathcal{S}, \pi_i) > 0$. After one iteration of the transfer scheme, $\pi_i^{(t+1)} = \pi_i^{(t)} + e(\mathcal{S}, \pi_i)\zeta(\mathcal{S}, \mathcal{C}_i)$. Then, for all $\pi_i^* \in \mathcal{O}_i$, $\|\pi_i^{(t+1)} - \pi_i^*\|_2 < \|\pi_i^{(t)} - \pi_i^*\|_2$.

As a final note for this section, it is worth pointing out that nonemptiness of the core can be checked in polynomial time if the values of all possible coalitions are available [54]. Since this is not possible here (see Remark 3.7), convergence properties of the transfer scheme are relevant. An interesting property is that, if the core is *empty*, a procedure analogous to that presented in this section can be used to show that the transfer sequence converges to the least-core, i.e.,

$$\mathcal{O}_i(\varepsilon) = \{\pi_i \in \mathcal{V}_i | \, e(\mathcal{S}, \pi_i) \leq \varepsilon, \forall \mathcal{S} \subseteq \mathcal{C}_i\}, \tag{3.36}$$

and $\varepsilon \geq 0$ is the minimum such that $\mathcal{O}_i(\varepsilon)$ is nonempty.

Remark 3.10. *Since we are dealing with dynamical systems, the value of any possible coalition $\mathcal{S} \subseteq \mathcal{N}$ is expected to vary at each time step. While the results in this section are relevant for the system in steady state, transient dynamics may degrade the outcome* *of the algorithm. Even if a coalitional structure* $\mathcal{P}(\mathcal{N}, \mathcal{G}) = \{\mathcal{C}_1, \ldots, \mathcal{C}_{N_c}\}$ *is maintained during a given time interval, it is possible that, for any* $\mathcal{C}_i \in \mathcal{P}$*, the value of subcoalitions* $\mathcal{S} \subset \mathcal{C}_i$ *evolves according to the state of the system. This means that the core is not a static set, and an allocation that is stable at time* k *may not show the same property at time* $k+1$*. In this case, the efficacy of the transfer scheme heavily relies on the available computation time between sampling times (notice that each iteration requires the computation of coalition values as described in Section 3.3.1). If it gives room for a limited number of iterations, we can still assume that at each time step the allocation provided to the members of any coalition in* $\mathcal{P}$ *is the best approximation toward a stable one.*

3.6 Illustrative case III: wide-area control of power grid

In order to test the proposed algorithm, we address the problem of wide-area control (WAC) of power networks. The objective of WAC is to control inter-area oscillations, involving mutual oscillation arising among a set of connected generators, causing undesired power transfers. Such oscillations are poorly controllable by means of local (decentralized) control. Exploiting the recent availability of phasor measurement units (PMUs) and flexible AC transmission systems (FACTS), along with a reliable real-time data network infrastructure, research has been focused on the development of WAC strategies based on inter-area communication [90, 95].

3.6.1 System description

The power network consists of several areas coupled by transmission lines (see Fig. 3.1). Local generation is available within each area. The goal is to provide automatic generation control (AGC) to *(i)* maintain the frequency around the nominal value, and *(ii)* reduce power transfers between areas.

The energy supply in each area is provided by a power station equipped with single-stage turbines. Let each area be identified by an index in the set $\mathcal{N} = \{1, \ldots, 5\}$. The linearized dynamics of synchronous generators in area $i \in \mathcal{N}$ result in the following continuous-time model [109]:

$$\dot{x}_i = A_{ii} x_i + B_{ii} u_i + D_i \Delta d_i + \sum_{j \in \mathcal{M}} A_{ij} x_j, \tag{3.37}$$

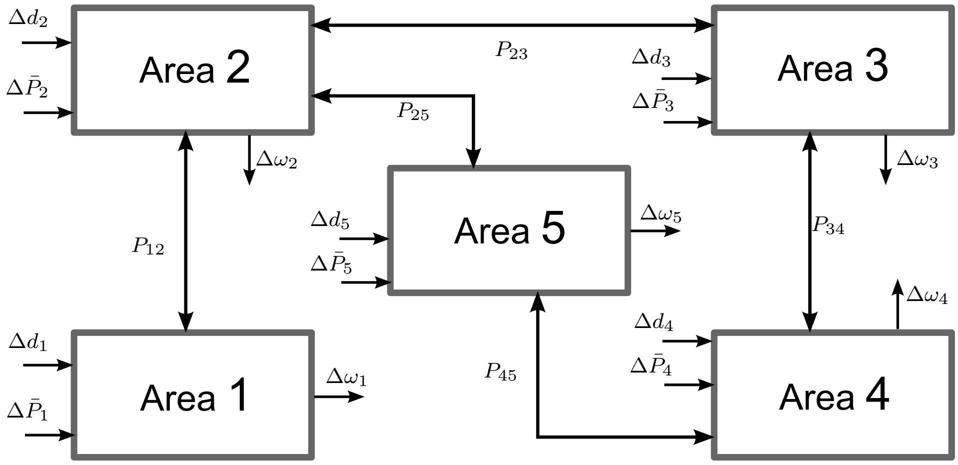

Figure 3.1: Power network composed of 5 areas with local supply [109]. The objective is to control inter-area oscillations—cause of undesired power transfers—and to minimize the deviation from the nominal frequency. Power transfers are possible between areas connected by transmission lines. Two cases are considered: *(i)* local production capacity is sufficient for locally matching the demand, *(ii)* the capacity of local generation is impaired, making energy transfers from neighboring areas necessary for demand satisfaction.

Table 3.3: Symbols employed in the power network example.

Symbol	Description	Unit
Δd	Deviation of the load from the nominal value (p.u.)	[-]
$\Delta\theta$	Variation in the rotor angle w.r.t. stator reference axis	[rad]
$\Delta\omega$	Deviation from the nominal frequency	[rad/s]
ΔP_m	Deviation from the nominal mechanical power (p.u.)	[-]
ΔP_v	Deviation from the nominal steam valve position (p.u.)	[-]
$\Delta\bar{P}$	Deviation of the power setpoint from the nominal value (p.u.)	[-]
H	Machine inertia constant	[s]
r_v	Rotor velocity regulation	[rad/s]
ρ_f	Load change / frequency variation (%)	[-]
τ_t	Prime mover time constant	[s]
τ_g	Governor time constant	[s]
P_{ij}^0	Slope of the power-angle curve at the initial angle between areas i and j	[rad^{-1}]

where $x_i \triangleq [\Delta\theta_i, \Delta\omega_i, \Delta P_{m_i}, \Delta P_{v_i}] \in \mathbb{R}^4$, $u_i = \Delta\bar{P}_i \in \mathbb{R}$, and $\Delta d_i \in \mathbb{R}$ is the variation in the demand (symbols are defined in Table 3.3).[12] The last term in (3.37) describes the influence of coupled areas, identified in the set $\mathcal{M}_i = \{j \in \mathcal{N} \setminus \{i\} |\, A_{ij} \neq \mathbf{0}\}$. Matrices are composed as

$$\begin{aligned} A_{ii} &= \begin{bmatrix} 0 & 1 & 0 & 0 \\ -\frac{\sum_{j\in\mathcal{M}_i} P_{ij}^0}{2H_i} & -\frac{\rho_{f_i}}{2H_i} & \frac{1}{2H_i} & 0 \\ 0 & 0 & -\frac{1}{\tau_{t_i}} & \frac{1}{\tau_{t_i}} \\ 0 & -\frac{1}{r_{v_i}\tau_{g_i}} & 0 & -\frac{1}{\tau_{g_i}} \end{bmatrix} \quad B_i = \begin{bmatrix} 0 \\ 0 \\ 0 \\ \frac{1}{\tau_{g_i}} \end{bmatrix} \\ A_{ij} &= \begin{bmatrix} 0 & 0\,0\,0 \\ \frac{P_{ij}^0}{2H_i} & 0\,0\,0 \\ 0 & 0\,0\,0 \\ 0 & 0\,0\,0 \end{bmatrix} \quad D_i = \begin{bmatrix} 0 \\ -\frac{1}{2H_i} \\ 0 \\ 0 \end{bmatrix}. \end{aligned} \tag{3.38}$$

For reasons of space, the values of the parameters are not reported here (the reader is referred to [109]). The coupling of the generation frequency between areas connected through transmission lines appears in the second row of A_{ii} and A_{ij}. Inter-area power transfers are modeled as

$$\Delta P_{ij} = P_{ij}^0(\Delta\theta_i - \Delta\theta_j),\ i, j \in \mathcal{N}, \tag{3.39}$$

where positive values indicate a transfer from area i to area j.

Classic discretization yields non-sparse structures, unless very small sampling steps are employed [1]. In order to preserve the topology of the system in the discrete-time model's structure, avoiding the dependence on the sampling time, the continuous-time model (3.37) is discretized following the method of [110], with $T_s = 1\,\mathrm{s}$. More specifically, by treating u_i as an exogenous input along with Δd_i and x_j, the input-decoupled structure of the continuous-time model is replicated in discrete time. Notice that the use of such a method is reasonable in this kind of framework, where one basic assumption is that system-wide knowledge of the model is not likely to be achieved (besides communication constraints, one further reason is the dependence of the time constants characterizing the linear model on the current setpoints [90]). From now on, any mention of the above matrices will refer to the discrete-time model.

[12]The load is assumed not sensitive to frequency variation.

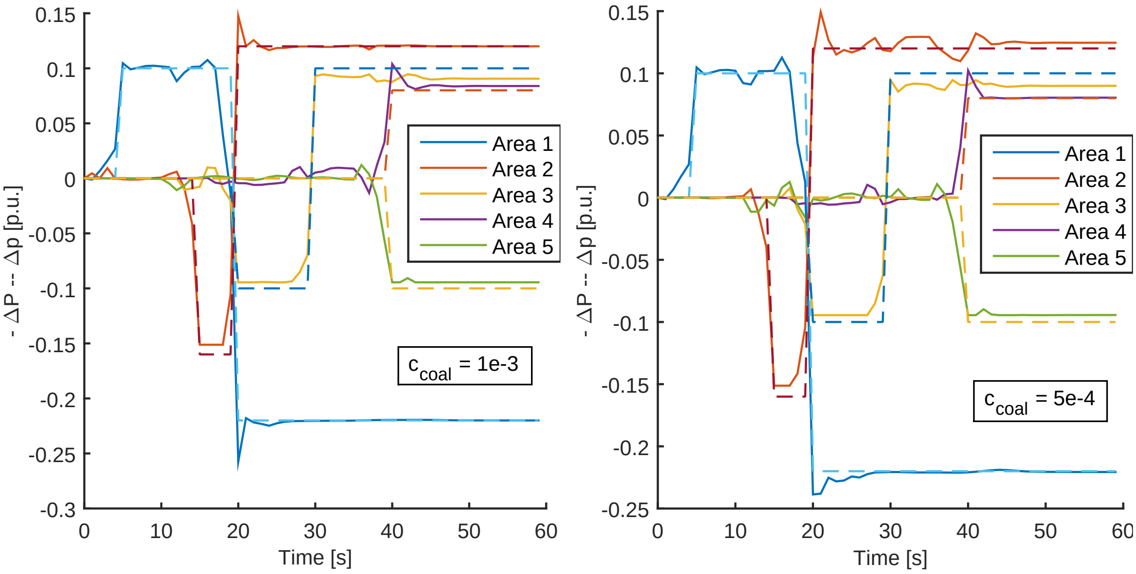

Figure 3.2: Scenario 2: the capacity of local generation is impaired, making energy transfers from neighboring areas necessary for demand satisfaction. Variation of the demand (dashed lines) and local power generation in the 5 areas. In the left plot, relative to $c_{\text{coal}} = 10^{-3}$, the lack of supply in Area 3 due to a 10% capacity drop w.r.t the demand value, is supplemented with energy transfers from Areas 4 and 5. Similarly, the right plot, corresponding to $c_{\text{coal}} = 5 \cdot 10^{-4}$, shows that Area 3 receives additional supply from Areas 2 and 5 (see Fig. 3.4). Power setpoints are computed with the RTO (3.41).

3.6.2 Controller design

It can be inferred from (3.39) that large energy transfers are caused by large differences in the angle deviation. The minimization of the energy transferred between connected areas can be implicitly addressed by penalizing large values of $\Delta\theta_i$; additionally, measures available from cooperating nodes can be exploited by penalizing the angle difference between the members of a given coalition. Therefore, the state weighting matrices in the objective function are chosen as

$$\begin{aligned} Q_{ii} &= \text{diag}(q_{ii}^{\theta} + \sum_{j \in \mathcal{M}_i} q_{ij}^{\theta} + q_{ji}^{\theta}, q_{ii}^{\omega}, q_{ii}^{P_m}, q_{ii}^{P_v}), \\ Q_{ij} &= \text{diag}(-\sum_{j \in \mathcal{M}_i} q_{ij}^{\theta} + q_{ji}^{\theta}, 0, 0, 0), \end{aligned} \tag{3.40}$$

where $Q_{ij} \in \mathbb{R}^{n_i \times n_j}$ is the submatrix of $Q \in \mathbb{R}^{n \times n}$ relative to the coupling between nodes i and j. For noncooperative control, $q_{ij} = q_{ji} = 0$; the rest of the values are defined as in [109], i.e., $Q_{ii} = \text{diag}(500, 0.01, 0.01, 10)$ and $R_i = 10$, $\forall i \in \mathcal{N}$. In case of cooperation, we set $q_{ij} = q_{ji} = 1000$.

Table 3.4: Constraints on local generation.

	$\|u_1\|_\infty \leq$	$\|u_2\|_\infty \leq$	$\|u_3\|_\infty \leq$	$\|u_4\|_\infty \leq$	$\|u_5\|_\infty \leq$
S1	0.2310	0.1680	0.1050	0.0840	0.1050
S2	0.3465	0.1512	0.0945	0.1260	0.0945

We test the capability of the coalitional controller based on autonomous coalition formation in achieving $\Delta\omega_i \to 0$, $\forall i \in \mathcal{N}$ in presence of step variations in the load Δd_i at any $i \in \mathcal{N}$. Two scenarios are considered: in the first, local production capacity is sufficient for locally matching any demand, and the objective is to track the reference $(\bar{x}, \bar{u})$, computed as a function of the change in the grid load. Since each area's load must be matched with the local production, the components of the setpoint vector are defined as $\bar{x}_i = [0, 0, \Delta d_i, \Delta d_i]$, $\bar{u}_i = \Delta d_i$, corresponding to the increment in the energy generation required to balance an increase in the demand. In the second scenario the capacity of local generation is impaired, making energy transfers from neighboring areas necessary for demand satisfaction (see Table 3.4). These transfers are described by the coalitional setpoints optimized by an RTO layer

$$\min_{\boldsymbol{\nu}_i^r, \boldsymbol{\xi}_i^r} \sum_{t=0}^{N_p-1} \|\nu_i^r(t|k) - \bar{\nu}_i(t|k)\|_{\mathbf{R}_i}^2 + \left\|\xi_i^r(t+1|k) - \bar{\xi}_i(t+1|k)\right\|_{\mathbf{Q}_i}^2 \tag{3.41a}$$

s.t.

$$\xi_i(t+1|k)(I - \mathbf{A}_{ii}) - \mathbf{B}_{ii}\nu_i(t|k) = \mathbf{D}_i\delta_i(t|k), \tag{3.41b}$$

$$\mathbf{1}^\intercal\nu_i(t|k) = \mathbf{1}^\intercal\delta_i(t|k), \tag{3.41c}$$

$$\nu_i(t|k) \in \Psi_i,\ t = 0, \ldots, N_p - 1, \tag{3.41d}$$

$$\sum_r P_{rj}(\Delta\theta_r - \Delta\theta_j) = (\Delta d_j - u_j^{\max})_+, \quad j \in \mathcal{C}_i,\ \forall r \in \mathcal{M}_j \cap \mathcal{C}_i, \tag{3.41e}$$

$$\delta(t|k) = \hat{\delta}_i(k+t),\ t = 0, \ldots, N_p - 1, \tag{3.41f}$$

where $\boldsymbol{\nu}_i^r \triangleq [\nu_i^r(k), \ldots, \nu_i^r(k+N_p-1)]$ is the input setpoint along the horizon N_p for $\mathcal{C}_i$, and $\boldsymbol{\xi}_i^r \triangleq [\xi_i^r(k+1), \ldots, \xi_i^r(k+N_p)]$ is the associated state reference. In the steady-state condition (3.41b), $\delta_i \triangleq (\Delta d_j)_{j\in\mathcal{C}_i}$ is the demand vector relative to all members of the coalition; (3.41c) defines the demand-supply equilibrium within a coalition, i.e., it is equivalent to $\sum_{j\in\mathcal{C}_i} \Delta\bar{P}_j = \sum_{j\in\mathcal{C}_i} \Delta d_j$. Weighting matrices in (3.41a) are defined as $\mathbf{Q}_i = \text{diag}(Q_{ii})$ and $\mathbf{R}_i = \text{diag}(R_{ii})$, with $Q_{ii} = (10, 0, 100, 100)$ and $R_{ii} = 100$. The setpoint $(\nu_i^r, \xi_i^r) \equiv (\bar{x}_i, \bar{u}_i)$ is assigned to singleton coalitions, since power transfers cannot be arranged for them.

At each time step, the procedure described in Section 3.4 is followed to evaluate the possible formation of coalitions, and then Problem (1.9) is solved independently by each resulting coalition to derive the control inputs $\nu_i^*(k)$ allowing the generation side of the grid to follow the reference (u^r, x^r). Cooperation costs are assumed increasing with the coalition size, $\chi = c_{\text{coal}}|\mathcal{C}|^2$, for $|\mathcal{C}| \geq 2$. The prediction and bargaining (see (3.9)) horizons length is set to $N_p = N_b = 5$. Following [111], the terminal cost in (3.8a) is chosen as

$$\boldsymbol{\ell}_i^{\mathrm{f}}(N_p|k) = (\xi_i(k) - \bar{\xi}_i)^\intercal \mathbf{Q}_i^{\mathrm{f}}(\xi_i(k) - \bar{\xi}_i), \tag{3.42}$$

where $\mathbf{Q}_i^{\mathrm{f}} = 20\mathbf{Q}_i$.

3.6.3 Results

In order to evaluate the variation of the controller performance over different degrees of cooperation, two indices are defined. The first is the average overall frequency deviation,

$$\eta(\omega) = \frac{1}{T_{\text{sim}}} \sum_{t=1}^{T_{\text{sim}}} \sum_{i \in \mathcal{N}} \Delta\omega_i^2, \tag{3.43}$$

and the second reflects the energy transferred between areas,

$$\psi(\theta) = \sum_{t=1}^{T_{\text{sim}}} \sum_{i \in \mathcal{N}} \sum_{j \in \mathcal{M}_i} \|\Delta P_{ij}(t) T_s\|^2, \tag{3.44}$$

where ΔP_{ij} is defined in (3.39), and T_s is the sampling time. These indices provide a measure of the global performance not dependent of the particular evolution of the coalition structure.

One instance of the evolving coalitional structure in Scenario 1 is represented in Fig. 3.3: notice that following the grid topology, coalitions are allowed only between interconnected areas. Similarly, results with the second scenario are shown in Fig. 3.4. One example of the energy supply provided by coalitional control in the second scenario is shown in Fig. 3.2. In this case, the supply capacity in Area 3 is not always sufficient to fulfill the local demand; meanwhile, generators in Area 5 cannot decrease their production to match the lowest local demand level, so the excess of production is transferred to other areas. As can be seen in Figure 3.2, the lack of supply capacity is covered by neighboring generators.

Figures 3.5 and 3.6 gather the results of a set of 200 simulations for the two scenarios, showing the performance for different values of c_{coal}. Coalition formation is

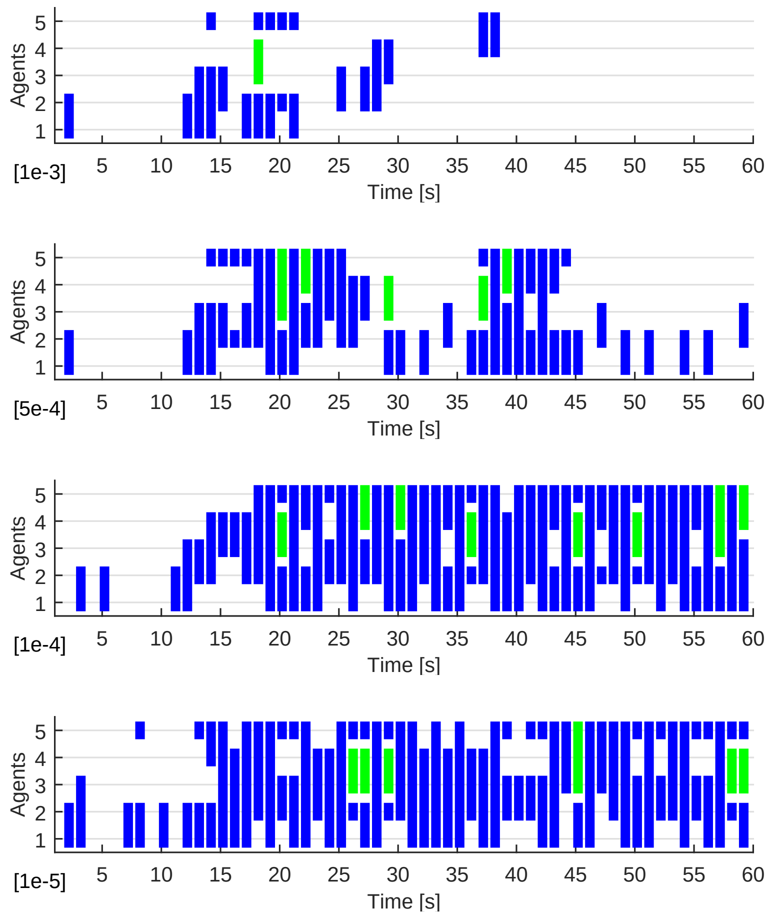

Figure 3.3: Scenario 1: production capacity is sufficient for locally matching any demand. Formation of coalitions for different values of c_{coal}. Costs of cooperation are increasing with the coalition size, i.e., $\chi = c_{\text{coal}}|\mathcal{C}|^2$, for $|\mathcal{C}| \geq 2$.

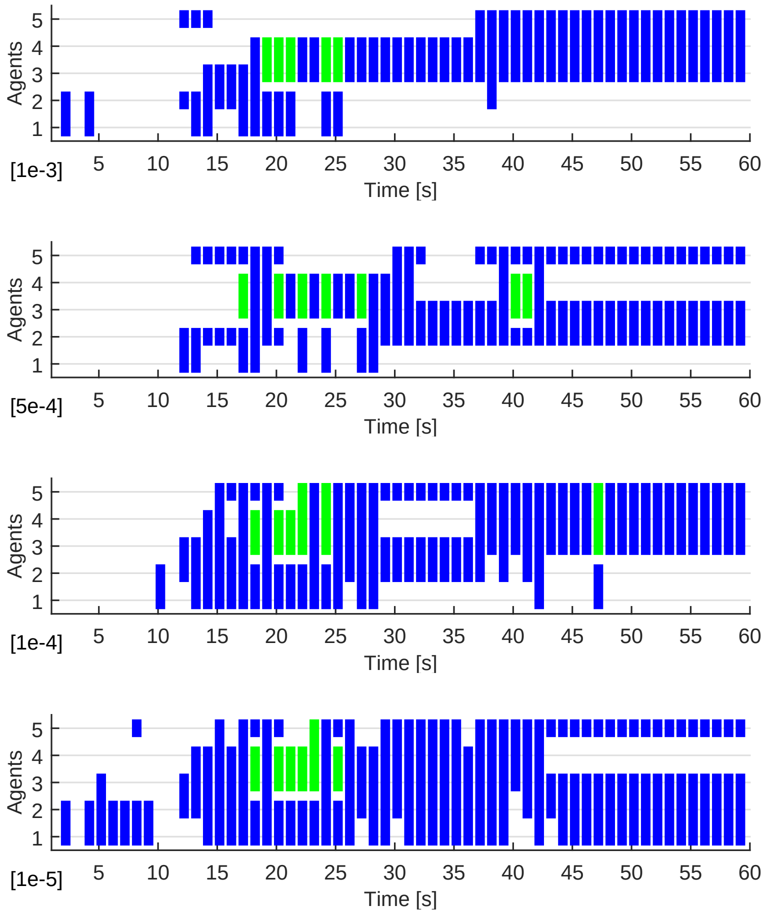

Figure 3.4: Scenario 2: the capacity of local generation is impaired, making energy transfers from neighboring areas necessary for demand satisfaction (see Fig. 3.2). The plots show the evolution of coalitions for different values of c_{coal}. Costs of cooperation increase with the coalition size, i.e., $\chi = c_{\text{coal}}|\mathcal{C}|^2$, for $|\mathcal{C}| \geq 2$. The cooperation in this case follows a more stable pattern.

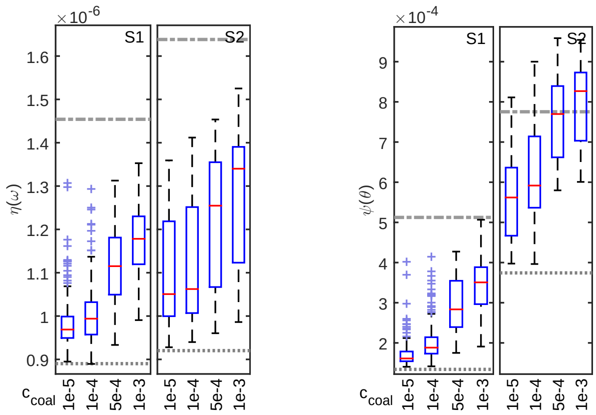

Figure 3.5: Performance index $\eta(\omega)$ (left) and $\psi(\theta)$ (right), respectively regarding the minimization of the frequency deviation and of inter-area energy transfers, for increasing values of c_{coal}. Plots marked with S1 are relative to Scenario 1, while S2 refers to the case in which areas 2, 3 and 5 experience limitations in their power generation. The dotted line marks the performance of the strictly cooperative strategy (centralized MPC), whereas the dashed-dotted line refers to the strictly noncooperative one. See Fig. 3.7 for details on the box representation. Even with scarce cooperation ($c_{\text{coal}} = 10^{-3}$), the performance improvement over noncooperative control is sensible: indices $\eta(\omega)$ and $\psi(\theta)$ are enhanced in Scenario 1 by about 18% and 31%, respectively. In Scenario 2, $\eta(\omega)$ is improved by about 18%; however, power transfers cannot be avoided in this scenario, and the low coordination between areas results in an increase of $\psi(\theta)$ by 5%.

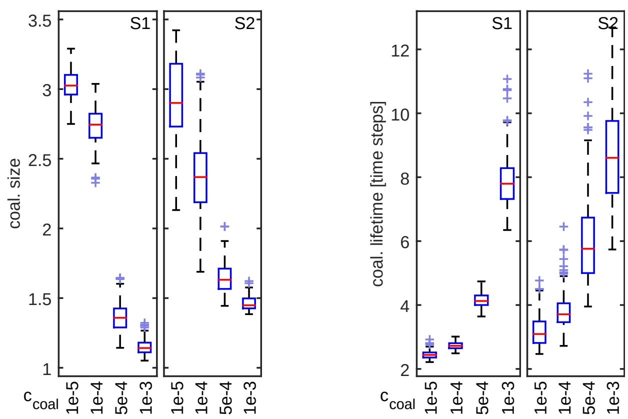

Figure 3.6: Average size of coalitions (left) and coalition lifetimes (right), for different values of c_{coal} (costs of cooperation are increasing with the coalition size, i.e., $\chi = c_{\text{coal}}|\mathcal{C}|^2$). Plots marked with S1 are relative to Scenario 1, while S2 refers to the case in which areas 2, 3 and 5 experience limits on the power generation. See Fig. 3.7 for details on the box representation.

Table 3.5: TU scheme allocation for the grand coalition.

	Dec. MPC	Centr. MPC	TU alg.	Shapley
Area 1	0.424	0.433	0.359	0.353
Area 2	0.365	0.268	0.329	0.333
Area 3	0.136	0.080	0.085	0.085
Area 4	0.057	0.052	0.054	0.052
Area 5	0.143	0.101	0.110	0.112

disincentivized as c_{coal} is increased, deteriorating the achievable performance. Roughly speaking, the performances of coalitional control fall between those obtained through fully-cooperative (centralized) and noncooperative MPC control. It is interesting to see how, even with a reduced cooperation effort, the performance improvement over the noncooperative control is sensible: with $c_{\text{coal}} = 10^{-3}$ (see top plot in Fig. 3.3), yielding an average coalition size of 1.2, indices $\eta(\omega)$ and $\psi(\theta)$ are enhanced by about 18% and 31%, respectively. In Scenario 2, $\eta(\omega)$ is improved by about 18%; however, power transfers cannot be avoided in this scenario, and the low coordination between areas results in an increase of $\psi(\theta)$ by 5%.

Table 3.5 shows the accumulated control costs for each area, in Scenario 1 (cooperation costs are not included). The allocation produced by the proposed iterative utility transfer algorithm is compared to the Shapley value. In order to better evaluate these two outputs, the agents were not allowed to leave the grand coalition in the simulations relative to Table 3.5. The first two columns show the control costs associated to centralized (fully cooperative) and noncooperative MPC: notice how for Area 1 cooperation implies an increase of the local cost. Individual rationality is achieved for all areas with both allocation methods. The results relative to the iterative transfer algorithm have been obtained with 10 iterations, i.e., the dissatisfaction w.r.t. the assigned allocation has been checked for 10 randomly selected subcoalitions (see Sections 3.4 and 3.5). Instead, the Shapley value required at each time step the evaluation of all possible subcoalitions, in this case $2^5 = 32$. These calculations are carried out by the procedure described in Sections 3.3.1 and 3.3.2.

Figures 3.7 and 3.8 show the accumulated control costs for the 5 areas, and their corresponding online reallocation, resulting over 200 simulations for the two scenarios. Notice how—particularly in Scenario 1—individual rationality is not always fulfilled when cooperation costs become appreciable. Online reallocation mitigates this issue and provides an incentive for the cooperation (see especially the case of Area 1).

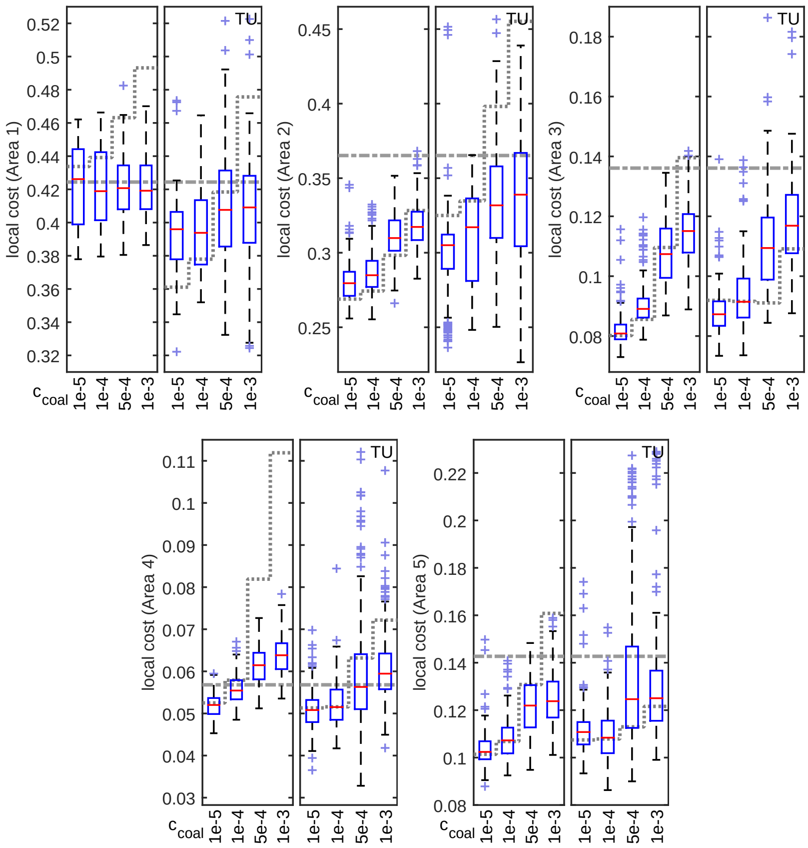

Figure 3.7: Scenario 1: production capacity is sufficient for locally matching any demand. Cost—involving both control and cooperation—locally incurred by agents, accumulated along the simulated interval. Plots marked with TU show the result of the online reallocation with the proposed algorithm. Box plots gather the results of 200 simulations, for different values of c_{coal} (costs of cooperation are increasing with the coalition size, i.e., $\chi = c_{\text{coal}}|\mathcal{C}|^2$, for $|\mathcal{C}| \geq 2$). As a reference, the costs corresponding to the fully cooperative strategy are denoted by the dotted line, showing the influence of cooperation costs. These—initially equally supported by the agents—are reallocated online with the proposed algorithm, as shown by the dotted line in 'TU' plots. The dashed-dotted line refers to the local cost with the noncooperative strategy. Boxes cover the range between the 25th and the 75th percentiles (the central mark is the median), and outliers (data exceeding a distance from the box extremes of 1.5 times the difference between the 25th and the 75th percentiles) are plotted separately.

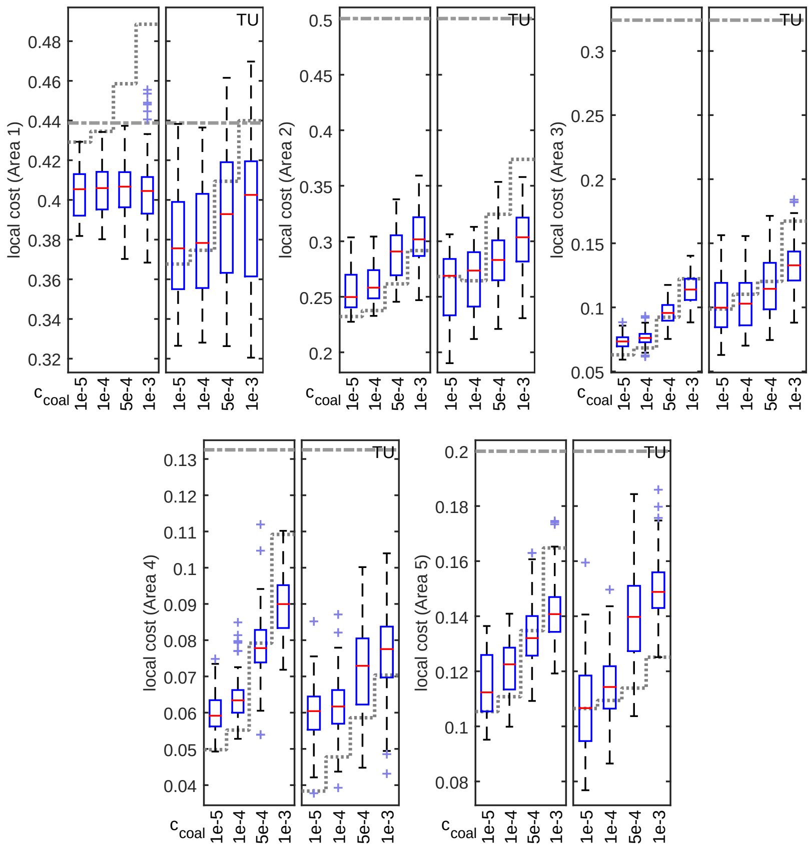

Figure 3.8: Scenario 2: the capacity of local generation is impaired, making energy transfers from neighboring areas necessary for demand satisfaction. Control cost locally incurred by agents, accumulated along the simulated interval. Plots marked with TU show the result of the online cost reallocation with the proposed algorithm. As a reference, the costs corresponding to the fully cooperative strategy are denoted by the dotted line, showing the influence of cooperation costs. These—initially equally supported by the agents—are reallocated online with the proposed algorithm, as shown by the dotted line in 'TU' plots. The dashed-dotted line refers to the local cost with the noncooperative strategy. See Fig. 3.7 for details on the box representation.

Chapter 4

Coalition formation of fast EV charging stations

The growing popularity of EVs induces the need of a novel infrastructure capable of efficiently supplying the associated energy demanded. It is expected that a significant portion of EV users' daily trip will exceed the range of the fully charged battery, thus requiring a recharge during daytime operation of the vehicle [112, 113, 114]. EV drivers will likely be uneasy with specific characteristics of EVs such as monitoring the state of charge (SoC) and best locating one of the available charging stations (CS). A recharging infrastructure whose service capability is as close as possible to the current gas station network is foreseen [115]. EV charger specifications are classified into three levels: level 1 (residential and commercial buildings), level 2 (specific charging facilities) and level 3 (fast charging). A 10 kWh battery would require about 5.5 hours with level 1 chargers, a couple of hours with a level 2 charger and about 15 minutes for level 3 [116].

Such novel infrastructure will likely encompass advanced power, communication, and control technologies. Information technologies applied to the transportation industry (intelligent transportation systems, ITS) strongly support this development, as vehicles and infrastructures are capable of exchanging traffic data in real-time. The advantages of the use of the ITS information for EV routing are shown in [115]. The focus is on minimal routing and queueing at fast CSs, comparing different scenarios characterized by an increasing level of knowledge—by EV drivers—about the real-time state of nearby CSs, allowing for an enhanced estimation of the waiting time. Results show that updated information about the estimated waiting time at each CS can be effectively employed for rerouting (choice is assumed unrelated to prices), providing significant improvement in the quality of service experienced by the users.

The problem of CS selection is also studied in [116], according to the distance to the station and the spot price. Knowledge about reciprocal location is assumed to be available, and the CS owners act such as to maximize their revenue. The setting is modeled as a noncooperative oligopoly game, providing a Nash equilibrium for prices and energy supply. A specific assumption made in [116] is that the same utility companies are the owners of CS facilities. As such, they can adjust the power generators setpoint to the CS demand in real-time, using updated information about all charging operations. Although it may seem a strong assumption at first, the availability of local generation devices (e.g., PV panels, small wind generators) makes this a plausible scenario.

CSs equipped with renewable power generators are considered in [117]. The study focuses on the pricing policy resulting by the competitive market interactions of CSs, modeled as a supermodular game. Constraints such as capacity of transmission lines and distance of the demanding EVs from the stations are taken into account.

The work of [100] addresses the pricing problem and the consequent selection of the best station by EV drivers. Besides the energy price, waiting times and travel distances are taken into account by drivers.[1] Due to the complexity of the problem, the analysis is carried out on a one-dimensional model (i.e., EVs moving along a line), with two competing charging stations and demand of recharges by EV approximated as a Poisson distribution. The market equilibrium is derived through the solution of a Stackelberg game model, where the stations announce their prices—based on predictions of the demand—upon which the EV drivers optimize their choice.

To estimate the average waiting time at charging stations, the authors of [100] assume a small penetration of EVs, in order to exploit the theory of $M/G/k$ queues. On the other hand, a sufficient number of EVs is assumed to allow modeling the CS selection as a population game, where a single player's decision has a negligible effect on the global equilibrium (and moreover, it will not affect the waiting time at a given station).

The EV charging station load is complicated and mutable, closely related to the user's schedule, driving and travel patterns, besides the CS availability [118]. Issues related to economical factors of CSs such as energy markets and dynamic pricing have already been considered in several works, involving as well the use of game theoretical tools [119, 14]. So far, most attention has been directed on the stress that uncontrolled daytime EV charging peaks may produce on the power system, which may even result

[1] However, just the instantaneous distance value, relative to the time when the decision is made, is considered. The influence of the driver's predefined route in the final decision is not taken into account in the model.

in grid outages. Concerned with the coordination of the demand, in order to avoid overloads of the existing electric grid, several works make use of pricing schemes and employ game theory concepts for the problem analysis [120, 121].

However, *the mobility of EVs is hardly taken into account*, since the most common scenario analyzed in the literature is household recharging [112]. On the distribution layer perspective, electric vehicle charging demand will constitute a unidentified quantity which may vary by space and time. The work of [122] formulates a mathematical model of the EV charging demand for a fast charging station. The arrival rate of vehicles is predicted by a fluid dynamic traffic model, whereas the charging demand forecast is based on multi-server queueing theory. Such model can allow the grid distribution planners to anticipate a charging profile for a specific CS. It is worth to remark that since the traffic flow is modeled by means of the fluid dynamic model, the work in [122] is specifically meant for CSs located on a highway, and not in urban environment. Furthermore, the model only considers EVs whose batteries are almost drained, thus requiring charging at the closest charging station.

The work of [112] brings out the concept of quality of service for charging stations, involving minimal waiting time for customers. In order to address the long delays caused by the fairly large charging time (compared with that of conventional gasoline vehicles), the authors of [112] propose a price admission mechanism at each CS. To achieve an efficient load across the grid, drivers are incentivized through price signals to recharge at less busy stations.

Although the above mentioned studies typically assume that vehicles follow a rigid (often monodimensional) trajectory, a number of methods have been proposed for the prediction of the EV load based on driving patterns, possibly obtained from data of real commuting habits [123]. Nevertheless, if on one hand the information available for light duty vehicles is limited, on the other hand it is arguable to expect that such data can be directly translated on EVs. The microsimulation environment employed in the present work was developed in cooperation with AYESA [124], which provided insights on the problem and data from the real benchmark Zem2All [125].

It is widely acknowledged that dynamic pricing policies offer the best performance in terms of efficient use of the infrastructures, since price variations allow to adjust the demand in real-time according to the system capacity. However, implementation of such pricing mechanisms is not straightforward, as it requires expensive real time monitoring. For this reason, static (e.g., flat rates) or myopic mechanisms (e.g., *congestion pricing* [112]) are eligible candidates for the application. The main goals of this case study are *(i)* to develop a model of the variation of the energy demand for EVs recharge operations in a urban setting, according to the spot prices, and *(ii)* to design a control strategy—based on such a model—to let each CS maximize its own economical benefit by either operating on its own or according to a joint planning derived through strategic coalitions.

4.1 Problem formulation of the case study

4.1.1 Scenario Description

The case study considers the interplay between several fast charging stations (CS) and the users of such public charging facilities. Since the primary recharging option will likely be constituted by (slow) charging posts located in house garages and parking lots, it is expected that the users of fast CS will be a subset of the whole EV population. The study by [126] estimates the portion of EV users demanding fast charging operations to be about 30% of the total EV population.

The choice of the charging station by EV drivers is a highly complex problem. Besides the natural dependence of the demand from the energy prices, the long time required for battery recharge (even with fast DC chargers) produces a significant coupling between the decisions of different drivers, unlike gas stations.

In order to facilitate the analysis, the problem has been so far approached in the literature through essential schemes, characterized by restrictions on the action space of both parties: simplifications may range from a unique price applied by all charging stations to neglecting the coupling between EV drivers' decisions (see [100] and references therein). Here, a price optimization problem is formulated from the charging manager (CM) standpoint, i.e., the owner of charging facilities. Demand at each CS is strongly correlated with its location as well as the location of the other CSs, and with the dominant traffic pattern. Motivated by this, we identified the sensitivity of the aggregate demand to recharge price variations on a microscopic traffic simulator. The open microsimulator SUMO [127] has been employed as the base engine for the simulation platform.

The possibility for any CM of cooperating with other CMs for a joint planning of the pricing strategy is considered to enhance the efficiency in the use of available charging infrastructures.

Behavior of EV drivers

The microsimulated urban scenario assumes that EV drivers looking for a recharge can access traffic data such as vehicle positions, velocities, etc. Indeed, such information can be accessed thanks to modern intelligent traffic infrastructures (ITS) and localization systems embedded in mobile phones (*floating car data*). Then, EV drivers rationally select a CS according to a function expressing their individual utility, expressed by (4.1), defined by a trade-off between charging cost minimization and getting the service as soon as possible. This function takes into account the state of charge (SoC) at the time of the decision, the desired final battery level, the time and energy required to reach the station and their equivalent monetary cost. In particular, the latter is a cost associated to the time required for the whole operation, converted into currency units (CU) for compatibility with energy prices.

$$J_i^{EV} = E_{\max,i}^{EV}(\mathrm{SoC}_f + \mathrm{SoC}_{(i,j)} - \mathrm{SoC}_o)p_j + (t_{(i,j)} + t_j^w - t_i^{\mathrm{tol}})\psi_i, \tag{4.1}$$

where $E_{\max,i}^{EV}$ is the battery capacity of EV i, SoC_f is the target SoC, SoC_o is the SoC at the time of the decision, $\mathrm{SoC}_{(i,j)}$ is the energy (in terms of SoC) required for EV i to get to CS j, and p_j is the price per kWh applied by CS j. The last term expresses the time cost, being $t_{(i,j)}$ the (estimated) time needed to reach the station, and ψ_i the price of user i's time, in CU per hour. The waiting time $t_{w,j}$ at CS j is estimated as in (4.2) for the station under consideration, on the basis of the number of vehicles in the line n_j^{EV}, of the mean individual demand $\bar{E}^{EV}$, and finally of the number of plugs n_j^{plug} and the power $P_{\max,j}$ available at CS j. An additional term in (4.1), designated as t_i^{tol}, expresses the tolerable queue time for user i.

$$t_{w,j} = \max\left\{0, n_j^{EV} - n_j^{\mathrm{plug}} + 1\right\} \bar{E}^{EV}/P_{\max,j}. \tag{4.2}$$

CS management

The demand at any given charging station is naturally related to the spatial and temporal distribution of EV traffic. Indeed, in real life the distribution of vehicles is far from being uniform: people tend to drive between points of interest, such as their home, school, workplace, and their typical routes may depend, e.g., on the day of the week. Such a stochastic behavior creates uneven customer demand among the charging facilities. Hence, the utility company on one hand, and managers of charging stations

Table 4.1: Table of symbols

$E^{EV}_{\max,i}$	EV i battery capacity	[kWh]
SoC_f	SoC after the recharge	%
SoC_o	current SoC	%
$\mathrm{SoC}_{(i,j)}$	drop in EV i SoC for reaching CS j	%
p_j	price of recharge at CS j	[CU/kWh]
$t_{(i,j)}$	time for reaching CS j	[h]
t^w_j	waiting time at CS j	[h]
t^{tol}_i	tolerable waiting time for EV i	[h]
ψ_i	cost of time for user i	[CU/h]
n^{EV}_j	vehicles in line at CS j	-
n^{plug}_j	plugs available at CS j	-
$P_{\max,j}$	power at CS j plugs	[kWh]
$\bar{E}^{EV}$	average recharge	[kWh]

on the other, both want to properly allocate the EVs to charging stations according to their interests.

The first scenario presented in this study considers four charging stations located in the urban area of Seville, Spain, each owned by a different charging manager. The objective is to study how different pricing strategies affect the economic benefit that each CS can achieve, and how coalitions between CMs influence their performance. The strategy of each CM is optimized on the basis of a simplified model of the behavior of EV drivers looking for fast recharging facilities in response to spot price variations:

$$E_i(k+1) = E_i(k) + B\Delta\mathbf{p}(k+1) + D\frac{\bar{p}(k+1) - p_{alt}}{p_{alt}}E_i(k), \tag{4.3}$$

where $\Delta\mathbf{p} \in \mathbb{R}^{|\mathcal{N}_{CS}|\times 1}$ is defined as

$$\Delta\mathbf{p}(k+1) \triangleq [p_i(k+1) - p_i(k)]_{i\in\mathcal{N}_{CS}},$$

E_i is the total recharged energy supplied at CS i, p_i is the price per kWh applied for the recharge, p_{alt} is the alternative price taken as reference. The parameters of the model are identified over different simulations on the developed microsimulation platform. Two terms compose the model: the first, taking into account the price differences between stations, evaluates the redistribution of the energy over the different CSs; the second expresses the tendency of the demand at decreasing when facing an overall rise of the perceived price, in presence of more competitive alternatives (the opposite holds when perceived price decrease). The manipulated variables are the daily prices (in

CU/kWh) applied at the stations for battery recharge, simultaneously made available by all charging managers.

The utility of the charging stations owner consists in maximizing its profit, which broadly speaking translates in serving as much EVs as possible while fulfilling the most restrictive constraint between the maximum power deliverable by the stations and the eventual limitations imposed by the grid operator. The next sections describe the formulation of the optimization problem.

4.1.2 Control objective

The objective of the control consists in maximizing the station's revenue derived by the recharging service. The revenue is formulated as $E_i p_i$, where E_i is the overall energy supplied by CS i, and p_i is the applied price per kWh. Notice that not all the revenue will constitute benefits for the CS. In this work, we model general costs for the use of infrastructures—that can be addressed to different aspects related with the energy provision and recharging operations—as a quadratic term depending on the delivered energy volume. Also, recall that each CS has a limited number of available charging plugs: as a byproduct of the optimization, such term will avoid to attract with low prices an excessive number of customers, since the station will not be able to satisfy the demand within a reasonable time slot. Hence, the CS utility is expressed by

$$U_i = E_i p_i - c_i E_i^2, \tag{4.4}$$

where c_i is a constant parameter associated with the infrastructural availability and supply-associated costs of CS i. Then the objective to maximize for CS i is defined as:

$$J_i(k) = \sum_{t=k}^{k+N_p} E_i(t) p_i(t) - c_i E_i^2(t), \tag{4.5}$$

over the prediction horizon N_p. For each station, the value of c_i is assumed to be in the order of 10^{-5} CU/kWh^2. Prices are considered in the range 0.275 – 0.325 CU/kWh. The steady-state demand distribution across the stations, when all four CSs apply the same price of 0.300 CU/kWh, is

$$E_0 = (296.63,\ 323.25,\ 264.75,\ 289.88)\ \text{kWh}.$$

Predictions employed for the solution of the problem of profit maximizing are based on the model (4.3), identified over a microsimulated traffic scenario.

4.2 Description of the applied management strategies

4.2.1 Coalition formation

The above setting is expanded by considering the possibility of coalition formation among CMs. The problem consists in deciding with whom to cooperate and under which conditions (namely, the allocation of the payoffs among the members of a coalition). We model such situation as a coalitional game in *characteristic form*. A coalitional game is uniquely defined by the pair $(\mathcal{N}, v)$, where $\mathcal{N}$ is the set of players and v is the *value* of a given coalition.

More specifically, a value is assigned to any possible coalition through a function $v : 2^{\mathcal{N}} \to \mathbb{R}$. The real value $v(\mathcal{C})$ associated with coalition $\mathcal{C}$ can be divided and transferred among its members (e.g., side-payments used to attract other players). The *payoff* ϕ_i is defined as the utility received by each agent $i \in \mathcal{C}$ by the division of $v(\mathcal{C})$. The vector of payoffs assigned to all the agents is referred to as the *allocation*.

Notice that such model cannot accurately reproduce the vast majority of real life scenarios. It is natural in engineering applications to encounter problems in which the value of a given coalition cannot be determined regardless of how the rest of the agents are organized. Games in *partition form* better fit to such type of problems: given a partition of the set of agents $\mathcal{N}$, i.e., a set of disjoint coalitions $\boldsymbol{\mathcal{C}} = \{\mathcal{C}_1, \dots, \mathcal{C}_l\}$, the value of a coalition $\mathcal{C}_i \in \boldsymbol{\mathcal{C}}$ is expressed as $v(\mathcal{C}_i, \boldsymbol{\mathcal{C}})$ [54]. Since it is not possible to derive a closed-form allocation in such setting, we approximate the partition function game with a characteristic function game by assigning values to coalitions *following a minmax approach*. The value of a given coalition will thus take into account the most unfavorable externalities given by any coalitional setup of the rest of agents.

Shapley Value

In order to compute a division of the coalition value across the coalition members, we consider here the closed-form expression provided by the Shapley value. Shapley defined the conditions to obtain a unique payoff mapping of the game $(\mathcal{N}, v)$ [29]. The Shapley value $\phi(v)$ satisfies the following three axioms:[2]

[2]Further axioms characterize the Shapley value. We mention here the ones related with our purpose.

1. *Efficiency*:
$$\sum_{i\in\mathcal{N}} \phi_i(v) = v(\mathcal{N}).$$

2. *Symmetry*: given two players i and j, if
$$v(\mathcal{C} \cup \{i\}) = v(\mathcal{C} \cup \{j\}),\ \forall \mathcal{C} | \mathcal{C} \cap \{i, j\} = \varnothing,$$
then $\phi_i(v) = \phi_j(v)$.

3. *Dummy*: if, for any player i, it holds that
$$v(\mathcal{C}) = v(\mathcal{C} \cup \{i\}),\ \forall \mathcal{C} | \mathcal{C} \cap \{i\} = \varnothing,$$
then $\phi_i(v) = 0$.

The symmetry axiom assigns the same payoff to players that equally improve a given coalition, while the dummy axiom assigns a null payoff to a player which does not contribute when joining a coalition. The formulation of the individual payoff assigned to player i according to the Shapley value's mapping is:

$$\phi_i(v) = \sum_{\mathcal{C}\subseteq\mathcal{N}\setminus\{i\}} \frac{|\mathcal{C}|!(|\mathcal{N}| - |\mathcal{C}| - 1)!}{|\mathcal{N}|!} \left[v(\mathcal{C} \cup \{i\}) - v(\mathcal{C})\right] \tag{4.6}$$

In words, the Shapley value expresses the individual *expected marginal contribution* of agent i to the coalition.

Despite the advantage of its closed form, the computational complexity of (4.6) increases significantly with the number of agents: some efficient techniques for its computation can be found in the literature (see, e.g., [128]). The sampling time of 12 h employed in this scenario leaves enough room for the computation; nevertheless, combinatorial explosion needs to be addressed when the number of independent charging stations grows.

4.2.2 Coalitional approach to the EV case study

The aim here is to explore the benefit brought in by the cooperative management of the set of CMs. Such benefit can be directly translated into economic units, and then possibly transferred (as recompense) from one agent to another in order to overcome what constrained the emergence of cooperation in the first place. This type of situations is designated in the game theory literature as transferable utility (TU) [51].

The following mechanism is implemented here for coalition formation. At each round (every 12 h in the simulations), all possible coalitions among CMs are evaluated, and the organization into a given coalitional structure will be decided as the outcome of a best matching algorithm. This operation is carried out on the basis of an increase of individual economic benefit for each agent, derived from the Shapley allocation of the value of the coalition the agent is affiliate with.

Remark 4.1. *For simplicity of presentation, we assume in the remainder that every CS belonging to a given CM will be involved in the coalition in which the CM participates. Nonetheless, a CM may in general choose to consider within a given coalition the management of only a subset of the CSs he owns.*

Given the above assumption, any set of CMs $\mathcal{C} \subseteq \mathcal{N}_{CM}$ straightforwardly maps into a set of CSs $\mathcal{C}' \subseteq \mathcal{N}_{CS}$, where $\mathcal{C}'$ contains all the CSs belonging to the CMs in $\mathcal{C}$.

The value of a coalition $\mathcal{C} \subseteq \mathcal{N}_{CS}$ are computed as the aggregate estimated revenue of the members

$$v(\mathcal{C}) = \sum_{i \in \mathcal{C}} E_i p_i - c_i E_i^2, \tag{4.7}$$

where the second term models usage and maintenance costs (see (4.4)). As mentioned in Section 4.2.1, the problem is approximated to a characteristic form game by assigning the value resulting by the worst-case scenario for any given coalition. Let $\mathbf{p}_i \triangleq (p_j)_{j \in \mathcal{C}}$, and $\mathbf{p}_{-i} \triangleq (p_j)_{j \in \mathcal{N}_{CS} \setminus \mathcal{C}_i}$. Both vectors are formed by subsets of components of the global vector $\mathbf{p} \triangleq (p_j)_{j \in \mathcal{N}_{CS}}$. The revenue prediction for CS i results by the solution of the minmax problem

$$\max_{\mathbf{p}_i} \min_{\mathbf{p}_{-i}} J_i \tag{4.8a}$$

s.t.

$$E(t+1) = E(t) + B(\mathbf{p}(t+1) - \mathbf{p}(t)) + D \frac{\bar{\mathbf{p}}(t+1) - p_{alt}}{p_{alt}} E(t), \tag{4.8b}$$

$$E(0) = E(k), \tag{4.8c}$$

$$\sum_t E_i(t) \leq 12 P^{CS}_{\max,i}, \tag{4.8d}$$

$$\mathbf{p}(t+1) \in \mathcal{U}, \tag{4.8e}$$

$$t = \{0, \ldots, Np - 1\},$$

where (4.8b) is the global energy prediction model relating all CS. Note that no limitations by the grid operator are considered in this problem. Once the $2^{|\mathcal{N}_{CM}|} - 1$ values for the possible coalitions among the CMs are available, the corresponding members' payoffs can be computed by means of the Shapley value. Notice that for the grand coalition, i.e., $\mathcal{C} \equiv \mathcal{N}_{CS}$, $\mathbf{p}_{-i}$ is not defined, and the problem reverts to mere minimization.

At this point, payoffs are used as input to a best matching algorithm in order to derive the best coalition(s) according to individually rational preference order. Since CMs will accept to form a coalition if and only if it implies a rise in their individual payoff, the algorithm matches CMs such that no player is left unsatisfied. However (due to the nonconvexity of this specific game) a conflict may arise between a pair of CMs when the respective preference orders are misaligned. This conflict are solved by assigning players to coalitions according to the lexicographical order. Let CM 1 and CM 2 be two players of the game, and $\{\mathcal{C}_A^{(i)}, \mathcal{C}_B^{(i)}\}$, with $i = \{1, 2\}$, the possible coalitions that can be joined by CM i. Consider the case where the formation of $\mathcal{C}_A^{(i)}$ and $\mathcal{C}_B^{(i)}$ is mutually exclusive. Then, the following order reflects the preference of CMs

$$\{\mathcal{C}_A^{(1)}, \mathcal{C}_A^{(2)}\} \preceq \{\mathcal{C}_B^{(1)}, \mathcal{C}_B^{(2)}\} \text{ iff } \begin{cases} \phi_1(\mathcal{C}_A^{(1)}) > \phi_1(\mathcal{C}_B^{(1)}) \text{ or} \\ \phi_1(\mathcal{C}_A^{(1)}) = \phi_1(\mathcal{C}_B^{(1)}) \text{ and } \phi_2(\mathcal{C}_A^{(2)}) \geq \phi_2(\mathcal{C}_B^{(2)}), \end{cases} \tag{4.9}$$

where $\phi_i(\mathcal{C})$ is the payoff defined by the Shapley value for the participation of player i in coalition $\mathcal{C}$, and $\preceq$ is the lexicographical preference operator.

Finally, the prices relative to the chosen coalitional structure are applied to the system. The profits derived by the energy sale at CS facilities are shared among all members of the corresponding coalition, according to the Shapley values previously computed. Note that since the Shapley values are based on estimated values, they cannot be directly applied to the realization of the profits. Instead, the ratios dictated by the Shapley's payoffs over the predicted coalition value are used for the division of the actual profits.

4.3 Technical description of the implementation

4.3.1 Microsimulations

The microsimulation platform employed for the macroscopic model identification and validation of coalitional strategies among CMs consists of two interdependent layers): the first layer is implemented on the open source microscopic traffic simulator SUMO [127], the second is implemented in Matlab. The two layers communicate via socket, employing the library TraCI4MATLAB [129] (Figure 4.1). The characterization of urban traffic (vehicle displacements, traffic congestion, velocities in each lane,

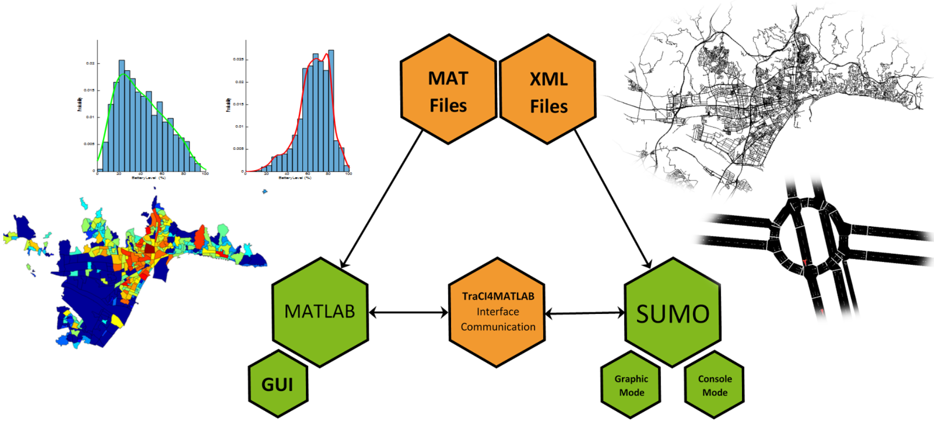

Figure 4.1: Implementation of the EV microsimulation platform over two software layers. Vehicle displacement, traffic congestion is modeled in SUMO. Energy management operations and CS choice is performed in the Matlab layer.

etc.) is performed in the first layer. Detailed street maps of the urban areas of Seville and Malaga (Spain) have been prepared for the purpose. A population of $n_v = 10000$ vehicles has been considered, including both electrical and conventional automobiles, of which $n_{EV} = 400$ (Seville) and $n_{EV} = 1000$ (Malaga) are possible customers of fast charging facilities.

The second layer is responsible for the specific management of electric vehicles. Each driver's decision of when, where and how much energy to recharge is defined at this layer. Other tasks are the modeling of the charging process and the battery discharge along each vehicle's route. For this, information extracted from the historical data (available from project *Zem2All*) about battery consumption as a function of the velocity has been employed. The data are relative to a specific brand and model, the Mitsubishi i-MiEV, featuring a 16 kWh battery. A charging curve has also been extracted from the database. Four independent CMs are considered, each characterized by different maintenance/usage cost factors c_i. For the Seville scenario, each CM owns one CS equipped with one charging post, capable of providing 50 kW output power. The Malaga scenario contemplates the availability of 60 CSs across the whole urban area, also equipped with a single 50 kW charging post.

Remark 4.2. *Although 50 kW can be viewed as the "entry level" power capacity for a level 3 charging post, the i-MiEV battery capacity of 16 kWh is fairly small if compared with the capacity of newer EV models. Therefore, the results of the microsimulation presented in the remainder also scale to higher CS power and larger battery capacities.*

The CS distribution for the two maps is shown in Figures 4.2 and 4.3.

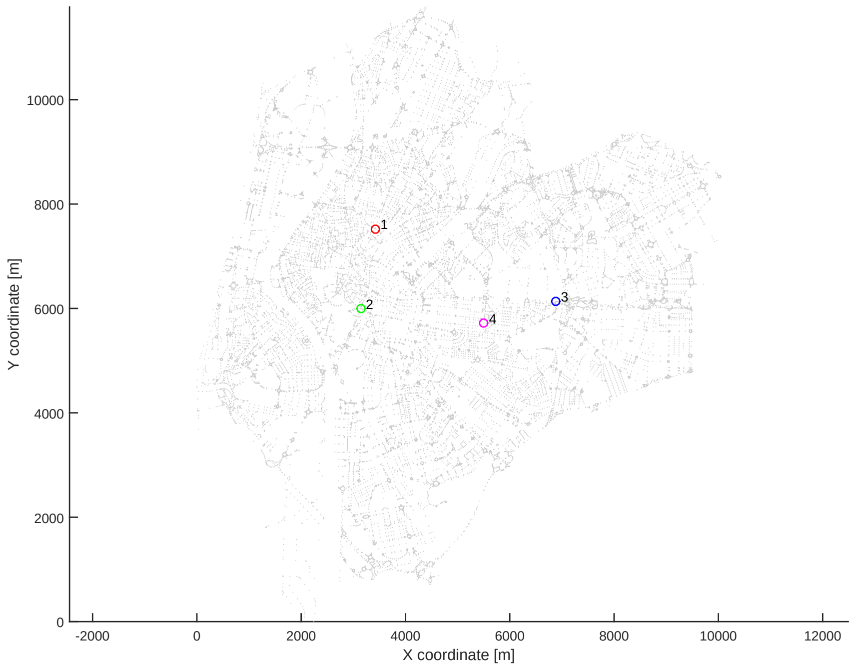

Figure 4.2: Location of CSs in Seville urban area. Colors show the different CM affiliation.

4.4 Validation of the management strategies for the case study

4.4.1 Scenario parameters

Values for the initial battery levels of the vehicles, the discharge rates as a function of the velocity as well as the locations of CSs are provided as initial data for the simulation. Any demand for recharge is triggered when the EV battery reaches a given (low) battery threshold. This threshold is expected to vary from one user to another: in this study, trigger values have been extracted from a probability distribution obtained over the Zem2All benchmark database. Similarly, the final battery level of each charging operation is inferred by real usage data. The first vehicle in line is served at the maximum power of the station $P_{\max,j} = 50$ kW. No limits are imposed on the size of the waiting queue.

In contrast with common non-electric or hybrid vehicles, the route length is limited by the autonomy of the batteries. Indeed, it is possible for an EV to run a distance greater than that allowed by its autonomy—without long charging stops—if a fast recharge is performed along the route. This is the usage pattern that we aim to

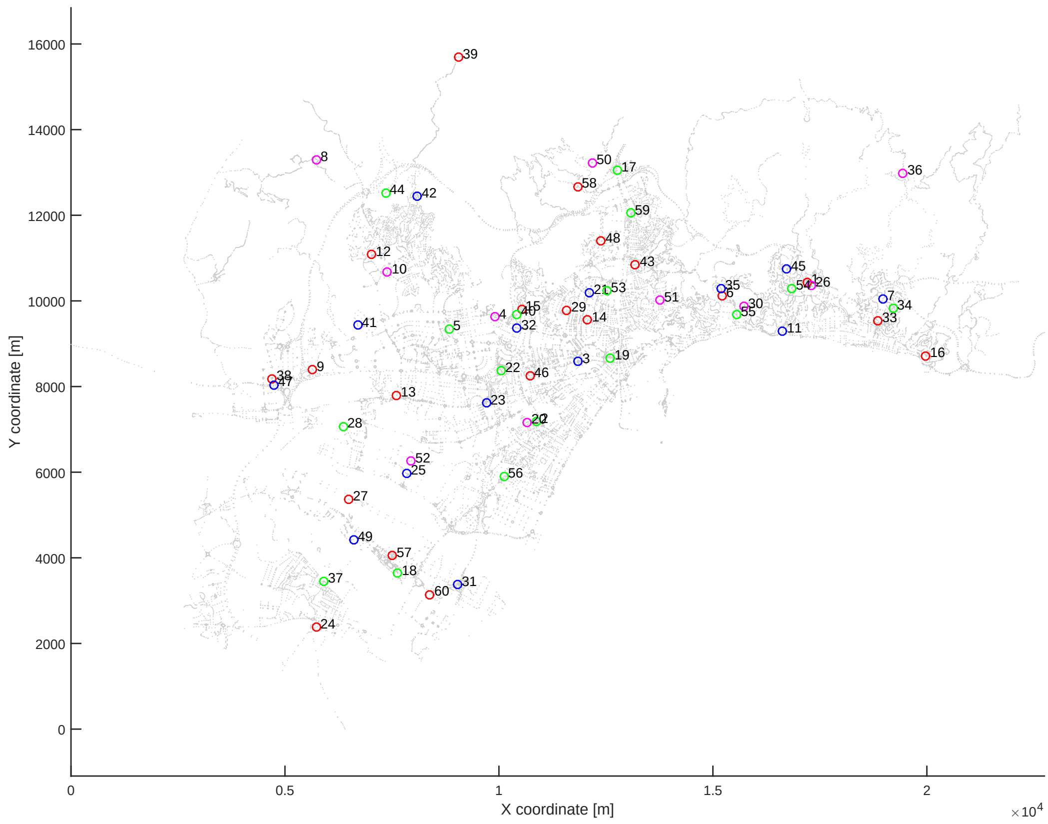

Figure 4.3: Location of the 60 CSs in Malaga urban area. Colors show their affiliation to the four CMs.

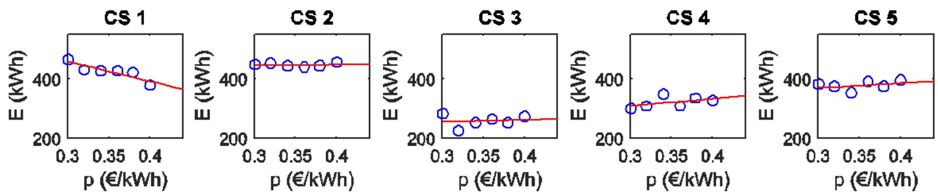

Figure 4.4: Malaga scenario: charging demand at five CSs sampled at different prices applied at CS 1 (all x axes refer to CS 1 price).

simulate in this study. Studies such as [126] estimate that about 30% of the EV routes will generate fast charging demand (see also [130]). To model this aspect, routes of proper length (25 km in average, according to [130], see deliverable D5.3 for further details) have been defined over the two urban areas, such that most of the n_{EV} drivers need to stop and recharge at least once along their route.[3]

4.4.2 Macroscopic model identification

The sensitivity matrices B and D have been identified through a series of simulations capturing the change in the aggregate daily demand to variation of the spot prices applied at CSs. In this particular study, a linearized response has been adjusted over the sampled space by least-square approach. Figure 4.4, relative to the Malaga scenario, shows an example of how the charging demand at five CSs is affected by the variation of the price applied at CS 1 (all x axes refer to CS 1 price). Notice that the coupling between demands at different CSs is a function of the routes followed by EVs and of the (relative) location of CSs, besides the prices and waiting times.

4.5 Results

4.5.1 Seville

Two scenarios are studied for the urban area of Seville, characterized by different maintenance/use costs. We have for scenario (i)

$$\mathbf{c} = [20 \quad 25 \quad 26 \quad 2] \cdot 10^{-5}\,\mathrm{CU/kWh^2}; \tag{4.10}$$

scenario (ii) is identical except the coefficients for CS1 and CS2 are swapped.

[3]Since the synthesis of the routes and the initial battery level are extracted from a probability distribution, some EVs can travel their entire route without having to stop.

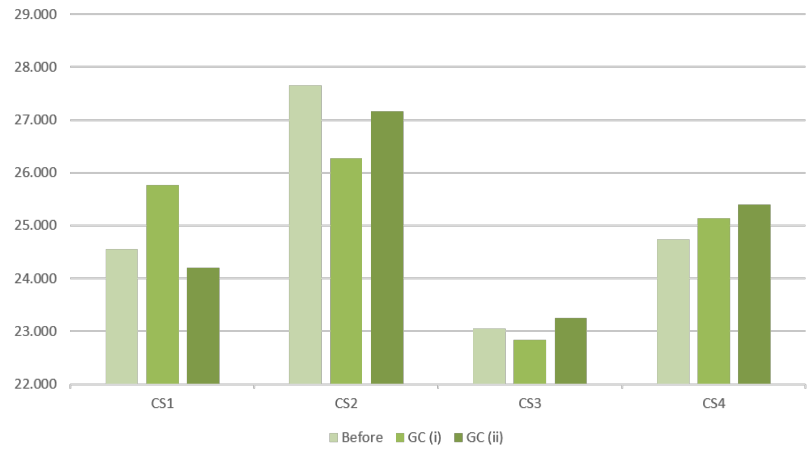

Figure 4.5: Redistribution of recharges (%) resulting by the grand coalition of CSs for scenarios (i) and (ii).

When coalition formation is not restrained, the four CMs reach a grand coalition agreement. The redistribution of the demand resulting by the coalitional strategy is accounted for by the difference maintenance costs (4.10) of CSs. The result for the two scenarios are shown in Figure 4.5. In particular, demand is redirected over CS1 due to its low maintenance costs (scenario (i)), while decreasing the demand at CS2, characterized by high usage costs. The opposite trends can be observed for scenario (ii). Figure 4.6 depicts the case where CS2 is left out from the grand coalition. As it can be seen, it is free to apply the most competitive prices when experiencing low usage costs (scenario (ii)). However, since the pricing strategy is not cooperative, it is not able to redirect the the demand towards other CSs in scenario (i). The cases in Figures 4.5 and 4.6 can be compared with the case where no coalition is formed. It can be seen in Figure 4.7 that CS 3—the best located among the CSs, but also characterized by the highest usage costs—is not able to reroute demand over other stations, and experiences significantly higher maintenance costs in both scenarios.

The effects of coalition formation on the spot prices are shown in Figure 4.8. It is clear how the grand coalition easily takes advantage of the monopoly to raise prices as most as possible. In such situation, users experience very short waiting times due to lower demand and even rerouting over CSs. When the formation of coalitions is forbidden instead, competitive strategies allow to keep prices as low as possible. Measures as limitations on the allowed market share of a single coalition (antitrust) demonstrate to be a means for keeping prices under control. An alternative means against the formation of monopoly is to impose an access costs to coalitions depending on the energy

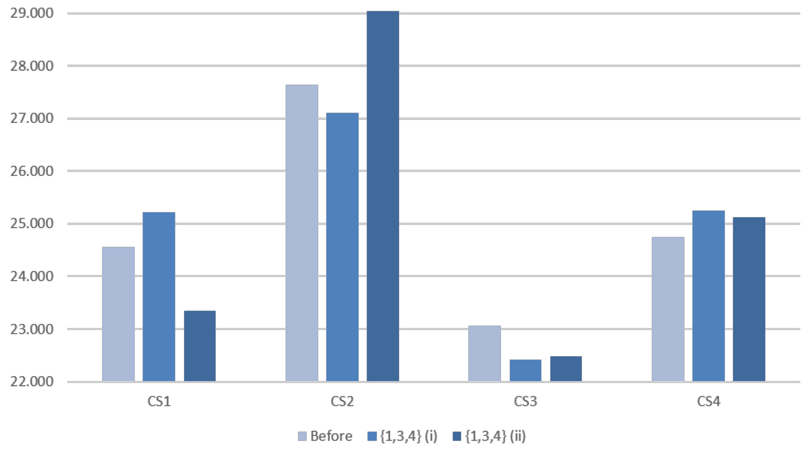

Figure 4.6: Redistribution of recharges (%) over CSs when CS 2 is left out of the grand coalition. Notice how it is free to apply the most competitive prices when experiencing low usage costs (scenario (ii)). However, it is not able to redirect the the demand to other CSs in scenario (i).

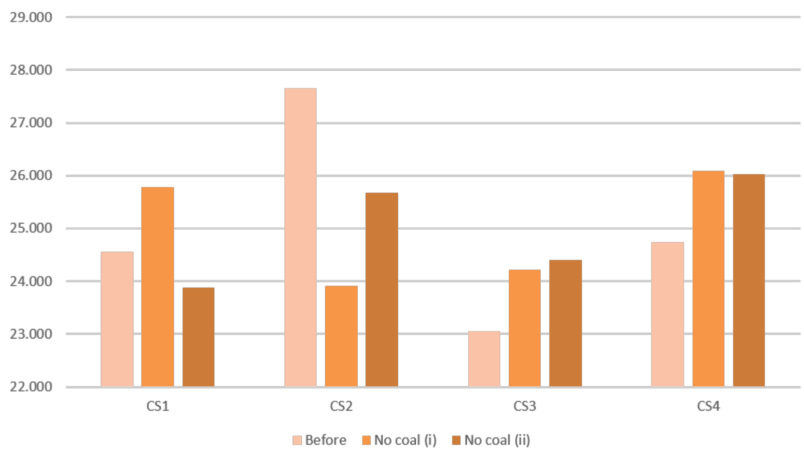

Figure 4.7: Redistribution of recharges (%) over CSs when no coalition is formed. CS 3 is characterized by high usage costs, but it is also the best located w.r.t. to the EV routes. For this reason it is not able to reroute demand over other CSs, and experiences significantly higher maintenance costs in both scenarios.

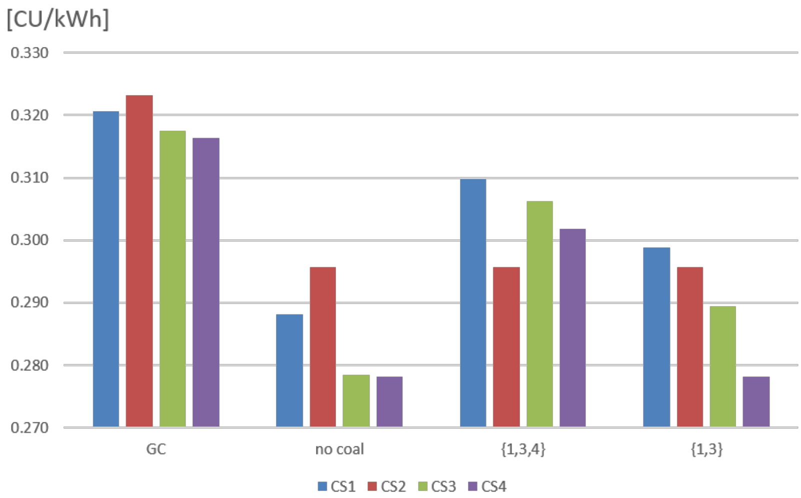

Figure 4.8: Effect of coalition formation on pricing strategies (short prediction horizon). The grand coalition translates into a monopoly management: prices are raised as most as possible. The only advantage for users is to experience the shortest waiting times. On the contrary, when the formation of coalitions is forbidden, competitive strategies allow to keep prices as low as possible. Measures as limitations on the allowed market share of a single coalition (antitrust) demonstrate to be a means for keeping prices under control. Access costs to coalitions depending on the energy volume are also useful against the formation of monopoly. In the above scenarios, CS 2 cannot access any coalition because of its high initial demand.

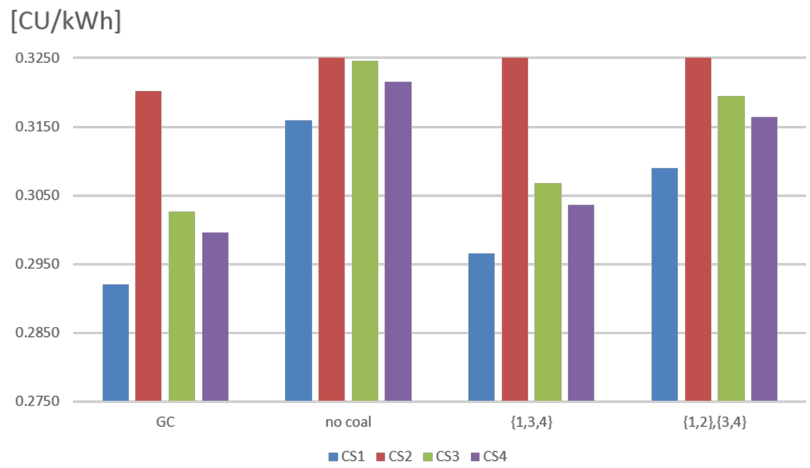

Figure 4.9: Effect of coalition formation on pricing strategies (extended prediction horizon). Employing a longer prediction horizon w.r.t. Figure 4.8, the trend is inverted. Due to uncertainty, smaller coalitions incur more risk on the market, and apply myopic strategies to save in the short run. Instead, the grand coalition can afford to offer the lowest prices on the market, in absence of any competition and uncertainty: the strategy is to keep the demand high through attractive prices and invest in the long run.

volume. In the above scenarios, CS 2 is characterized by a high initial demand, and as such its access to any coalition is forbidden.

Nonetheless, the monopoly issue is smoothened by employing a longer prediction horizon, as pointed out in Figure 4.9. Due to uncertainty, smaller coalitions incur more risk on the market, and apply myopic strategies to save in the short run. Instead, the grand coalition can afford to offer the lowest prices on the market, in absence of any competition and uncertainty: interestingly, the strategy is to keep the demand high through attractive prices and invest in the long run.

Concerning the estimate error on the predicted revenue, Figure 4.10 illustrates how, over the members of the same coalition the prediction error is reduced, whereas it increases significantly for the CSs which are left out. It is worth to notice that prediction error is low when no coalitions are formed, due to the strong competition of the CSs, which makes worst-case approach fit.

Finally, Figures 4.11 and 4.12 show how the Shapley value allocation defines a re-distribution of the revenue over the members of a coalition. In particular, the case described in Figure 4.11 shows how CS 3—the most influential station due to its advantageous location—is compensated a posteriori for jointly planning a pricing strategy capable of redirecting the demand to the other CSs. The result depicted in Figure 4.12 refer to the coalition structure $\{\{1,3,4\},\{2\}\}$. In the second scenario, CS 1 has the

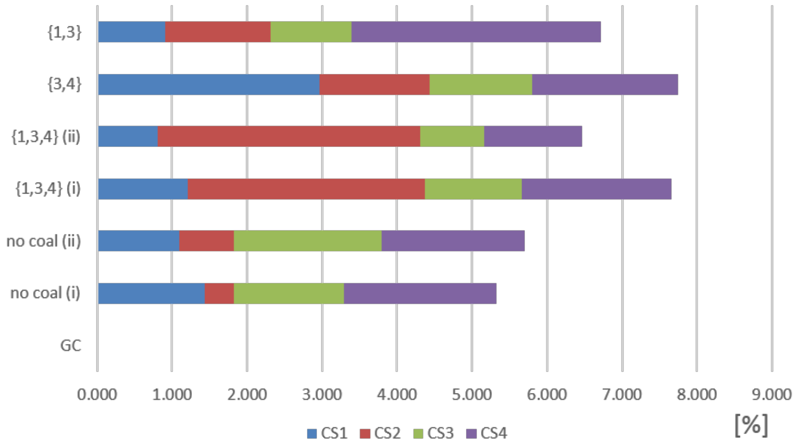

Figure 4.10: Error (%) on the estimate revenue. Prediction error is low when no coalitions are formed, due to the strong competition of the CSs, which makes worst-case approach fit. However, when coalitions form, the prediction error increases significantly for the CSs which are left out.

(a) Scenario (*i*)

(b) Scenario (*ii*)

Figure 4.11: Benefit redistribution (Shapley value) for the grand coalition. CS 3 is the most influential CS. Through the jointly planned pricing strategies, the demand is redirected to other CSs. However, CS 3 is compensated a posteriori by adjusting the payoff on the basis of the Shapley value.

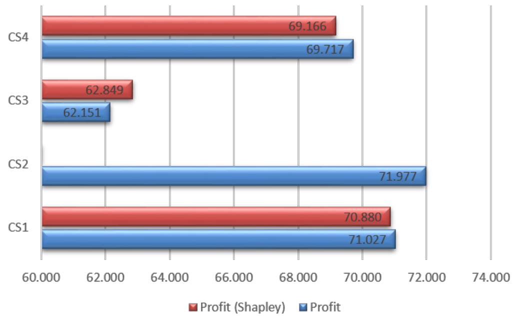

(a) Scenario (*i*)

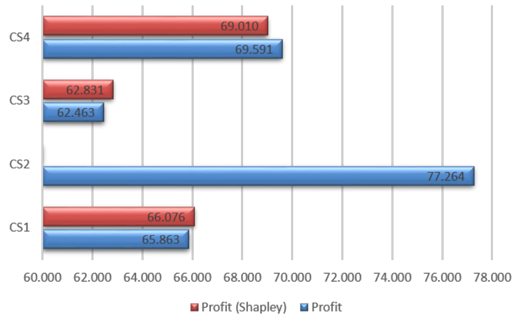

(b) Scenario (*ii*)

Figure 4.12: Benefit redistribution (Shapley value) for the coalition structure $\{\{1,3,4\},\{2\}\}$. In the second scenario, CS 1 has the highest cost-of-use along with CS 3. CS 4 has the lowest costs, and its gain is redistributed across the other members of the coalition. Revenue for CS 2 is high because of its high initial demand, and also because of the strongly competitive prices it can apply in scenario (ii), due to its low costs of use (see Fig. 4.6).

highest cost of use along with CS 3. CS 4 has the lowest cost instead, and its revenue is redistributed across the other members of the coalition.

4.5.2 Malaga

The following results are relative to the Malaga scenario, involving 60 CSs owned by 4 CMs (see Figure 4.3). The maintenance cost factors relative to each CM's infrastructures have been defined as

$$\mathbf{c} = [30 \quad 47 \quad 56 \quad 66] \cdot 10^{-6}\,\mathrm{CU/kWh^2};$$

Figures 4.13–4.15 show the aggregate demands over a ten-day time frame. More specifically, Figure 4.13 shows a comparison between the demand resulting by maintaining a fixed price of 0.3 CU/kWh at all CSs (designated as the reference case), and the strategy resulting by the grand coalition. Prices are slightly raised in order to take advantage of the monopoly, and to reduce demand in stations characterized by high cost-of-use. Although it may seem that the outcome is not consistent with CM 4 incurred costs, the plot in Figure 4.18 shows how the grand coalition's pricing strategy actually provides a uniform distribution of the costs of use (COU) w.r.t. the energy supplied. Moreover, the grand coalition achieves sensible overall reduction of the COU/revenue ratio: 31% in average, versus 38% resulting from the competitive strategies. Moreover, revenue redistribution through the Shapley value covers the bigger costs sustained by CM 4,

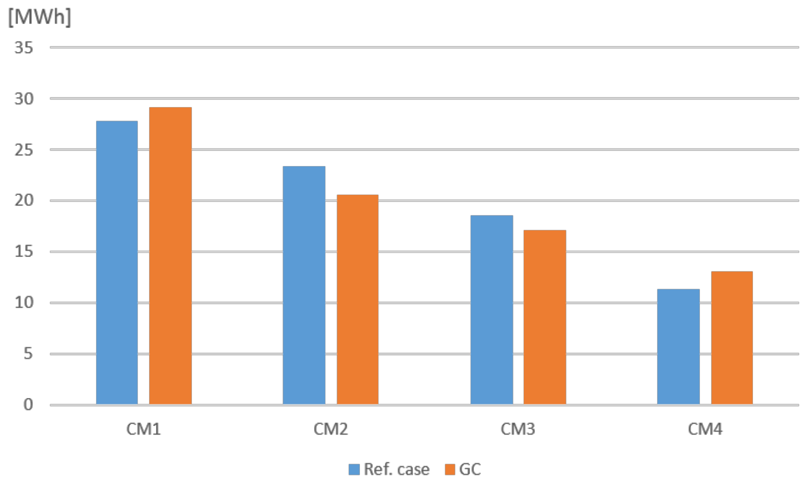

Figure 4.13: Redistribution of recharges ([MWh]) resulting by the grand coalition of CMs. The values in the y axis refer to the aggregate demand at all CSs owned by a given CM, over a timespan of 10 days. The plot shows a comparison between the demand resulting by maintaining a fixed price of 0.3 CU/kWh at all CSs (ref. case), and the strategy resulting by the grand coalition. Prices are slightly raised in order to take advantage of the monopoly, so demand is reduced in CSs characterized by high cost-of-use. The outcome is not consistent with CM 4 incurred costs, mainly due to prediction errors resulting by the linearized model: however, revenue redistribution through the Shapley value covers this issue, as shown in Figure 4.16.

as shown in Figure 4.16. For the case where no coalition is formed (Figure 4.14) and the case relative to the coalition structure $\{\{1,4\},\{2,3\}\}$ (Figure 4.15), worst-case approach implemented to derive prices leads to competitive strategies, resulting in the same minimal price sequence applied over the considered timespan. Overall demand increases due to the low prices, while the distribution over the CMs facilities remains constant. Interestingly, over the same pricing strategy, the Shapley value provides a reallocation of the revenues towards the CM incurring the highest cost (here CM 4, see Figure 4.16).

Finally, Figure 4.17 shows the average profit (total revenue − cost-of-use) over 9 simulated days. The grand coalition provides a net improvement of the profit of CMs, whereas strictly competitive strategies yield a poor economic performance. In average, a daily average profit of 1947.55 CU is achieved with the grand coalition, versus the 1542.46 CU of the strictly competitive strategy. As can be seen in Figure 4.18, this is due to the poor efficiency of the strategy in adapting to the different infrastructural limitations of the CMs.

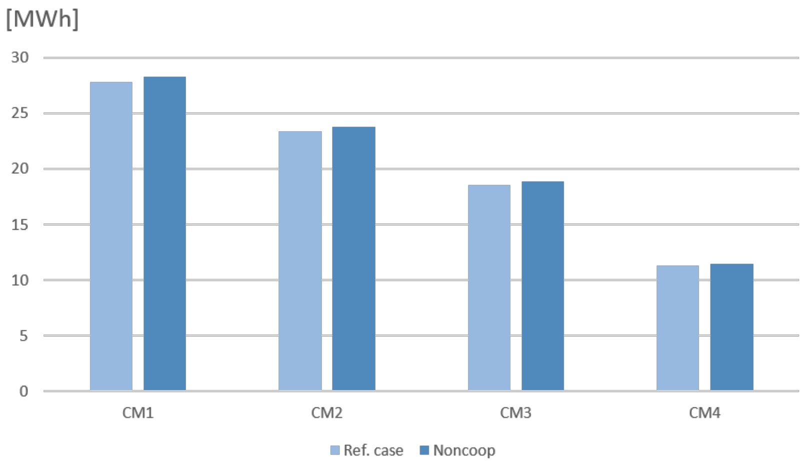

Figure 4.14: Redistribution of recharges ([MWh]) resulting by the grand coalition of CMs. The values in the y axis refer to the aggregate demand at all CSs owned by a given CM, over a timespan of 10 days. The worst-case approach implemented yields competitive strategies, resulting in the minimal price sequence possible. Overall demand increases due to the low prices, while the distribution over CMs facilities remains constant.

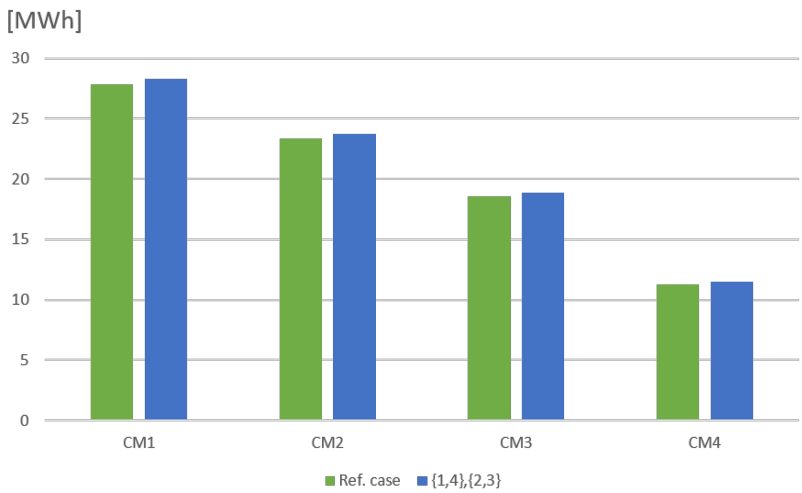

Figure 4.15: Redistribution of recharges ([MWh]) relative to the CM coalition structure $\{\{1,4\},\{2,3\}\}$. The values in the y axis refer to the aggregate demand at all CSs owned by a given CM, over a timespan of 10 days. The worst-case approach leads to competitive strategies, resulting in the same minimal price sequence of the no coalition case. Interestingly here, over this same pricing strategy, the Shapley value provides a reallocation of the revenues towards the CM incurring the highest cost (CM 4), as can be seen in Figure 4.16.

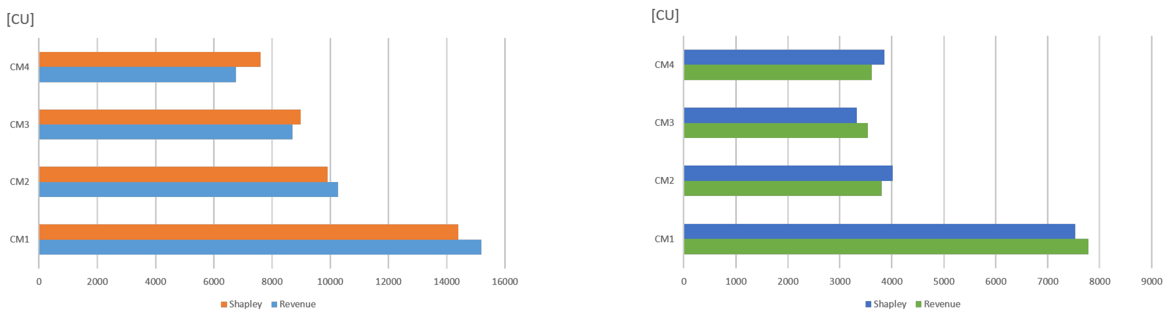

(a) Grand coalition (b) $\{\{1,4\},\{2,3\}\}$

Figure 4.16: Benefit redistribution (Shapley value) for the grand coalition and the coalition structure $\{\{1,4\},\{2,3\}\}$, relative to the Malaga scenario. The plot shows how the revenue is reallocated towards the owners of facilities characterized by the highest costs.

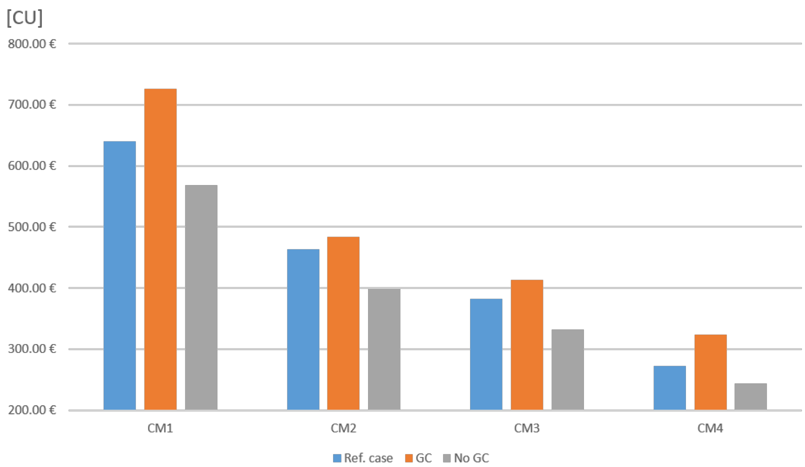

Figure 4.17: Average profit over 9 days of simulation (total revenue − cost-of-use). The grand coalition (GC) provides a net improvement of the profit of CMs, whereas strictly competitive strategies ("No GC") yield a poor economic performance. In average, 1947.55 CU are earned in average with the GC, versus the 1542.46 CU of the strictly competitive strategy. As can be seen in Figure 4.18, this is due to the poor efficiency of the strategy, associated with high costs-of-use w.r.t. the achievable revenue. Notice that the reference case should be viewed just as an initial condition, since the competition between CMs would not allow to keep its associated prices.

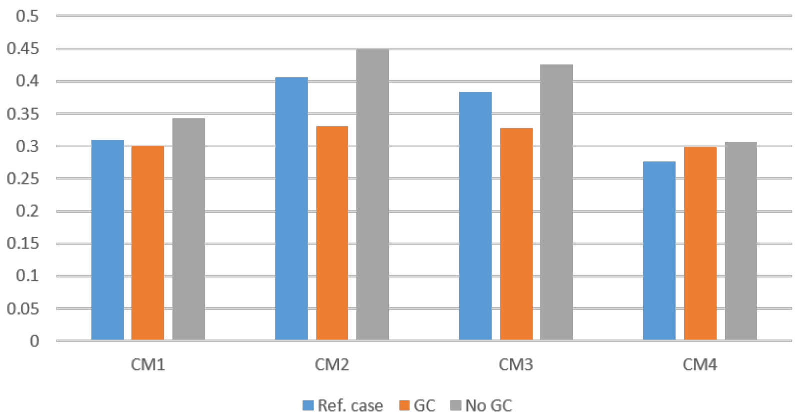

Figure 4.18: Ratio of the costs of use over the total revenue. The pricing strategy optimized by the grand coalition (GC) provides a uniform distribution of the costs of use w.r.t. the energy supplied. Moreover, the GC achieves sensible overall reduction of the ratio: 31% in average, versus 38% resulting from the competitive strategies.

4.6 Conclusion

The work presented in this chapter is a study of a near future scenario regarding plug-in electric vehicles population. Considering the standpoint of the owners of battery recharge infrastructures, the problem of the energy refill pricing is analyzed, involving possible cooperative strategies. The price sensitivity of EV fast charging facilities users has been modeled over a microsimulated scenario representing a finite population of EVs and four independent and selfish CMs. Then, following an approach to incentive coalition formation based on the Shapley value's allocation, the possibilities offered by the coalitional management of CSs are studied. Results from simulations have shown that a joint planning of pricing strategies allows to increase the profit (about 25%) and the quality of service for the users. Interestingly, the increase in the profit can be mainly attributed to a better management of the charging infrastructure, allowed by the possibility of demand reshaping offered by coalitional strategies. Naturally, for such a framework to be feasible, a more transparent management of charging infrastructures is required.

In this work, only on-the-fly recharge operations have been considered. Ongoing work is concerned with the possibility of booking recharge slots in advance. The case study admits further analysis of competition issues (oligopoly), that need to be specifically addressed through computationally-viable tools. Finally, as an important byproduct of this work, the prediction model object of this study could be employed for decentralized routing mechanism that can enhance the quality of service provided to EV drivers, fulfill grid capacity constraints, or optimize some other specific charging facility's owner objective function. This currently constitutes a large body of research in the intelligent transportation systems field.

4.7 Acknowledgments

The study presented in this chapter has been carried out in collaboration with Ezequiel González Debada and David Cerero Tejero.

CHAPTER 5

Conclusion and outlook

As the architecture of multiagent systems becomes more complex—featuring reconfigurable topologies [10, 9, 94, 11], misaligned individual interests [12, 131, 132, 15], human-in-the-loop control [133], plug and play capabilities [58]—the relationship between possible restrictions on the global availability of information and the system performance is increasingly unclear [134]. Some of the challenges and open issues for coalitional control are summarized in the remainder.

Criteria for coalition formation How to determine the most appropriate coalitional structure for the overall system is a problem that shows fundamental analogies with model partitioning. Two different perspectives on coalition formation can be considered. The first is a *top-down* approach, where the global coalitional structure is optimized at a supervisory layer. Of fundamental importance is the criterion used to break the overall system into coalitions. Some possibilities have been already explored, such as the minimization of an index that combines optimal control performance and communication costs [10], or an H_∞ robustness index—reflecting model-plant mismatches due to nonlinearities or inaccurate identification—as proposed in [21]. To address *individual rationality* as well, the second consists of a *bottom-up* approach: here the formation of coalitions is produced as the outcome of an autonomous bargaining procedure. While the first approach may offer some advantages in view of global system stability guarantees, the second appeals as a more appropriate scheme for real-world (plug and play) applications.

Information exchange Information plays a fundamental role in the coordination of multiagent systems. Either attained through direct sensing or communication, in-

formation is the basis for the local decisions of agents and, as such, decisive to the emergent global behavior [134]. Despite the huge effort dedicated to the development of distributed controllers for large-scale systems, communication has been mainly studied from a transmission perspective, covering issues such as bandwith limitations, data loss, or the effects of noisy channels [135]. The very nature of the information exchange has received little attention. Indeed, in order to allow fundamental properties of centralized control, such as system-wide optimality and stability, the majority of the literature about distributed control overlooked privacy-related issues in order to focus on the overall system performance.
Does providing agents with additional information always lead to improvements in the performance? On the other hand, can the excess of information be detrimental under some given system-wide perspectives? These questions have been partially addressed in works such as [134, 34]. In [134], a graph-coloring problem is used as a simple platform for studying the effect of information on multiagent collaboration. Results demonstrate that an increased amount of information is able to improve the efficiency of the Nash equilibria; on the other hand, it degrades the convergence rate of the distributed algorithm, where the agents seek to maximize their utility.

Constraints on coalition formation Bigger coalitions provide better control performance at the cost of increasing cooperation requirements. The enforcement of limitations on the composition of coalitions may be necessary. Some limitations can be of direct application (as for example size constraints), whereas others can implicitly derive by the penalization of specific metrics (use of the network infrastructure, identity of the participants, optimization variables, time expected to solve the control problem). In either case, this is a problem that requires attention. See [136] for a detailed analysis about constraints in the coalition formation process.

Partial cooperation and information When dealing with systems characterized by a strong heterogeneity, selfish interests may hinder the sharing of knowledge relevant for control purposes and cooperation as well. It is possible that only a subset of the control agents is willing to exchange information about their subsystems. It is therefore necessary to explore the performance bounds of the control loop possibly achievable with *partial system information*. Similar issues have been already studied in the field of Economics, using tools provided by the game theory. The authors of [34] extend a performance metric introduced by [137]—the *competitive ratio*—for the purpose of quantifying the distance from the optimum of the distributed solution of an LP problem when the information is locally segmented. From the coalitional control standpoint, it is arguably critical to characterize the improvement provided by a broader knowledge of the system, and promote the formation of coalitions accordingly. Notice that the previous question can be reversed: *what is the minimal partition of the system model information necessary to guarantee some performance goal?* In order to address this question, the authors of [34] point out that additional metrics need to be formulated in order to allow the characterization of the different partitioning possibilities and the relative *minimality* notion. Again, possible candidate for such task are already available in the game theory literature about multi-agent decision making under partial information.

Performance metrics The development of the coalitional control field requires the definition of key performance indicators, especially those capable of capturing the trade-off between the information exchanged by the control agents and the performance of the system. For example, in [34] the connection between closed-loop performance and the amount of exchanged information is characterized for distributed linear quadratic controllers. Bounds are provided on the minimal information exchange needed to achieve an improvement over the performance of the best decentralized (communication-less) scheme.
By addressing a networked resource allocation problem, the work of [138] identifies how a measure of locality in the individual control laws can be translated into a bound on the overall achievable efficiency. The relationship between the redundancy of information in the control laws implemented by agents and the achievable efficiency of the overall behavior is then characterized, providing bounds on the efficiency of the stable solutions. When full information regarding the mission space is available to the agents, the efficiency of the resulting stable solutions is guaranteed to lie within 50% of the optimal. However, as the reach of the information becomes more limited, the efficiency of the stable solutions may be as low as $1/N$ of the optimal, where N designates the number of agents.

Commitment between cooperating agents Depending on the type of information exchanged and its purpose, it is possible to classify the cooperation in decreasing degrees of subsystems' integration, ranging from full information (the coalition is formally equivalent to a unique subsystem) to binding to a prearranged output interval, or sharing planned trajectories, interaction models, objectives. Data for different degrees of cooperation can be computed offline and retrieved during system operation, in order to implement control schemes with varying requirements (from completely decentralized to centralized) on top of the same control infrastructure [8, 10]. This includes the possibility of reserving some backup strategies for the case of communication failure [94].

Theoretical guarantees Classical theoretical properties such as stability or robustness for the closed-loop system are more challenging in this context, specially in the case of bottom-up approaches, where little global information may be available at the individual subsystem level.

Coalitional guarantees Research on the novel properties specific of this type of control systems is needed. An example would be the degree of robustness of the coalitions with respect to the external incentives that their members may have for leaving.

Combinatorial explosion Another issue is linked with the number of possible structures of the controller under a given data network. Approaching the problem of finding the optimal coalitional structure with exhaustive search can become unviable even for relatively small number of agents, due to the exponential growth of the number of possible coalitions. Constraints on the communication topology and the number of agents in a coalition might help to relieve this issue, since the realization of some configurations would be denied. Alternatively, limitations on the number of links that can be switched during a certain period would reduce the search space and ease the on-line implementation of coalitional control schemes.

At this point, the coalitional control framework reveals itself as a wide open field for novel and diverse investigation. In the complex networked systems falling within its scope, information about the relevance of the agents and data links involved in the distributed control problem is of critical importance [27, 26]. Game theory can be useful in this sense. The role of cooperation costs on the outcome of the coalition formation, as well as its relation with control optimality, constitutes an interesting topic for future research. Allocation criteria from game theory may be employed to redistribute the control effort over the agents participating in cooperative tasks [139], or for dynamic model partitioning in a distributed control architecture. Reconfiguration capabilities provided to the controlled system through the evolving coalitional structure are suited for fault-tolerance needs or plug-and-play settings [140].

When only a subset of the control agents is able/willing to exchange information about their subsystems, it might be interesting to investigate the performance bounds of the overall control loop. These questions have been already addressed in fields such as economics and computer science, but remain an open challenge in the framework of dynamical systems control. Privacy-related issues—inherent in SoS—have been generally overlooked in order to focus on the overall system performance or on specific data transmission problems (e.g., limited bandwith, channel noise, data loss). The impact of (partially) restricted knowledge of the global system by local control agents has received relatively little attention [141]. Conversely, by exploiting available real-time data exchange infrastructures, it can be interesting to characterize the improvement provided by a broader knowledge of the system [90], and promote the formation of coalitions accordingly.

Incentive mechanisms from game theory can be applied in intelligent transportation systems, for traffic or service demand reshaping [99], also in competing markets like EV charging [119, 100].

Finally, there is still room for the analysis of the coalitions stability (average coalition lifetime), and the associated conditions on benefit redistribution among cooperating controllers [98] (especially if the objective function has an economical meaning), as well as the sufficient conditions for the stability of the system in control theoretic sense, i.e., guarantees of reaching the desired setpoint.

Appendix A

Coalitional control and game theory

The formation of coalitions among the control agents in a distributed control framework is the foundation of *coalitional control*. This section presents the notions of game theory most related with coalitional control and, in general, with distributed control. For its wide application in the design and the analysis of distributed control strategies, the concept of Nash equilibrium is first introduced. The remainder of the section is dedicated to the basic tools for the analysis of coalitional stability. Finally, the dynamic coalition formation problem is briefly introduced.

A.1 Introduction

Game theory aims at mathematically characterizing the behavior of independent agents interacting within a complex environment, in the presence of conflicting interests. Two main branches can be identified in this field, addressing *noncooperative* and *cooperative* games, respectively. Noncooperative games model situations in which a number of independent agents, that have (partially) conflicting interests, optimize their individual strategy on the basis of a utility index affected by other agents' actions, *without any coordination* between them. Notice that this does not preclude cooperation: indeed, cooperation can arise from the specific architecture of the game, without any agreement among the agents. A particular class of games is related to incentive system design. Here, the top level of an organization chooses a reward scheme and the lower levels make decisions trying to maximize their individual reward. The problem consists in *choosing a reward scheme so that the lower-level decision makers end up minimizing* *a global cost function* [13]. A typical example of application is distributed resource allocation [48]. Cooperative games are appropriate to model situations in which some commonalities are found among the agents [142]. As a consequence, the individual benefit can be improved through the joint operation of the players. Especially related with the work of this thesis are the *dynamic coalition formation* games. These games contemplate the evolution of the cooperative structure implemented by the players in order to operate jointly. Such evolution can be ascribed, e.g., to variations in the degree of coupling among different parts of the system, or to players that enter or leave the game in a plug & play setting.

In game theory, the term *strategy* designates a well-defined sequence of actions (also *moves*) performed by an agent, generally resulting from a particular response algorithm reflecting the behavior of the agent. Games contemplate a set of actions available for each agent to pick at each turn, which can be translated into the control engineering terminology as the input constraint set. An *action* is intended as an input applied to the system.

A basic distinction is made between actions applied in a sequential or simultaneous fashion. The first category allows to consider the case where the players are aware of the strategy implemented by others: the outcome of *sequential* games (also known as dynamic games, or games in extensive form) can be represented by trees. The second category, known as games in *strategic* (or normal) form, is considered for modeling scenarios in which the players act simultaneously or, in general, are not aware of the actions taken by others. The outcome of such games is generally represented on a table [142].

Games can also be classified depending on the quality of information available to the players: a *complete information* game is characterized by the knowledge of the strategies and payoffs *available* to the other players (this does not necessarily include information of the strategy actually implemented by the others). The designation *perfect information* identifies the complete knowledge of actions taken by all players [142] (although in simultaneous games the players can only be aware of past actions). To give an example, in a game with complete and imperfect information players are aware of the actions available to everyone, and of the corresponding payoffs, but their decisions cannot be based on the knowledge of the decisions of the others.

Static games model situations in which the agents apply a one-shot strategy, as opposed to *repeated game* models. The scenarios encountered in control engineering show, in general, analogies with both dynamic games—in which time has a fundamental role in the decision making (the strategy can be based on the knowledge of past

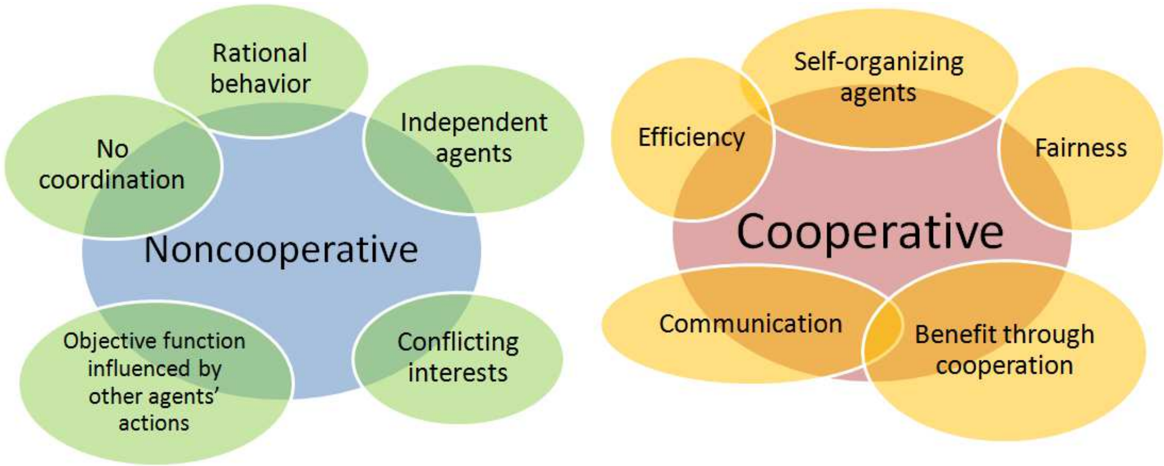

Figure A.1: Noncooperative vs. cooperative game theory

implemented actions)—and repeated games, since the agents can act more than once. One class of games is dedicated to the analysis of *infinitely repeated* games, where the horizon is not known a priori (in this class of games, the focus is on the existence of a winning strategy) [142].

One of the foundations of game theory is the assumption that the agents are *rational*, i.e., all the actions taken are meant to improve utility. However, due to the suboptimality of the control strategy, or to other factors such as failures or delays, this assumption does not always hold in practice. In general, the notion of rationality may be better interpreted as each player's knowledge of its objectives, evaluated on the basis of its own value system to synthesize the strategy to be implemented [142]. It is important to design algorithms capable of preventing the system to deviate from the desired equilibrium due to possible nonrational decisions. Game theory provides proper frameworks to deal with such errors, e.g., the concept of perturbed equilibrium, games with imperfect information or imperfect observability. The study of games with *bounded rationality* is an emerging field that addresses situations where nonrational decisions may be taken [14].

A.2 Noncooperative games

A game is defined through three elements: a set $\mathcal{N}$ of agents (players), a set of allowed actions $\mathcal{A}_i$ and a utility function u_i for each agent $i \in \mathcal{N}$. In a noncooperative game, each agent i chooses the action $a_i \in \mathcal{A}_i$ that maximizes its utility $u_i(a_i, \mathbf{a}_{-i})$, which depends as well on the actions $\mathbf{a}_{-i}$ of the rest of the agents. When the game is dynamic, additional elements are also reflected in the utility function, such as time, past actions, information sets [14]. Sequences of actions applied in a deterministic manner are defined as *pure strategies*; sequences of actions picked according to a given probability distribution are defined as *mixed strategies*.

A.2.1 Dominant and dominated strategies

From the point of view of each player, strategies may be characterized as dominant and dominated. A strategy is referred to as *dominant* if the player has the incentive to play it regardless of the strategies played by other players. On the other hand, a strategy is *dominated* if the player always has better alternatives regardless of the strategies played by the others.

A.2.2 Equilibria in noncooperative games

The solution of a strategic game (i.e., where the players are not aware of the actions taken by others) is represented by possible equilibria of the strategies applied by the agents. The Nash equilibrium corresponds to a stable state in which no agent can improve its utility by changing its strategy, once the other agents' choices are fixed. It can be reached with little or absent coordination in decentralized settings, and may be not unique. In particular, the Nash equilibrium of a static noncooperative game with pure strategy is the set of actions $\mathbf{a}^* \in \mathcal{A}_1 \times \mathcal{A}_2 \times \ldots \times \mathcal{A}_{|\mathcal{N}|}$ such that for all the agents $i \in \mathcal{N}$ holds

$$u_i(a_i^*, \mathbf{a}_{-i}^*) \geq u_i(a_i, \mathbf{a}_{-i}^*),\ \forall a_i \in \mathcal{A}_i. \tag{A.1}$$

For mixed strategies a similar definition is given, based on the probability distribution of the actions to take. A Nash equilibrium is guaranteed to exist in mixed strategy games. A Nash equilibrium cannot involve any dominated strategy.

In presence of multiple Nash equilibria, several metrics can be used to study the efficiency of each one of them, such as the price of anarchy and the price of stability [143, 14].

For sequential games, a different concept—known as *subgame perfect equilibrium*—is used. In such games, agents synthesize their strategies according to the actions already taken by others, and the consequent range of future outcomes. Thus, each agent will focus on the subtree showing the possible evolution of the game (and whose root represents the current state).

A.3 Bargaining theory

Bargaining theory studies situations in which two or more agents have a common interest to cooperate, but at the same time they have conflicting interests about the conditions of such cooperation (e.g., two or more agents have a common interest to trade, but conflicting interests on the price at which to trade). In other words, agents would like to reach an agreement rather than disagree; however, each agent would like to reach an agreement that is as advantageous as possible for itself [142]. Truthfulness of the participants is an essential element in bargaining. For this reason, a consistent branch of game theory is dedicated to the development of *pricing mechanisms* aimed at discouraging cheating among the players.

A.3.1 Nash bargaining

The Nash bargaining model applies to situations in which two individuals bargain over the partition of a fixed payoff: the set of possible agreement is the set of partitions whose sum is the total payoff. In case of disagreement, each player is assigned a penalty referred to as the *disagreement point* of the game. The *useful payoff* for each player is thus defined as the difference between the payoff received in case of agreement and the disagreement point. The partition that maximizes the *product* of the agents' useful payoffs is referred to as the Nash bargaining solution or the Nash product [142].

A.3.2 Rubinstein bargaining

The Rubinstein bargaining game models a sequential bargaining where offers and counteroffers are made by turns. In order to preclude an infinite negotiation, a cost is incurred in case the agreement is delayed. In other words, at each additional round the size of the available payoff becomes smaller. Thus, at any given round of the bargaining, the power of a player is determined by the magnitude of this cost. The factor by which the payoff is decreased can be different for each player, and it is referred to as the player's discount factor. The Rubinstein bargaining shows a unique subgame perfect equilibrium: any offer made by a player should be at least equal to the discounted value that the opponent is able to get in the next round.

A.4 Bayesian games

The Bayesian games framework can be used to model scenarios in which the set of agents may be characterized by several behavior profiles (e.g., some agents might favor cooperation, while others may want to cheat). In particular, an agent does not know in advance the exact behavior that the other agents will apply to a certain situation, although it may know the whole set of possible behaviors. The uncertainty about the characteristics of other players is modeled by introducing a set of possible states, called player's *types*, with their associated (guessed) probability of occurrence.

Example A.1. *In a bargaining situation for the allocation of a given payoff, the information disclosed by the agents (e.g., about the costs of operating their systems) may or may not be truthful, in order to take advantage and receive a greater share of the payoff; in such a case, Bayesian game model can be used to extract a profile of the other agents' actions.* ■

When choosing the strategy to be implemented next, a player should take into account the probability of occurrence of each of the other players' types, and thus their possible actions.

A.5 Multi-agent learning

An important line of research related with game theory is the development of learning algorithms in order to achieve a desired cooperative equilibrium. A learning algorithm is typically composed of three steps: *(i)* observation of the state of the environment; *(ii)* estimation of the *prospective utility*; *(iii)* update of the strategy [14].

The *best response* represents the simplest form of such algorithms: at each iteration, every agent applies the strategy which maximizes its utility. However, the outcome of such a scheme is very sensitive to the initial condition. Convergence to an equilibrium is only guaranteed with particular types of utility functions, and the convergence to an efficient equilibrium cannot be ensured [14].

In [14] some relevant categories of advanced learning algorithms are introduced:

- *Fictitious play*: algorithms in this category are based on the estimation of the frequency with which other agents implement a given strategy. On the basis of its estimate, each agent can choose the best strategy. For some type of games (e.g., zero-sum games) this scheme converges to a Nash equilibrium.

- *Regret matching*: this class of algorithms is based on the minimization of the *regret from applying a certain strategy*, i.e., the difference between the utility of *always* applying that strategy and the utility achieved by implementing the current strategy.

- *Reinforcement learning.*

- *Stochastic learning.*

In order to overcome instability issues due to possible errors (i.e., nonrational strategies) during the learning procedure, these algorithms are commonly designed so that *the agents are allowed to choose unintended strategies*, so as to perturb the reached equilibrium and seek for any opportunity of improvement. This kind of approach, called *learning by experimentation*, is receiving significant attention in game theory and multiagent learning, and has shown good performances in communication applications [14].

A.6 Coalitional game theory

Cooperative game theory provides means of analyzing the behavior of self-organizing agents that can communicate and decide to cooperate in order to achieve some benefit. Also, cooperative game theory focuses on the design of mechanisms for the cooperation so to guarantee *fairness* and efficiency. However, since most research has been focused on noncooperative games so far, specialized tools are still needed for the design of such mechanisms, in particular those suited for the dynamical environments naturally encountered in engineering applications.

Under cooperative game theory, *coalitional games* and *Nash bargaining* provide tools for the analysis of situations in which the agents have to decide with whom to cooperate and under which conditions [14]. Nash bargaining focuses on the negotiation of the conditions for the cooperation within a given coalition (e.g., allocation of the payoffs among the members of a coalition). A coalitional game is uniquely defined by the pair $(\mathcal{N}, v)$, where $\mathcal{N}$ is the set of players, and $v(\mathcal{C})$ is the *value* of a given coalition $\mathcal{C} \subseteq \mathcal{N}$ in the game. The definition of this value determines the form and the type of the game [48].

The basic category of coalitional games is represented by games in *characteristic form*, where the value of $\mathcal{C}$ depends only on the members that compose it, with no regard to how the rest of the agents are organized. In games with *transferable utility* (TU), a value is assigned to any possible coalition through a function $v : 2^{\mathcal{N}} \to \mathbb{R}$. The real value $v(\mathcal{C})$ associated with coalition $\mathcal{C}$ can be divided and transferred among its members (e.g., side-payments used to attract other players). The *payoff* p_i is defined as the utility received by each agent $i \in \mathcal{C}$ after the division of $v(\mathcal{C})$. The vector of payoffs assigned to all the agents is referred to as the *allocation*.

For the members of any given coalition, an allocation is said to be *efficient* when it is obtained by splitting the entire value of the coalition, i.e., when the following condition holds:

Definition A.1 (Efficiency).

$$\sum_{i \in \mathcal{C}} p_i = v(\mathcal{C}) \tag{A.2}$$

Furthermore, an allocation is said to be *individually rational* when it satisfies:

Definition A.2 (Individual rationality).

$$p_i \geq v(\{i\}), \forall i \in \mathcal{C} \tag{A.3}$$

In other words, individual rationality implies that the payoff offered to any member of a coalition has to be at least equivalent to the payoff that can be achieved by playing independently. An allocation satisfying both (A.2) and (A.3) is designated as *imputation* [49].

In different cases, the payoff is assigned *directly to the members* of a coalition, according to given rules (or possible constraints on the division of the utility). The individual payoffs cannot be redistributed (transferred) among the players. Such situations are modeled by coalitional games with *nontransferable utility* (NTU). Hence, the value of a coalition $\mathcal{C}$ is not expressed by a single real value; instead, $v(\mathcal{C}) \subseteq \mathbb{R}^{|\mathcal{C}|}$ is a *set* of allocations, each one relative to a given coalition's strategy.[1]

Games in characteristic form allow to model a wide spectrum of scenarios. In engineering applications, however, it is natural to encounter problems in which the value of a given coalition cannot be determined regardless of how the rest of the agents are organized. Games in *partition form* model such type of problems. Given a partition of the set of agents $\mathcal{N}$, i.e., a set of disjoint coalitions $\boldsymbol{\mathcal{C}} = \{\mathcal{C}_1, \dots, \mathcal{C}_l\}$, the value of a coalition $\mathcal{C}_i \in \boldsymbol{\mathcal{C}}$ is expressed as $v(\mathcal{C}_i, \boldsymbol{\mathcal{C}})$ (this value can be either TU or NTU).

The two game forms introduced so far do not consider any underlying communication infrastructure among the agents. Indeed, either in characteristic or in partition form, the value of a coalition does not depend on how the agents are connected. Coalitional games in *graph form* have been introduced to model situations in which the

[1]The notation $|\cdot|$ denotes the cardinality of a set.

connections between the agents influence the utility that they can achieve. As the name suggests, these connections are modeled by means of a graph (either directed or undirected) whose nodes represent the agents. The value of a coalition $v(\mathcal{G}_\mathcal{C})$ is thus expressed on the basis of the topology of the edges connecting the agents of $\mathcal{C}$; depending on the scenario, the value $v(\mathcal{G}_\mathcal{C}, \mathcal{G}_{\mathcal{N}\setminus\mathcal{C}})$ can be a function of how the rest of the agents are connected [48].

A.7 Canonical coalitional games

Canonical coalitional games are in characteristic form (TU or NTU). The main feature of games belonging to this category is that *cooperation is always beneficial.* More specifically, the *superadditivity* property always holds:

$$v(\mathcal{C}_1 \cup \mathcal{C}_2) \geq v(\mathcal{C}_1) + v(\mathcal{C}_2) \tag{A.4}$$

which implies that the members of two disjoint coalitions $\mathcal{C}_1$ and $\mathcal{C}_2$ are able to achieve *at least* the same payoff allocation if participating in the coalition produced by the union $\mathcal{C}_1 \cup \mathcal{C}_2$. This, in turn, leads to the formation of the *grand coalition*, since the payoff allocation that can be obtained from $v(\mathcal{N})$ is at least as good as those obtained through the coalition of any possible subset of agents. Hence, the theory on canonical coalitional games focuses on two main problems:

- *stability*: how to find a payoff allocation guaranteeing that no agent would prefer to leave the grand coalition;
- *fairness*: it can be interpreted as a notion allowing to model the influence of "global goals" on the agents' behavior. The members of a coalition may care about receiving a payoff that is balanced with the individual contributions (thus, each agent care about both its own payoff and the payoff assigned to the others) [144].

A.8 The core

The set of payoff allocations able to guarantee that no agent has an incentive to leave the grand coalition $\mathcal{N}$ to form a coalition $\mathcal{C} \subset \mathcal{N}$ is called the *core*. In particular, a payoff allocation $\mathbf{p} \equiv \{p_i\}_{i\in\mathcal{N}}$ belonging to the core satisfies the following two conditions[2]:

[2]The examples refer to a TU game. For NTU games the definition of the core is similar, although based on the individual payoff instead of their sum.

- *Efficiency* (budget rationality): $\sum_{i \in \mathcal{N}} p_i = v(\mathcal{N})$, i.e., the entire value of the grand coalition has to be shared among its members.

- *Group rationality*: $\sum_{i \in \mathcal{C}} p_i \geq v(\mathcal{C}), \ \forall \mathcal{C} \subseteq \mathcal{N}$, i.e., the payoff p_i obtained by each member of the grand coalition has to be greater (or equal) to the one obtained by acting alone or within a smaller coalition.

A payoff allocation $\mathbf{p}$ belonging to the core is said to be *stabilizing* [49]. The core is not guaranteed to exist for all canonical games. When the core is empty, the grand coalition cannot be stabilized. The existence of the core in a TU game is related to the feasibility of the following LP problem:

$$\begin{aligned} \min_{\mathbf{p}} \ & \sum_{i \in \mathcal{N}} p_i \\ s.t. \ & \sum_{i \in \mathcal{C}} p_i \geq v(\mathcal{C}), \ \forall \mathcal{C} \subseteq \mathcal{N} \end{aligned} \tag{A.5}$$

Since the growth of the number of constraints in (A.5) is exponential in the number of agents, finding the existence of the core is an NP-complete problem. In practice, however, the search of imputations can be narrowed by considering those of most interest (possibly already known to be fair) in a given scenario.

Nonemptiness of the core is assured in *convex* games.

Definition A.3 (Convex game)**.** *A TU canonical game is convex if the following condition holds:*[3]

$$v(\mathcal{C}_1) + v(\mathcal{C}_2) \leq v(\mathcal{C}_1 \cup \mathcal{C}_2) + v(\mathcal{C}_1 \cap \mathcal{C}_2), \quad \forall \mathcal{C}_1, \mathcal{C}_2 \subseteq \mathcal{N} \tag{A.6}$$

or alternatively, for all $i \in \mathcal{N}$ and any pair of coalitions $\mathcal{C}_1 \subseteq \mathcal{C}_2 \subseteq \mathcal{N}$ such that $\mathcal{C}_1 \cap \{i\} = \mathcal{C}_2 \cap \{i\} = \varnothing$,

$$v(\mathcal{C}_1 \cup \{i\}) - v(\mathcal{C}_1) \leq v(\mathcal{C}_2 \cup \{i\}) - v(\mathcal{C}_2) \tag{A.7}$$

Definition (A.7) relates the convexity of the game to the marginal contribution of each agent i: in a convex game, the marginal contribution of any agent i is *nondecreasing* w.r.t. set inclusion (i.e., the size of the coalition it joins). In other words, a game is convex if an agent's marginal contribution increases if it joins a larger coalition [145]. However, convexity is a strong condition, hard to find in real-world scenarios. *Balanced-*

[3] The definition can be extended to NTU games as well.

ness of a game is a weaker condition—which holds for a wide class of problems—that also guarantees a nonempty core, as stated by the Bondareva-Shapley theorem [49].

Definition A.4 (Balanced map). *Let $\alpha : 2^{\mathcal{N}} \to [0,1]$ be a function that assigns a weight to each possible coalition in a set $\mathcal{N}$ of agents. The function α is said to be a* balanced map *if*

$$\sum_{\mathcal{C} \in 2^{\mathcal{N}}} \alpha(\mathcal{C}) \mathbf{1}\{i \in \mathcal{C}\} = 1, \quad \forall i \in \mathcal{N} \tag{A.8}$$

i.e., α is a balanced map if, for any agent i, the sum of the weights assigned by α to every coalition containing i equals 1.[4]

Definition A.5 (Balanced game). *A game $(\mathcal{N}, v)$ is said to be balanced if for any balanced map α it holds that*

$$\sum_{\mathcal{C} \in 2^{\mathcal{N}}} \alpha(\mathcal{C}) v(\mathcal{C}) \leq v(\mathcal{N})$$

Theorem A.1 (Bondareva-Shapley). *A coalitional game has a nonempty core iff it is* balanced.

A.9 Shapley Value

As mentioned in Section A.7, it is not uncommon to find the core to be an empty set or, vice versa, to be so large to make the choice of a suitable imputation a hard task. Furthermore, an allocation belonging to the core does not necessarily guarantee fairness to every agent (e.g., Bird's allocation rule).

Shapley tackled these issues by defining the conditions to obtain a unique payoff mapping, i.e., the *Shapley value* of the game $(\mathcal{N}, v)$. Any Shapley allocation ϕ must satisfy the following four axioms:[5]

1. *Efficiency*: $\sum_{i \in \mathcal{N}} \phi_i(v) = v(\mathcal{N})$.
2. *Symmetry*: given two players i and j, if $v(\mathcal{C} \cup \{i\}) = v(\mathcal{C} \cup \{j\})$, $\forall \mathcal{C} | \mathcal{C} \cap \{i, j\} = \varnothing$, then $\phi_i(v) = \phi_j(v)$.
3. *Dummy*: if, for any player i, $v(\mathcal{C}) = v(\mathcal{C} \cup \{i\})$ holds $\forall \mathcal{C} | \mathcal{C} \cap \{i\} = \varnothing$, then $\phi_i(v) = 0$.

[4] The notation $\mathbf{1}\{\cdot\} : \mathcal{N} \to \{0,1\}$ designates the *indicator function*, which takes the value 1 if $i \in \mathcal{C}$, or 0 if $i \notin \mathcal{C}$ [146].

[5] The definition is given here for TU games. Definitions of the Shapley value for NTU games are also available.

4. *Additivity*: let u and v be characteristic functions. Then $\phi(u+v) = \phi(u) + \phi(v)$.

The symmetry axiom assigns the same payoff to players that equally improve a given coalition, while the dummy axiom assigns a null payoff to a player which does not contribute when joining a coalition. The additivity axiom states the uniqueness of the mapping ϕ over the space of all coalitional games, relating the Shapley values of two different games characterized by u and v [48]. The formulation of the individual payoff assigned to player i according to the Shapley value's mapping is:

$$\phi_i(v) = \sum_{\mathcal{C} \subseteq \mathcal{N} \setminus \{i\}} \frac{|\mathcal{C}|!(|\mathcal{N}| - |\mathcal{C}| - 1)!}{|\mathcal{N}|!} \left[v(\mathcal{C} \cup \{i\}) - v(\mathcal{C}) \right] \tag{A.9}$$

The weight factor of the marginal contribution $v(\mathcal{C} \cup \{i\}) - v(\mathcal{C})$ expresses the probability —for any agent i— of joining a given coalition $\mathcal{C} \subseteq \mathcal{N} \setminus \{i\}$, assuming that the agents form the grand coalition *in a random order*. Thus, the value assigned by Shapley's criterion corresponds to the individual *expected marginal contribution*.

A Shapley allocation that also belongs to the core of a game combines the fairness properties of the Shapley value with the stability of the core. Note that for convex games, the Shapley value provides a closed-form expression of an imputation belonging to the core. However, in nonconvex games the Shapley value is generally not related to the core [49].

Despite the advantage of its closed form, the computational complexity of (A.9) increases significantly with the number of agents: alternative techniques for its computation can be found in the literature (the interested reader is referred to [48] and references therein).

A.10 The nucleolus

Another important allocation criterion for canonical games is the *nucleolus*. It consists in the allocation $\mathbf{p} = (p_i)_{i \in \mathcal{N}}$ (for the grand coalition) able to minimize the *dissatisfaction* of all the agents for all the possible coalitions in $\mathcal{N}$. The dissatisfaction is defined for each coalition $\mathcal{C} \subseteq \mathcal{N}$ as the excess

$$e(\mathbf{p}, \mathcal{C}) = v(\mathcal{C}) - \sum_{i \in \mathcal{C}} p_i \tag{A.10}$$

Consider the vector $\theta(\mathbf{p}) \in \mathbb{R}^{2^{\mathcal{N}}}$ containing the excess values for every coalition in the set of agents, arranged in nonincreasing order, relative to an imputation $\mathbf{p}$. Then, the nucleolus is the imputation $\mathbf{p}^*$ providing the minimum dissatisfaction according to the lexicographic order, i.e.:

$$\theta(\mathbf{p}^*) <_{\text{lex}} \theta(\mathbf{p})$$

where the $<_{\text{lex}}$ operator designates the lexicographic order, defined as:

$$(e_1, \ldots, e_{2^{|\mathcal{N}|}}) <_{\text{lex}} (e'_1, \ldots, e'_{2^{|\mathcal{N}|}})$$

iff

$$\exists i \leq 2^{|\mathcal{N}|} \mid e_i < e'_i \wedge e_j = e'_j, \forall j < i$$

Definition A.6 (Nucleolus [49]). *The nucleolus of a game* $(\mathcal{N}, v)$ *is the lexicographically minimal imputation.*

As a consequence of the efficiency and group rationality conditions, only imputations with negative or null dissatisfaction belong to the core. If the core of a game is not empty then the nucleolus is in the core; following Theorem A.1 this condition is surely verified in balanced games (which include convex games).

The nucleolus of a canonical coalitional game always exists and is unique. It is group and individually rational, and satisfies the symmetry and dummy Shapley's axioms. Moreover, it always belongs to the kernel of a game.[6] The nucleolus has so far been defined only for TU games, and its computation requires the solution of $\mathcal{O}(2^{\mathcal{N}})$ linear programs, each with $|\mathcal{N}| + 1$ decision variables [49].[7]

A.11 Power indices

Power indices express the influence of players on the formation of coalitions and on the outcome of the game [142]. A fair allocation rule can be based on (normalized) power indices. Widely used power indices are the one proposed by Shapley and Shubik (also known as Shapley value, see Section A.9), the Banzhaf index, and the Holler-Packel index.

The Shapley value assumes an equal distribution of the probability of the order in which any agent joins all possible coalition. The Banzhaf power index assumes instead that all possible coalitions containing agent i are equally probable. The measure of the

[6]Given two players i and j, the kernel of a game is the set of allocations such that the maximum dissatisfaction of a player i belonging to any coalition not including player j is equal to the maximum dissatisfaction of player j belonging to any coalition without i.

[7]One decision variables corresponding to the payoff of each agent, plus an additional slack variable representing the excess for that coalition.

power of agent i according to the Banzhaf index is defined as:

$$\mathrm{BPI}_i = \frac{1}{2^{|\mathcal{N}|-1}} \sum_{\mathcal{S} \subseteq \mathcal{N} | i \in \mathcal{S}} (v(\mathcal{S}) - v(\mathcal{S} \setminus \{i\})).$$

The Holler-Packel index is based as well on the marginal contribution of agent i, but it focuses on the coalitions whose allocations are in the core:[8]

$$\mathrm{HPI}_i = \sum_{\mathcal{S} \in \mathfrak{C}(\mathcal{N}, v)} (v(\mathcal{S}) - v(\mathcal{S} \setminus \{i\})),$$

where $\mathfrak{C}(\mathcal{N}, v)$ denotes the set of coalitions whose payoff allocations constitute the core of the game (i.e., the best that can be achieved by the members of these coalitions, such that no one of them has an incentive to leave in search of a greater payoff).

Depending on the situation, some indices may be more suited than others. In particular, the Shapley value is based on the assumption that the agent commits to stay in the coalition it joins. On the other hand, the Banzhaf value is based on the idea that agents are free to join and leave any coalition.

A.12 Dynamic coalition formation

In this class of games the focus is directed on the evolution of the coalitional structure due to variations in the nature of the game (e.g., variations in the degree of coupling among different parts of the system, players that enter or leave the game in a plug & play setting). The purpose of the coalition formation process is to maximize the total utility (social welfare) in TU games, or to achieve a Pareto optimal payoff allocation in NTU games.

In general, the optimization of the composition of coalitions is an NP-complete problem, since it requires the evaluation of all the possible partitions of the set $\mathcal{N}$ of agents, whose number—known as the Bell number—grows exponentially with the number of agents. Let $\mathcal{K}_s$ denote the set of possible coalitional structures (that is, partitions of $\mathcal{N}$) composed by s coalitions. The cardinality of this set is expressed by the Stirling number of the second kind [147]:

$$|\mathcal{K}_s| = \frac{1}{s!} \sum_{j=0}^{s-1} (-1)^j \binom{s}{j} (s-j)^n \tag{A.11}$$

[8] See Section A.8 for a definition of the core.

Then $|\mathcal{K}| = \sum_{s=1}^{|\mathcal{N}|} |\mathcal{K}_s|$ is the number of possible coalitional structures given a set $\mathcal{N}$ of agents [103]. For example, a set of 10 agents originates 115975 possible partitions.

As a consequence, a centralized approach for the optimization of the coalitional structure is impractical. In many cases the properties of the game (e.g., the way its value v is defined) can be used as a guide for reducing the computational complexity. Nevertheless, since coalition formation naturally involves several autonomous agents, a distributed approach is generally desired for the solution of such problem. Several techniques have been proposed so far, based on heuristic methods, Markov chains, set theory, bargaining and other negotiation algorithms from economics (the interested reader is referred to [48] and references therein).

The work of Apt and Witzel [57] focuses on the outcome of a coalition formation process resulting from the application of two rules, namely merge and split. The aim is to identify the conditions under which the outcome of the process is a unique coalitional structure, irrespective of the initial condition. The rules proposed in [57] are based on the comparison of different partitions of the set of players involved in a given merge or split operation, according to preference criteria such as Nash, utilitarian or leximin order (these ordering criteria provide advantageous properties, namely irreflexivity, transitivity, and monotonicity).

Definition A.7 (Merge [57])**.**

$$\{\mathcal{C}_1, \dots, \mathcal{C}_k\} \cup \mathcal{P} \rightarrow \{\bigcup_{i=1}^{k} \mathcal{C}_i\} \cup \mathcal{P} \quad \text{iff} \quad \{\bigcup_{i=1}^{k} \mathcal{C}_i\} \triangleright \{\mathcal{C}_1, \dots, \mathcal{C}_k\}$$

Definition A.8 (Split [57])**.**

$$\{\bigcup_{i=1}^{k} \mathcal{C}_i\} \cup \mathcal{P} \rightarrow \{\mathcal{C}_1, \dots, \mathcal{C}_k\} \cup \mathcal{P} \quad \text{iff} \quad \{\mathcal{C}_1, \dots, \mathcal{C}_k\} \triangleright \{\bigcup_{i=1}^{k} \mathcal{C}_i\}$$

In definitions A.7 and A.8, the symbol $\triangleright$ denotes the *local* preference operator. The rest of the agents not concerned with the transformation is denoted as $\mathcal{P} \equiv \mathcal{N} \setminus \bigcup_{i=1}^{k} \mathcal{C}_i$.

The application of supplementary basic rules can be studied to improve the convergence of the coalition formation process. For example, *transfers* (moving a subset of agents from one coalition to another) and *swaps* (exchanging subsets of agents between two coalitions) are considered in [148].

A.12.1 Preferences for TU games

Consider a coalitional TU game $(\mathcal{N}, v)$, where the value v maps a given coalition to a nonnegative real value, such that $v(\varnothing) = 0$. Then consider two different partitions of a given set of agents, i.e., two *sets of coalitions* $\mathcal{A} \equiv \{\mathcal{C}_1, \ldots, \mathcal{C}_l\}$ and $\mathcal{B} \equiv \{\mathcal{C}'_1, \ldots, \mathcal{C}'_m\}$. For a TU game, the preference operator can be based on the value of the coalitions:

$$\mathcal{A} \triangleright \mathcal{B} \quad \text{iff} \quad v(\mathcal{A}) \triangleright v(\mathcal{B}) \tag{A.12}$$

where $v(\mathcal{A}) \equiv \{v(\mathcal{C}_1), \ldots, v(\mathcal{C}_l)\}$.

Several criteria can be used for the comparison of two given coalitional structures. Let $a = (a_1, \ldots, a_l)$ and $b = (b_1, \ldots, b_m)$. The following ordering criteria fulfill the properties desired for the preference operator, namely irreflexivity, transitivity, and monotonicity [57]:[9]

- *Utilitarian order*:
$$a \succ_{\text{ut}} b \quad \text{iff} \quad \sum_{i=1}^{l} a_i > \sum_{i=1}^{m} b_i$$
- *Nash order*:
$$a \succ_{\text{Nash}} b \quad \text{iff} \quad \prod_{i=1}^{l} a_i > \prod_{i=1}^{m} b_i$$
- *Leximin order*:
$$a \succ_{\text{lex}} b \quad \text{iff} \quad \check{a} >_{\text{lex}} \check{b}$$

where $\check{a}$ is the sequence of the components of a arranged in nonincreasing order, and the $>_{\text{lex}}$ operator designates the lexicographic order, defined as:

$$(a_1, \ldots, a_l) >_{\text{lex}} (b_1, \ldots, b_m)$$

iff

$$\exists i \leq \min(l, m) \mid a_i > b_i \,\wedge\, a_j = b_j, \forall j < i$$

or

$$\forall i \leq \min(l, m), a_i = b_i \,\wedge\, l > m.$$

Notice that the Nash order implicitly promotes an equal distribution, since for a fixed $\sum_{i=1}^{l} a_i$, $\prod_{i=1}^{l} a_i$ is maximum when all a_i are equal [57].

[9] Examples of different ordering criteria that does not satisfy such properties are also shown in [57], such as the elitist or the egalitarian order.

A.12.2 Individual payoffs

The preference criteria presented in Section A.12.1 are based on the entire coalition's value. However, in practice each agent may base its preference on the *individual payoff* that it achieves by joining a certain coalition. In [57], the notion of *individual value function* is used in order to map the value $v(\mathcal{C})$ of a given coalition $\mathcal{C}$ to each agent's payoff. The individual value function $\phi_i(\mathcal{C})$ is assumed to be *efficient*, i.e.:

$$\sum_{i \in \mathcal{C}} \phi_i(\mathcal{C}) = v(\mathcal{C})$$

Let $\mathcal{A} \equiv \{\mathcal{C}_1, \ldots, \mathcal{C}_l\}$ and $\mathcal{A}' \equiv \{\mathcal{C}'_1, \ldots, \mathcal{C}'_m\}$ be two different partitions of the same (sub)set $\mathcal{S}$ of agents, i.e.,

$$\bigcup_{i \in \mathcal{A}} \mathcal{C}_i = \bigcup_{i \in \mathcal{A}'} \mathcal{C}'_i = \mathcal{S} \subseteq \mathcal{N} \tag{A.13}$$

Furthermore, let $\Phi(\mathcal{A})$ be the vector of the allocations of the coalitions in the partition $\mathcal{A}$. According to [57], no general relation can be found between orderings based on $v(\mathcal{C})$ and orderings based on $\phi(\mathcal{C})$. An exception to this is represented by the utilitarian order, since by definition (see Section A.12.1) it compares the sum of the payoffs, that in turn, following the efficiency assumption (A.13) on $\phi(\mathcal{C})$, coincides with the coalitional value $v(\mathcal{C})$.

The *Pareto order* can be used as a preference criterion for two different set of allocations $\Phi(\mathcal{A})$ and $\Phi(\mathcal{A}')$. Notice that in this case the comparison is on the payoff achieved by each agent in the set $\mathcal{S}$:

$$(\phi_1, \ldots, \phi_n) \succ_P (\phi'_1, \ldots, \phi'_n) \quad \text{iff} \quad \forall i \in \{1, \ldots, n\},\, \phi_i \geq \phi'_i \wedge \exists j \,|\, \phi_j > \phi'_j \tag{A.14}$$

where $\succ_P$ designates the Pareto order, and n is the number of agents in $\mathcal{S}$. The Pareto order satisfies the transitivity, irreflexivity and monotonicity properties desired for the preference operator [57].

Bibliography

[1] R. Vadigepalli and F. J. Doyle III, "Structural analysis of large-scale systems for distributed state estimation and control applications," *Control Engineering Practice*, vol. 11, no. 8, pp. 895 – 905, 2003.

[2] R. R. Negenborn, Z. Lukszo, and H. Hellendoorn, Eds., *Intelligent Infrastructures.* Springer, 2010.

[3] R. Scattolini, "Architectures for distributed and hierarchical model predictive control - a review," *Journal of Process Control*, vol. 19, pp. 723–731, 2009.

[4] R. R. Negenborn and J. M. Maestre, "Distributed model predictive control: An overview and roadmap of future research opportunities," *Control Systems, IEEE*, vol. 34, no. 4, pp. 87–97, Aug 2014.

[5] B. T. Stewart, J. B. Rawlings, and S. J. Wright, "Hierarchical cooperative distributed model predictive control," in *American Control Conference (ACC), 2010*, June 2010, pp. 3963–3968.

[6] D. D. Šiljak, *Decentralized control of complex systems.* Boston: Academic Press Inc., 1991.

[7] A. Zečević and D. D. Šiljak, *Control of complex systems.* Springer US, 2010.

[8] J. B. Rawlings and B. T. Stewart, "Coordinating multiple optimization-based controllers: New opportunities and challenges," *Journal of Process Control*, vol. 18, no. 9, pp. 839 – 845, 2008.

[9] J. M. Maestre, D. Muñoz de la Peña, A. Jiménez Losada, E. Algaba, and E. F. Camacho, "A coalitional control scheme with applications to cooperative game theory," *Optimal Control Applications and Methods*, 2013.

[10] F. Fele, J. M. Maestre, S. M. Hashemy, D. Muñoz de la Peña, and E. F. Camacho, "Coalitional model predictive control of an irrigation canal," *Journal of Process Control*, vol. 24, no. 4, pp. 314 – 325, 2014.

[11] A. Núñez, C. Ocampo-Martínez, J. M. Maestre, and B. De Schutter, "Time-varying scheme for noncentralized model predictive control of large-scale systems," *Mathematical Problems in Engineering*, vol. 2015, 2015.

[12] F. Fele, J. M. Maestre, and E. F. Camacho, "Coalitional control: A bottom-up approach," in *2015 American Control Conference (ACC)*, Chicago, IL, July 2015, pp. 4074–4079.

[13] J. Tsitsiklis, "Problems in decentralized decision making and computation," Ph.D. dissertation, Massachusetts Institute of Technology, 1984.

[14] W. Saad, Z. Han, H. Poor, and T. Basar, "Game-theoretic methods for the smart grid: An overview of microgrid systems, demand-side management, and smart grid communications," *Signal Processing Magazine, IEEE*, vol. 29, no. 5, pp. 86–105, Sept 2012.

[15] F. Malandrino, C. Casetti, and C.-F. Chiasserini, "A holistic view of ITS-enhanced charging markets," *IEEE Transactions on Intelligent Transportation Systems*, vol. 16, no. 4, pp. 1736–1745, Aug. 2015.

[16] T. Larsson and S. Skogestad, "Plantwide control - A review and a new design procedure," *Modeling, Identification and Control*, vol. 21, no. 4, pp. 209–240, 2000.

[17] W. Al-Gherwi, H. Budman, and A. Elkamel, "Robust distributed model predictive control: A review and recent developments," *The Canadian Journal of Chemical Engineering*, vol. 89, no. 5, pp. 1176–1190, 2011. [Online]. Available: http://dx.doi.org/10.1002/cjce.20555

[18] M. Jilg and O. Stursberg, "Optimized Distributed Control and Topology Design for Hierarchically Interconnected Systems," in *European Control Conference*, Zurich, Switzerland, Jul. 2013, pp. 4340 – 4346.

[19] ——, "Hierarchical Distributed Control for Interconnected Systems," in *13th IFAC Symposium on Large Scale Complex Systems: Theory and Applications*, Shanghai, China, Jul. 2013, pp. 419–425.

[20] Y. Samyudia, P. Lee, and I. Cameron, "A methodology for multi-unit control design," *Chemical Engineering Science*, vol. 49, no. 23, pp. 3871 – 3882, 1994. [Online]. Available: http://www.sciencedirect.com/science/article/pii/0009250994001960

[21] W. Al-Gherwi, H. Budman, and A. Elkamel, "Selection of control structure for distributed model predictive control in the presence of model errors," *Journal of Process Control*, vol. 20, no. 3, pp. 270 – 284, 2010. [Online]. Available: http://www.sciencedirect.com/science/article/pii/S0959152409002224

[22] E. M. B. Aske, S. Strand, and S. Skogestad, "Coordinator MPC for maximizing plant throughput," *Computers & Chemical Engineering*, vol. 32, pp. 195 – 204, 2008, process Systems Engineering: Contributions on the State-of-the-Art Selected extended Papers from ESCAPE '16/PSE 2006. [Online]. Available: http://www.sciencedirect.com/science/article/pii/S009813540700138X

[23] N. Motee and B. Sayyar-Rodsari, "Optimal partitioning in distributed model predictive control," in *Proceedings of the 2003 American Control Conference*, vol. 6, 2003, pp. 5300–5305.

[24] B. T. Stewart, A. N. Venkat, J. B. Rawlings, S. J. Wright, and G. Pannocchia, "Cooperative distributed model predictive control," *Systems and Control Letters*, 2010.

[25] P. J. Antsaklis and A. N. Michel, *Linear systems*. New York: McGraw-Hill,, 1997.

[26] Y.-Y. Liu, J.-J. Slotine, and A.-L. Barabasi, "Controllability of complex networks," *Nature*, vol. 473, pp. 167–173, 2011.

[27] T. H. Summers and J. Lygeros, "Optimal Sensor and Actuator Placement in Complex Dynamical Networks," in *IFAC World Congress*, Aug. 2014.

[28] C. Ocampo-Martínez, S. Bovo, and V. Puig, "Partitioning approach oriented to the decentralised predictive control of large-scale systems," *Journal of Process Control*, vol. 21, no. 5, pp. 775 – 786, 2011. [Online]. Available: www.sciencedirect.com/science/article/pii/S0959152410002398

[29] L. Shapley, "A value for n-person games," *Annals of Math. Studies*, vol. 28, pp. 307–317, 1953.

[30] F. J. Muros, J. M. Maestre, E. Algaba, C. Ocampo-Martínez, and E. F. Camacho, "An application of the Shapley value to perform system partitioning," in *Proceedings of the 2015 American Control Conference*, 2015, pp. 2143–2148.

[31] I. Alvarado, D. Limon, D. Muñoz de la Peña, J. M. Maestre, F. Valencia, H. Scheu, R. R. Negenborn, M. A. Ridao, B. De Schutter, J. Espinosa, and M. W., "A comparative analysis of distributed MPC techniques applied to the hd-mpc four tank benchmark," *Submitted to Journal of Process Control*, 2010.

[32] J. M. Maestre, M. A. Ridao, A. Kozma, C. Savorgnan, M. Diehl, M. D. Doan, A. Sadowska, T. Keviczky, B. De Schutter, H. Scheu, W. Marquardt, F. Valencia, and J. Espinosa, "A comparison of distributed mpc schemes on a hydro-power plant benchmark," *Optimal Control Applications and Methods*, vol. 36, no. 3, pp. 306–332, 2015, oca.2154. [Online]. Available: http://dx.doi.org/10.1002/oca.2154

[33] P. Trodden and A. Richards, "Adaptive cooperation in robust distributed model predictive control," in *Control Applications, (CCA) Intelligent Control, (ISIC), 2009 IEEE*, July 2009, pp. 896–901.

[34] C. Langbort and J. Delvenne, "Distributed design methods for linear quadratic control and their limitations," *Automatic Control, IEEE Transactions on*, vol. 55, no. 9, pp. 2085–2093, Sep. 2010.

[35] H. Ishii and R. Tempo, "The PageRank problem, multiagent consensus, and web aggregation: A systems and control viewpoint," *Control Systems, IEEE*, vol. 34, no. 3, pp. 34–53, June 2014.

[36] J. M. Maestre and H. Ishii, "A cooperative game theory approach to the PageRank problem," in *2016 American Control Conference (ACC)*, Boston, MA, USA, Jul. 2016, pp. 3820–3825.

[37] Y. Sun and N. H. El-Farra, "Quasi-decentralized model-based networked control of process systems," *Computers and Chemical Engineering*, vol. 32, pp. 2016–2029, 2008.

[38] J. M. Maestre, D. Muñoz de la Peña, E. F. Camacho, and T. Alamo, "Distributed model predictive control based on agent negotiation," *Journal of Process Control*, vol. 21, no. 5, 2011.

[39] P. Trodden and A. Richards, "Cooperative distributed MPC of linear systems with coupled constraints," *Automatica*, vol. 49, no. 2, pp. 479 – 487, 2013.

[40] R. R. Negenborn, P. J. van Overloop, T. Keviczky, and B. De Schutter, "Distributed model predictive control of irrigation canals," *Networks and Heterogeneus Media*, vol. 4, pp. 359–380, 2009.

[41] H. Scheu, J. Busch, and W. Marquardt, "Nonlinear distributed dynamic optimization based on first order sensitivities," in *Proceedings of the American Control Conference*, Baltimore, Maryland, USA, July 2010.

[42] J. M. Maestre and R. R. Negenborn, *Distributed Model Predictive Control Made Easy*, ser. Intelligent Systems, Control and Automation: Science and Engineering. Springer, 2014, vol. 69.

[43] M. Lopes de Lima, E. Camponogara, D. Limon Marruedo, and D. Muñoz de la Peña, "Distributed satisficing MPC," *Control Systems Technology, IEEE Transactions on*, vol. 23, no. 1, pp. 305–312, Jan. 2015.

[44] A. Núñez, C. Ocampo-Martínez, B. De Schutter, F. Valencia, J. López, and J. Espinosa, "A multiobjective-based switching topology for hierarchical model predictive control applied to a hydro-power valley," in *3rd IFAC International Conference on Intelligent Control and Automation Science*, Chengdu, China, Sep. 2013, pp. 529–534.

[45] F. V. Arroyave, "Game theory based distributed model predictive control: An approach to large-scale systems control," Ph.D. dissertation, GAUNAL, Universidad Nacional de Colombia, September 2012.

[46] M. Slikker and A. van den Nouweland, *Social and Economics Networks in Cooperative Game Theory*. Kluwer Academic Publishers, 2001.

[47] T. Rahwan, T. Michalak, M. Wooldridge, and N. R. Jennings, "Anytime coalition structure generation in multi-agent systems with positive or negative externalities," *Artificial Intelligence*, vol. 186, no. 0, pp. 95 – 122, 2012. [Online]. Available: www.sciencedirect.com/science/article/pii/S0004370212000288

[48] W. Saad, Z. Han, M. Debbah, A. Hjorungnes, and T. Basar, "Coalitional game theory for communication networks," *IEEE Signal Processing Magazine, Special Issue on Game Theory*, vol. 26, no. 5, pp. 77–97, September 2009.

[49] E. Baeyens, E. Y. Bitar, P. P. Khargonekar, and K. Poolla, "Coalitional aggregation of wind power," *Power Systems, IEEE Transactions on*, vol. 28, no. 4, pp. 3774–3784, Nov 2013.

[50] F. Malandrino, C. Casetti, C.-F. Chiasserini, and M. Reineri, "A game-theory analysis of charging stations selection by EV drivers," *Performance Evaluation*, vol. 83–84, pp. 16–31, Jan. 2015.

[51] D. Ray, *A game-theoretic perspective on coalition formation.* Oxford University Press, 2007.

[52] T. Sandholm, K. Larson, M. Andersson, O. Shehory, and F. TohmÃľ, "Coalition structure generation with worst case guarantees," *Artificial Intelligence*, vol. 111, no. 1âĂŞ2, pp. 209 – 238, 1999. [Online]. Available: www.sciencedirect.com/science/article/pii/S0004370299000363

[53] G. de O. Ramos, J. Rial, and A. Bazzan, "Self-adapting coalition formation among electric vehicles in smart grids," in *Self-Adaptive and Self-Organizing Systems (SASO), 2013 IEEE 7th International Conference on*, Sept 2013, pp. 11–20.

[54] G. Chalkiadakis, E. Elkind, and M. Wooldridge, *Computational aspects of cooperative game theory.* USA: Morgan & Claypool, 2012.

[55] R. B. Myerson, *Game Theory: Analysis of Conflict.* Cambridge, MA: Harvard University Press, 1997.

[56] R. Aumann and J. Dreze, "Cooperative games with coalition structures," *International Journal of Game Theory*, vol. 3, no. 4, pp. 217–237, 1974. [Online]. Available: http://dx.doi.org/10.1007/BF01766876

[57] K. R. Apt and A. Witzel, "A generic approach to coalition formation," *International Game Theory Review (IGTR)*, vol. 11, no. 3, pp. 347–367, 2009.

[58] S. Riverso, M. Farina, and G. Ferrari-Trecate, "Plug-and-play model predictive control based on robust control invariant sets," *Automatica*, vol. 50, no. 8, pp. 2179–2186, 2014.

[59] P. A. Trodden, P. R. Baldivieso Monasterios, and J. M. Maestre, "Distributed MPC with minimization of mutual disturbance sets," in *2016 American Control Conference (ACC)*, Boston, MA, USA, Jul. 2016, pp. 5193–5198.

[60] R. R. Negenborn and J. M. Maestre, "Distributed model predictive control: An overview and roadmap of future research opportunities," *IEEE Control Systems*, vol. 34, no. 4, pp. 87–97, Aug 2014.

[61] F. Fele, J. M. Maestre, and E. F. Camacho, "Coalitional control: cooperative game theory and control," *IEEE Control Systems Magazine*, 2016, accepted.

[62] F. Fele, E. G. Debada, J. M. Maestre, and E. F. Camacho, "Coalitional control for self-organizing agents," *IEEE Transactions on Automatic Control*, 2016, submitted.

[63] F. Fele, J. Maestre, F. Muros, and E. Camacho, "Coalitional control: an irrigation canal case study," in *Proceedings of the 37th IEEE International Conference on Networking, Sensing and Control*, Paris, France, April 2013.

[64] F. Fele, J. M. Maestre, and E. F. Camacho, "Coalitional MPC control applied to an irrigation canal," in *ACROSS workshop on cooperative systems*, Dubrovnik, Croatia, Sep. 2014.

[65] ——, "Coalitional control: a bottom-up approach," in *Proceedings of the 2015 American Control Conference*, Chicago, IL, USA, Jul. 2015.

[66] F. Fele, P. Báez-González, and E. F. Camacho, "Coalition formation of charging stations in an EV population scenario," *IEEE Transactions on Smart Grid*, 2016, to be submitted.

[67] C. Ocampo-Martínez, D. Barcelli, V. Puig, and A. Bemporad, "Hierarchical and decentralised model predictive control of drinking water networks: Application to Barcelona case study," *Control Theory Applications, IET*, vol. 6, no. 1, pp. 62–71, 2012.

[68] M. V. Kothare, V. Balakrishnan, and M. Morari, "Robust constrained model predictive control using linear matrix inequalities," *Automatica*, vol. 32, no. 10, pp. 1361–1379, 1996.

[69] P. Malaterre, D. Rogers, and J. Schuurmans, "Classification of canal control algorithms," *Journal of Irrigation and Drainage Engineering*, vol. 124, no. 1, pp. 3–10, 1998.

[70] A. J. Clemmens and J. Schuurmans, "Simple optimal downstream feedback canal controllers: Theory," *Journal of Irrigation and Drainage Engineering*, vol. 130, no. 1, pp. 26–34, 2004.

[71] P. J. van Overloop, "Model predictive control on open water systems," Ph.D. dissertation, Delft University of Technology, Delft, The Netherlands, 2006.

[72] R. R. Negenborn, P. J. van Overloop, T. Keviczky, and B. De Schutter, "Distributed model predictive control for irrigation canals," *Networks and Heterogeneous Media*, vol. 4, no. 2, pp. 359–380, 2009.

[73] H. Fawal, D. Georges, and G. Bornard, "Optimal control of complex irrigation systems via decomposition-coordination and the use of augmented lagrangian," in *1998 IEEE International Conference on Systems, Man, and Cybernetics*, vol. 4, 1998, pp. 3874–3879.

[74] A. Zafra Cabeza, J. M. Maestre, M. A. Ridao, E. F. Camacho, and L. Sánchez, "A hierarchical distributed model predictive control approach in irrigation canals: A risk mitigation perspective," *Journal of Process Control*, vol. 21, no. 5, pp. 787–799, 2011.

[75] SOBEK, "Manual and technical reference," WL|Delft Hydraulics, Delft, The Netherlands, Tech. Rep., 2000.

[76] J. Schuurmans, "Control of water levels in open-channels," Ph.D. dissertation, TUDelft, 1997.

[77] P. J. van Overloop, R. R. Negenborn, B. De Schutter, and N. C. Giesen, "Predictive control for national water flow optimization in the netherlands," in *Intelligent Infrastructures*, ser. Intelligent Systems, Control and Automation: Science and Engineering, R. R. Negenborn, Z. Lukszo, and H. Hellendoorn, Eds. Springer Netherlands, 2010, vol. 42, pp. 439–461. [Online]. Available: http://dx.doi.org/10.1007/978-90-481-3598-1_17

[78] A. Clemmens, "Water-level difference controller for main canals," *Journal of Irrigation and Drainage Engineering*, vol. 138, no. 1, pp. 1–8, 2012.

[79] S. Hashemy, M. Monem, J. Maestre, and P. Van Overloop, "Application of an in-line storage strategy to improve the operational performance of main irrigation canals using model predictive control," *Journal of Irrigation and Drainage Engineering*, vol. 139, no. 8, pp. 635–644, 2013.

[80] P. J. van Overloop, S. Weijs, and S. Dijkstra, "Multiple model predictive control on a drainage canal system," *Control Engineering Practice*, vol. 16, no. 5, pp. 531 – 540, 2008. [Online]. Available: http://www.sciencedirect.com/science/article/pii/S0967066107001190

[81] P. J. van Overloop, J. Schuurmans, R. Brouwer, and C. Burt, "Multiple-model optimization of proportional integral controllers on canals," *Journal of Irrigation and Drainage Engineering*, vol. 131, no. 2, pp. 190–196, 2005.

[82] J. M. Maestre, D. Muñoz de la Peña, A. Jiménez Losada, E. Algaba, and E. F. Camacho, "An application of cooperative game theory to distributed control," in *Proceedings of the 18th IFAC World Congress*, 2011.

[83] G. Pannocchia and J. B. Rawlings, "Disturbance models for offset-free model-predictive control," *AIChE Journal*, vol. 49, no. 2, pp. 426–437, 2003.

[84] S. Isapoor, A. Montazar, P. J. van Overloop, and N. van de Giesen, "Designing and evaluating control systems of the Dez main canal," *Irrigation and Drainage*, vol. 60, no. 1, pp. 70–79, 2011. [Online]. Available: http://dx.doi.org/10.1002/ird.545

[85] S. Hashemy and P. Van Overloop, "Applying decentralized water level difference control for operation of the dez main canal under water shortage," *Journal of Irrigation and Drainage Engineering*, 2013.

[86] W. Saad, Z. Han, and H. Poor, "Coalitional game theory for cooperative micro-grid distribution networks," in *Communications Workshops (ICC), 2011 IEEE International Conference on*, June 2011, pp. 1–5.

[87] G. K. Larsen, N. D. van Foreest, and J. M. Scherpen, "Power supply–demand balance in a smart grid: An information sharing model for a market mechanism," *Applied Mathematical Modelling*, vol. 38, no. 13, pp. 3350 – 3360, 2014.

[88] S. Engell, R. Paulen, M. A. Reniers, C. Sonntag, and H. Thompson, *Core Research and Innovation Areas in Cyber-Physical Systems of Systems*. Cham: Springer International Publishing, 2015, pp. 40–55.

[89] A. Gusrialdi and S. Hirche, "Performance-oriented communication topology design for large-scale interconnected systems," in *49th IEEE Conference on Decision and Control (CDC)*, Dec 2010, pp. 5707–5713.

[90] F. Dörfler, M. R. Jovanović, M. Chertkov, and F. Bullo, "Sparsity-promoting optimal wide-area control of power networks," *IEEE Transactions on Power Systems*, vol. 29, no. 5, pp. 2281–2291, Sept 2014.

[91] J. M. Maestre, H. Ishii, and E. Algaba, "A cooperative game theory approach to the PageRank problem," in *Proceedings of the 2016 American Control Conference*, Boston, MA, USA, Jul. 2016.

[92] F. Lin, M. Fardad, and M. R. Jovanović, "Design of optimal sparse feedback gains via the alternating direction method of multipliers," *IEEE Transactions on Automatic Control*, vol. 58, no. 9, pp. 2426–2431, Sept 2013.

[93] R. Schuh and J. Lunze, "Design of the communication structure of a self-organizing networked controller for heterogeneous agents," in *Control Conference (ECC), 2015 European*, July 2015, pp. 2194–2201.

[94] D. Gross, M. Jilg, and O. Stursberg, "Design of Distributed Controllers and Communication Topologies Considering Link Failures," in *2013 European Control Conference*, Zurich, Switzerland, Jul. 2013, pp. 3288 – 3294.

[95] S. Riverso, M. Farina, and G. Ferrari-Trecate, "Plug-and-play decentralized model predictive control for linear systems," *IEEE Transactions on Automatic Control*, vol. 58, no. 10, pp. 2608–2614, Oct 2013.

[96] R. E. Stearns, "Convergent transfer schemes for n-person games," *Transactions of the American Mathematical Society*, vol. 134, no. 3, pp. 449–459, 1968.

[97] J. C. Cesco, "A convergent transfer scheme to the core of a TU-game," *Revista de Matemáticas Aplicadas*, vol. 19, pp. 23–25, 1998.

[98] A. Nedić and D. Bauso, "Dynamic coalitional TU games: Distributed bargaining among players' neighbors," *Automatic Control, IEEE Transactions on*, vol. 58, no. 6, pp. 1363–1376, June 2013.

[99] J. Pfrommer, J. Warrington, G. Schildbach, and M. Morari, "Dynamic vehicle redistribution and online price incentives in shared mobility systems," *Intelligent Transportation Systems, IEEE Transactions on*, vol. 15, no. 4, pp. 1567–1578, Aug 2014.

[100] W. Yuan, J. Huang, and Y. Zhang, "Competitive charging station pricing for plug-in electric vehicles," *Smart Grid, IEEE Transactions on*, vol. PP, no. 99, pp. 1–13, 2015.

[101] J. M. Maestre, D. Muñoz de la Peña, and E. F. Camacho, "Distributed MPC: a supply chain case study," in *Proceedings of the Conference on Decision and Control*, 2009.

[102] E. Camponogara and L. de Oliveira, "Distributed optimization for model predictive control of linear-dynamic networks," *Systems, Man and Cybernetics, Part A: Systems and Humans, IEEE Transactions on*, vol. 39, no. 6, pp. 1331–1338, Nov 2009.

[103] T. Rahwan, T. Michalak, M. Wooldridge, and N. R. Jennings, "Anytime coalition structure generation in multi-agent systems with positive or negative externalities," *Artificial Intelligence*, vol. 186, pp. 95 – 122, 2012.

[104] E. F. Camacho and C. Bordons, *Model Predictive Control*, 2nd ed. London, England: Springer-Verlag, 2004.

[105] J. B. Rawlings and D. Q. Mayne, *Model Predictive Control: Theory and Design.* Nob Hill Publishing, 2009.

[106] T. S. Ferguson, *Game Theory, Second Edition*, Mathematics Department, UCLA, 2014.

[107] M. O. Jackson, *Social and Economic Networks.* Princeton, NJ, USA: Princeton University Press, 2010.

[108] L. S. Shapley, "On balanced sets and cores," *Naval Research Logistics Quarterly*, vol. 14, no. 4, pp. 453–460, 1967.

[109] S. Riverso and G. Ferrari-Trecate, "Hycon2 Benchmark: Power Network System," *ArXiv e-prints*, Jul. 2012.

[110] M. Farina, P. Colaneri, and R. Scattolini, "Block-wise discretization accounting for structural constraints," *Automatica*, vol. 49, no. 11, pp. 3411 – 3417, 2013.

[111] D. Limon, T. Alamo, F. Salas, and E. F. Camacho, "On the stability of constrained MPC without terminal constraint," *IEEE Transactions on Automatic Control*, vol. 51, no. 5, pp. 832–836, May 2006.

[112] I. Bayram, G. Michailidis, I. Papapanagiotou, and M. Devetsikiotis, "Decentralized control of electric vehicles in a network of fast charging stations," in *Global Communications Conference (GLOBECOM), 2013 IEEE*, Dec 2013, pp. 2785–2790.

[113] PlugShare, "EV charging station map," 2016. [Online]. Available: www.plugshare.com

[114] T. Motors, "Tesla supercharger map," 2016. [Online]. Available: www.tesla.com/supercharger

[115] J. Johnson, M. Chowdhury, Y. He, and J. Taiber, "Utilizing real-time information transferring potentials to vehicles to improve the fast-charging process in electric vehicles," *Transportation Research Part C: Emerging Technologies*, vol. 26, pp. 352 – 366, 2013. [Online]. Available: http://www.sciencedirect.com/science/article/pii/S0968090X12001313

[116] J. Escudero-Garzas and G. Seco-Granados, "Charging station selection optimization for plug-in electric vehicles: An oligopolistic game-theoretic framework," in *Innovative Smart Grid Technologies (ISGT), 2012 IEEE PES*, Jan 2012, pp. 1–8.

[117] W. Lee, L. Xiang, R. Schober, and V. W. S. Wong, "Electric vehicle charging stations with renewable power generators: A game theoretical analysis," *IEEE Transactions on Smart Grid*, vol. 6, no. 2, pp. 608–617, March 2015.

[118] X. Feixiang, H. Mei, Z. Weige, and L. Juan, "Research on electric vehicle charging station load forecasting," in *Advanced Power System Automation and Protection (APAP), 2011 International Conference on*, vol. 3, Oct 2011, pp. 2055–2060.

[119] F. Malandrino, C. Casetti, C.-F. Chiasserini, and M. Reineri, "A game-theory analysis of charging stations selection by EV drivers," *Performance Evaluation*, vol. 83–84, pp. 16–31, Jan 2015. [Online]. Available: http://www.sciencedirect.com/science/article/pii/S0166531614001163

[120] Z. Ma, D. S. Callaway, and I. A. Hiskens, "Decentralized charging control of large populations of plug-in electric vehicles," *Control Systems Technology, IEEE Transactions on*, vol. 21, no. 1, pp. 67–78, Jan 2013.

[121] F. Parise, M. Colombino, S. Grammatico, and J. Lygeros, "Mean field constrained charging policy for large populations of plug-in electric vehicles," in *IEEE Conference on Decision and Control*, Los Angeles, California, USA, Dec. 2014.

[122] S. Bae and A. Kwasinski, "Spatial and temporal model of electric vehicle charging demand," *Smart Grid, IEEE Transactions on*, vol. 3, no. 1, pp. 394–403, March 2012.

[123] E. Xydas, C. Marmaras, L. Cipcigan, A. Hassan, and N. Jenkins, "Forecasting electric vehicle charging demand using support vector machines," in *Power Engineering Conference (UPEC), 2013 48th International Universities'*, Sept 2013, pp. 1–6.

[124] Ayesa, "Ayesa website," 2013. [Online]. Available: www.ayesa.com

[125] Zem2All, "Zem2all project website," 2013. [Online]. Available: www.zem2all.com

[126] R. J. Flores, B. P. Shaffer, and J. Brouwer, "Electricity costs for an electric vehicle fueling station with level 3 charging," *Applied Energy*, vol. 169, pp. 813 – 830, 2016. [Online]. Available: http://www.sciencedirect.com/science/article/pii/S0306261916302082

[127] D. I. of transport systems, "Simulation of Urban MObility (SUMO)," 2016. [Online]. Available: www.dlr.de/ts/sumo/en/

[128] N. Nisan, T. Roughgarden, E. Tardos, and V. V. Vazirani, *Algorithmic Game Theory*. New York, NY, USA: Cambridge University Press, 2007.

[129] A. Acosta, "TraCI4Matlab, an implementation of the TraCI interface for Matlab," 2016. [Online]. Available: www.mathworks.com/matlabcentral/fileexchange/44805-traci4matlab

[130] Q. Wu, A. Nielsen, J. Ostergaard, S. T. Cha, F. Marra, Y. Chen, and C. Traeholt, "Driving pattern analysis for electric vehicle (ev) grid integration study," in *Innovative Smart Grid Technologies Conference Europe (ISGT Europe), 2010 IEEE PES*, Oct 2010.

[131] J. Barreiro-Gomez, C. Ocampo-Martínez, J. M. Maestre, and N. Quijano, "Multi-objective model-free control based on population dynamics and cooperative games," in *54th IEEE Conference on Decision and Control (CDC)*, Osaka, Japan, Dec. 2015, pp. 5296–5301.

[132] A. Nedić and D. Bauso, "Dynamic coalitional TU games: Distributed bargaining among players' neighbors," *Automatic Control, IEEE Transactions on*, vol. 58, no. 6, pp. 1363–1376, June 2013.

[133] J. M. Maestre, P. J. Van Overloop, M. Hashemy, A. Sadowska, and E. F. Camacho, “Human in the Loop Model Predictive Control: an Irrigation Canal Case Study,” in *Proceedings of the 2014 Control and Decision Conference*, Los Angeles, CA, USA, Dec. 2014.

[134] J. R. Marden, B. Touri, R. Gopalakrishnan, and J. P. O’Brien, “Impact of information in a simple multiagent collaborative task,” in *2015 54th IEEE Conference on Decision and Control (CDC)*, Dec 2015, pp. 4543–4548.

[135] G. N. Nair, F. Fagnani, S. Zampieri, and R. J. Evans, “Feedback control under data rate constraints: An overview,” *Proceedings of the IEEE*, vol. 95, no. 1, pp. 108–137, Jan 2007.

[136] T. Rahwan, T. Michalak, E. Elkind, P. Faliszewski, J. Sroka, M. Wooldridge, and N. Jennings, “Constrained coalition formation,” in *Proceedings of the Twenty-Fifth AAAI Conference on Artificial Intelligence.* AAAI, August 2011, pp. 719–725.

[137] C. H. Papadimitriou and M. Yannakis, “Linear programming without the matrix,” in *25th ACM Symp. Theory Comput.*, 1993, pp. 121–127.

[138] J. R. Marden, “The role of information in multiagent coordination,” in *2014 53rd IEEE Annual Conference on Decision and Control (CDC)*, Dec 2014, pp. 445–450.

[139] A. Zambelli, S. Erhart, L. Zaccarian, and S. Hirche, “Dynamic load distribution in cooperative manipulation tasks,” in *Proceedings of the 2015 IEEE/RSJ International Conference on Intelligent Robots and Systems (IROS)*, Hamburg, Germany, Sep 2015.

[140] S. Riverso, F. Boem, G. Ferrari-Trecate, and T. Parisini, “Plug-and-play fault detection and control-reconfiguration for a class of nonlinear large-scale constrained systems,” *IEEE Transactions on Automatic Control*, 2016.

[141] F. Deroo, M. Meinel, M. Ulbrich, and S. Hirche, “Distributed stability tests for large-scale systems with limited model information,” *IEEE Transactions on Control of Network Systems*, vol. 2, no. 3, Sept 2015.

[142] J. Antoniou and A. Pitsillides, *Game theory in communication networks: cooperative resolution of interactive networking scenarios.* CRC Press, 2012.

[143] J. R. Marden and J. S. Shamma, "Game theory and distributed control," in *Handbook of Game Theory Vol. 4*, H. P. Young and S. Zamir, Eds. Elsevier Science, 2013, forthcoming.

[144] C. Korth, *Fairness in Bargaining and Markets*, ser. Lecture Notes in Economics and Mathematical Systems. Springer, 2009.

[145] E. Baeyens, E. Y. Bitar, P. P. Khargonekar, and K. Poolla, "Wind energy aggregation: A coalitional game approach," in *50th IEEE Conference on Decision and Control and European Control Conference (CDC-ECC)*, Dec 2011, pp. 3000–3007.

[146] Wikipedia, "Indicator function — Wikipedia, the free encyclopedia," 2014, [Accessed 13/03/2014]. [Online]. Available: http://en.wikipedia.org/w/index.php?title=Indicator_function&oldid=594891923

[147] V. H. Moll, *Numbers and functions*. American Mathematical Society (AMS), 2012.

[148] K. R. Apt and T. Radzik, "Stable partitions in coalitional games," *CoRR*, vol. abs/cs/0605132, 2006.